Role of the Asf1-Rad53 interaction in genomic stability in S.cerevisiae

Yue Jiao

Gènes, Génomes, Cellules

UNIVERSITÉ PARIS-SUD 11

Université Paris-Sud 11
THÈSE

Pour obtenir le titre de

Docteur de l'Université Paris-Sud 11
L'Ecole Doctorale Gènes, Génomes, Cellules

Présentée et soutenue publiquement par

Yue JIAO

Le 4 Juillet 2011

RÔLE DE L'INTERACTION ASF1-RAD53 DANS LA STABILITE GENOMIQUE CHEZ *S.CEREVISIAE*

Jury

Dr. Benoît ARCANGIOLI	Rapporteur
Dr. Serge GANGLOFF	Rapporteur
Dr. Françoise OCHSENBEIN	Examinatrice
Dr. Carl MANN	Directeur de thèse
Pr. Herman VAN TILBEURGH	Président du Jury

Thèse préparée au sein du laboratoire
Stabilité génomique
DSV/SBIGeM/ iBiTec-S/LSOC
CEA-Saclay

Acknowledgments

First of all, I would like to thank my supervisor Dr. Carl MANN for giving me the opportunity to work on this project and for his continual guidance and advice in every aspect of the work.

Thank you to my committee members for their valuable suggestions and feedback in evaluating my research. I would also like to sincerely thank Dr. Françoise Ochsenbein for always having time for me, her valuable help, collaboration and guidance.

A big thank you to all the members of our laboratory, both past and present members, who have provided support and humor during the last 3.5 years. In praticular I would like to thank Régis Courbeyrette for sharing his valuable experiences in yeast technologies and Michael Montblanc for his help with the GST-pull down experiment.

Especial thanks are due to my dearest friends Sandrine Ragu, Kévin Contrepois Maryssa Nassour and Jean-Yves Thuret for their personal and professional support and so much encouragement. It was a pleasure to be a part of such a wonderful group in my daily work. Special thanks to my yeast-roomate Aeid Igbaria for the stimulating scientific and non-scientific discussions.

Additionally, I would like to acknowledge my collaborators for their excellent experimental contribution and scientific interest, especially Karsten Seeger, Albane Gaubert, Aurélie Lautrette, Armelle Lengronne and Philippe Pasero.

I am very grateful to my funding sources that allowed me to undertake this research: CEA-Irtelis (The International PhD Program) and ARC (Association pour la recherche sur le cancer).

Finally thanks to my mom LiLi Ma and my dad XiaoMing Jiao for encouraging and inspiring me throughout my life and their unconditional love. Thank you for believing in me even when I didn't believe in myself. A massive thanks to Isabelle San Martin for always giving me a warm hug when I was tired. I am thankful to Arhamatoulay Maiga, Arounie Tavenet, Céline Bon, Aubrey Poulizac and Yan Li for their amazing friendship and the positive attitude towards life. I will always remember the good times.

Abstract

Asf1 is a histone chaperone, which participates in the assembly and disassembly of histones H3/H4 on DNA. Asf1 is not essential for cell viability in yeast, but the DNA damage checkpoints are constitutively activated in cells lacking Asf1 and they are hypersensitive to several types of genotoxic stress. In yeast, Asf1 forms a stable complex with Rad53 in the absence of genotoxic stress. Our results suggest that this complex involves at least three interaction surfaces. One site involves the H3-binding surface of Asf1 with an as yet undefined surface of Rad53, probably reside in the kinase domain of Rad53. A second site is formed by the Rad53-FHA1 domain binding to Asf1-T270. The third site involves the C-terminal 21 aa of Rad53 bound to the conserved Asf1 N-terminal domain, where Rad53 competes with histone H3/H4 and co-chaperones HirA/CAF-1 for binding to the same surface of Asf1. Rad53 is phosphorylated and activated upon genotoxic stress. The Asf1-Rad53 complex dissociated when cells were treated with hydroxyurea but not methyl methane sulfonate, suggesting a regulation of the complex as a function of the stress.

In addition to these results, we also found that the *rad53-A806R+L808R* mutation at the C-terminus of Rad53 destabilized the Asf1-Rad53 interaction and increased the viability of *rad9* and *rad24* mutants to genotoxic stress. The *rad53-ALRR* mutant also appeared to re-enter the cell cycle and/or traverse S-phase more rapidly than wild type and increased repair or adaptation when combined with the *rad24* mutant.

Abbreviations

4-NQO : 4nitroquinoline 1-oxide
9-1-1 : Rad9-Rad1-Hus1
ARS : Autonomous replicating sequence
Asf1 : Anti-silencing factor-1
ATM : Ataxia telangiectasia mutated
ATR : Ataxia telangiectasia and Rad3 related
BrdU : Bromodeoxyuridine
bp : base pair
CAF-1 : chromatin assembly factor-1
CDK : Cyclin-dependent kinase
CIP : Calf intestinal phophatase
CK2 : Casein kinase 2
CPT : Camptothecin
CDK : cyclin-dependent kinase
DDK : Dbf4-dependent kinases
DDR : DNA damage response
DNA : deoxyribonucleic acid
dNTP: deoxyribonukleotide
DSB : double strand break
DTT : dithiothreitol
Csm3 : chromosome segregation in meiosis
FACS : Fluorescence activated cell sorting
FHA : forkhead-associated domain
GCR : gross chromosomal rearrangement
GST : Glutathione-S-transferase
HIR : Histone regulation
HA : Hemagglutinin
HR : Homologous recombination
HU : hydroxyurea
IP: Immunoprecipitation
IPTG: Isopropyl-β-D-thiogalaktopyranosid
kd : kinase dead
MCM : minichromosome maintenance
Mec1 : Mitosis entry checkpoint mutant 1

MMS : Methylmethanesulfonate

MRN : Mre11, Rad50, Nbs1

MRX : Mre11, Rad50,Xrs2

NHEJ : Non-homologous end joining

NLS : Nuclear localization signal/sequence

PCNA : proliferating cell nuclear antigen

PCR : Polymerase chain reaction

PI3K : Phosphoinositide-3 kinase

Pol : Polymerase

Rad53 : Radiation sensitive mutant 53

RNR : ribonucleotide reductase

RPA : replication protein A

S.cerevisiae : Saccharomyces cerevisiae

SCD : SQ/TQ cluster domain

SDS-PAGE : Sodium dodecyl sulfate polyacrylamide gel electrophoresis

S.pombe : Schizosaccharomyces pombe

ssDNA : single-strand DNA

TAP : Tandem Affinity Purification

Tel1 : Telomere maintenance mutant 1

Tof1 : Topoisomerase I interacting factor

WT : Wildtype

YFP : Yellow fluorescent protein

YPD: Yeast extract peptone dextrose

Table of contents

List of Figures

List of Tables

Introduction

Model: Saccharomyces cerevisiae

The budding yeast *Saccharomyces cerevisiae* is a useful model for studying higher eukaryotic organisms. *S.cerevisiae* has many technical advantages such as rapid growth, dispersed cells, mutant isolation, a well-defined genetic system, numerous selective markers and easy gene manipulation. The genome of *S.cerevisiae* was completely sequenced in 1996 (Goffeau et al, 1996). It is composed of about 13,000,000 bp and 6,275 genes. It is estimated that 23% of yeast genes have homologs in the human genome, and 30% of known genes involved in human diseases have yeast orthologs. Additionally, the conservation of many cellular processes in eukaryotes, such as DNA replication, DNA damage checkpoints and cell cycle control also establishes the usefulness of yeast in the study of human disease (Johnson and O'Donnell, 2005; Lee and Nurse, 1987; Perego et al, 2000; Zhou and Elledge, 2000).

1.1 Genome stability

The maintenance of genomic stability is beneficial for the survival of an individual cell and crucial for cancer avoidance. Cells invest huge resources to maintain genomic stability, and cancer cells undergo an array of genetic changes to escape these barriers.

Defects in chromatin modulation and choromosomal aberrations, including altered chromatin structure in repetitive DNA, chromosome rearrangements and chromosome loss, are reflective of genomic instability and are a hallmark of cancer cells (Myung et al, 2003; Prado et al, 2004; Melo et al, 2007; Kops et al, 2005; Mitelman et al, 2007).

In addition, the DNA checkpoint pathway was originally identified in *S.cerevisiae,* because their loss of fuction resulted in defects in cell cycle progression in response to DNA damge. The absence of checkpoints can be lethal to cells. In cells mutated for checkpoint components, the spontaneous and induced chromosomal rearrangements are significantly increased (Hartwell et al, 1994; Myung et al. 2001; Kolodner et al. 2002; Myung and Kolodner, 2002). These results demonstrate that checkpoint proteins also play important roles in maintaining genomic stability.

1.2 Chromatin

1.2.1 Nucleosome and chromatin structure

In eukaryotic cells, genomic DNA is packaged in chromatin as nucleosomes. The basic unit of chromatin is the nuclesome, consisting of 147bp of DNA wrapped around a histone octamer containing two copies each of histones H2A, H2B, H3 and H4 (Figure 1). The histone proteins are highly conserved across all eukaryotes. Histone proteins contain two functional domains: a core histone-fold domain involved in histone/histone and histone/DNA interactions, and a flexible N-terminal tail domain where a variety of covalent post-translational modifications sites have been studied (Luger et al, 1997). However, little is known about the conformation of the histone tails.

Two nuclesome core particles are separated by linker DNA varying in length from 10 to 80 bp. Histone H1 locks the linker DNA at the entry and exit points of the nucleosome. H1 participates in nucleosome positioning or spacing and formation of the higher-order chromatin structure (Ramakrishnan, 1997; Widom, 1998; Thomas, 1999; Maier et al. 2008).

The primary chromatin structure consisting of nucleosomes assembled along DNA resembles ‘beads on a string’ as seen by electron microscopy (Woodcock et al, 2006). This chromatin fiber may then be further folded and compacted into higher-order chromatin structure that allows the packaging of the genomic DNA into the nucleus (Horn et al, 2002).

The light-microscopy studies have revealed at least two types of chromatin: heterochromatin that stays condensed after cell division and euchromatin that decondenses during interphase (Grewal et al. 2002; Elgin et al. 2003; Maison et al. 2004). Euchromatin can either be actively transcribed or repressed whereas heterochromatin is commonly defined as transcriptionally repressed appearing in large units at the centromeres and telomeres (Grewal et al. 2007).

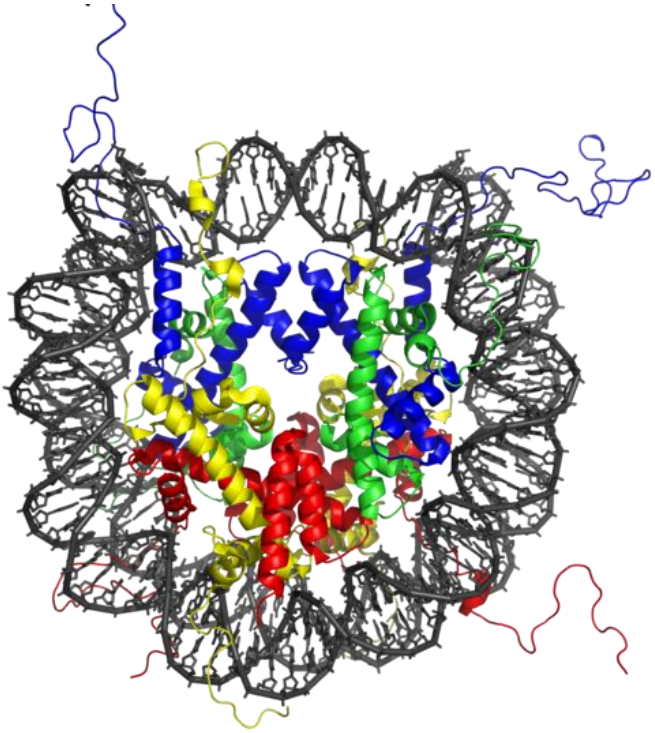

Figure 1. The structure of a nucleosome core particle defined by X-ray crystallography at 2.8 Å resolution. The core particle contains of two copies of H2A, H2B, H3 and H4 and DNA. The view is from the top through the superhelical axis (Lunger et al, 1997). The histone globular domain consists of three α helices connected by two flexible loops and is referred to as the histone fold domain which allows histones to dimerize head to tail in a handshake manner (Arents and Moudrianakis, 1995).

1.2.2 Chromatin dynamics

Chromatin structure and packaging of the genome is important for regulating the cellular processes such as transcription, replication and repair (Kornberg et al, 1999). Therefore, factors that can alter chromatin structure are essential for and provide additional regulatory points in these cellular processes. The chromatin structure is highly dynamic to enable rapid unfolding, disassembly and refolding. Three main mechanisms that control the dynamics of chromatin structure have been identified: histone post-translational modification (PTMs), histone variants and ATP-dependent chromatin remodeling factors (remodelers).

1.2.2.1 Histone modifications

PTMs constitute reversible covalent modifications of amino acidic residues, such as serine and threonine phosphorylation, lysine acetylation, lysine and arginine methylation and lysine ubiquitination, among others. These PTMs modulate chromatin structure and/or recruit proteins to chromatin to mediate distinct cellular processes, including gene transcription, DNA replication and DNA repair (Strahl and Allis, 2000; Turner, 2000; Jenuwein and Allis, 2001; Vidanes et al., 2005). Each of these modifications is catalyzed by a specific family of enzymes. For example, histone acetyltransferases, methyltransferases, kinases and ubiquitin ligases, as well as the enzymes that remove these modifications.

The majority of histone PTMs were found in the N-terminal tails of histones that extend out from the globular core of the nucleosome, creating chromatin structures favourable either for activation or repression of genes through altering the degree of chromatin compaction (Luger et al, 1998). However, recent work has shown that modifications in the globular core play crucial roles in regulating the structure and function of chromatin and controlling biological function, such as H3K56 and H4K91 acetylation (Cosgrove et al, 2004; Masumoto et al, 2005; Xu et al, 2005; Hyland et al, 2005; Ye et al, 2005).

Some histone PTMs are induced in response to DNA damage (Figure 2). These histone PTMs may increase the plasticity of chromatin and facilitate the access of DNA repair and checkpoint proteins to sites of DNA lesions. After repair of lesions, PTMs are cleared for restoration of the chromatin structure and the shut down of checkpoint signaling. Several typical conserved PTMs are introduced here.

In mammals, phosphorylation of serine-139 in the C-terminal SQE motif of histone H2AX is rapidly induced at DSBs, and was named γ-H2AX (Rogakou et al, 1998). In yeast, this phosphorylation (γ-H2A) occurs at serine 129 in the most abundant form of histone H2A (Downs et al, 2000). This phosphorylation is catalysed by DNA damage checkpoint protein kinases: ATM, ATR and DNA-PK kinases in human cells (Burma et al, 2001; Ward et al, 2001; Stiff et al, 2004) or their homologues Mec1 and Tel1 in budding yeast (Downs et al, 2000; Redon et al, 2003; Nakamura et al, 2004) These kinases are recruited to DSBs through their association with partner proteins that recognise DNA lesions either directly or indirectly (Zou et al, 2003; Falck et al, 2005). The formation of γH2AX nuclear foci has been proven to be a DSB marker in mammalian cells. Although γH2AX is not essential for the initial recruitment of DSB response factors, it stabilizes the binding of the checkpoint factors, and it is required for effective repair of DSBs by both the NHEJ and HR pathways (Karagiannis et al, 2007; Celeste et al, 2002; 2003). Dephosphorylation of γH2AX by HTP-C (Histone phosphatase H2A complex) is necessary for the efficient recovery from DNA

damage after DNA repair. γH2AX recruits ubiquitin ligases that participate in the further recruitment of downstream players in the DNA damage response (Huen et al, 2007; Mailand et al, 2007; Kolas et al, 2007).

In yeast, H3K56 acetylation by Rtt109 is important for DNA damage response signaling and histone reassembly after DNA repair (Schneider et al, 2006). These acetylations regulate the binding of H3-H4 with histone chaperone CAF-1, but not Rtt106, to promote nucleosome assembly (Burgess et al, 2010). H3K56-Ac has been shown to require the histone chaperone Asf1 and occurs at the S phase in unstressed cells. Its role will be discussed in chapter 3.2.2.

The methyltransferase Dot1 mediates H3K79 methylation in both yeast and mammalian cells. In budding yeast, increased accessibility of H3K79me3 at DSBs is implicated in the recruitment of the Rad9 checkpoint adaptor protein (Bonilla et al, 2008; Huyen et al, 2004; Wysocki et al, 2005).

The recent studies have revealed that histone acetylation is important for promoting nucleosome assembly by enhancing histone binding with distinct histone chaperones. For example, the most highly-conserved mark of newly-synthesized histones is H4-K5, 8, 12, 16 acetylation which is conserved from yeast to humans. They are generally acetylated by a number of HATs such as NuA4, Gcn5 and in yeast. These acetylations may facilitate histone assembly into nucleosomes and facilitate DNA repair by non-homologous end joining (NHEJ) and homologous recombination (HR) (Sobel et al, 1995; Parthun et al, 1996; Bird et al, 2002; Murr et al, 2006; Murr et al, 2007). Following deposition onto the DNA, the newly synthesized H4 is rapidly deacetylated, which is required for proper chromatin maturation (Sobel et al, 1995; Loyola et al, 2006). H4-K16Ac inhibits the formation of compact 30-nanometer–like fibres and impedes the ability of chromatin to form cross-fibre interactions (Shogren-Knaak et al, 2006). In addition, methylation of histone H4-K20 is essential for recruiting the orthologous checkpoint proteins 53BP1 (mammals) and Crb2 (fission yeast) to sites of DSBs and subsequent activation of a DNA damage checkpoint.

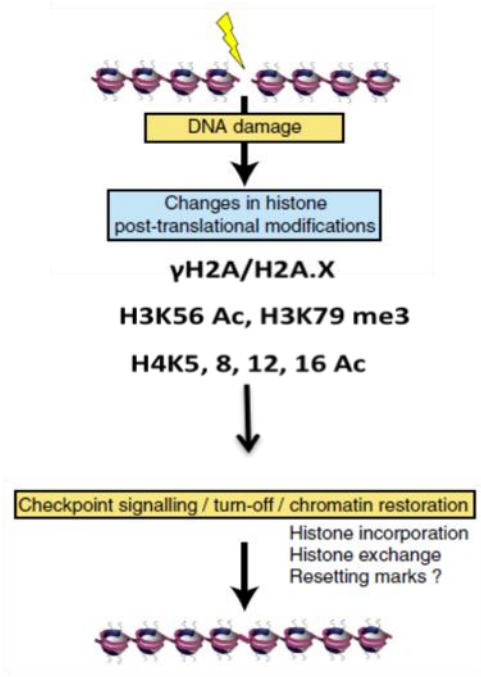

Figure 2. Some histone PTMs are induced in response to DNA damage in yeast, such as γH2A/H2A.X, H3K56 Ac, H3K79 me3 and H4K5, 8, 12,16 Ac, which may increase the plasticity of chromatin, facilitate the access of DNA repair and checkpoint proteins to sites of DNA lesions.

1.2.2.2 Histone variants

Histone variants are distinct, non-allelic isoforms of the major histone types (Redon et al, 2002). The incorporation of the histone variants into nucleosomes may specify chromatin for particular biological roles (Malik and Henikoff, 2003; Talbert and Henikoff, 2010).

In mammals, there are three major classes of histone H3 variants: the replicative histones H3.1 and H3.2, the replacement histone H3.3, and the centromeric protein A (CENP-A) (Loyola et al, 2007). The replicative variants H3.1 and H3.2 represent the bulk of the histones and are expressed and deposited mostly in a replication-coupled manner during S phase. The replacement variant H3.3 is expressed constitutively at low levels throughout the cell cycle and incorporated in a replication-independent (RI) manner. *S.cerevisiae* has only a single H3 variant, most closely related to H3.3 (Tagami et al, 2004 ; Nakatani et al., 2004; Henikoff and Ahmad, 2005; Kamakaka and Biggins, 2005). CENP-A is a centromere specific form of the H3 and essential for centromere function in yeast and mammals (Black and Bassett, 2008).

Histone H2A has the largest number of variants, including H2A.X, H2A.Z, macroH2A and H2A.Bbd. H2A.Z (Htz1 in yeast) is essential in mammals but not in yeast (Faast et al, 2001), and its deletion increases the need for chromatin remodeling enzymes to promote

transcription (Santisteban et al, 2000). H2A.Z stabilizes the nucleosome and facilitates the formation of higher order structures (Park et al, 2004; Hoch et al, 2007; Fan et al, 2002), and is also required for the expression of genes that cluster near the sub-telomeric region where it has been proposed to act as a boundary element to stop the spread of heterochromatin (Meneghini et al. 2003; Raisner and Madhani, 2006). H2AX is similar to canonical H2A and is involved in the repair of DSBs as described above. In yeast there is no histone H2AX variant, but the major form of H2A is phosphorylated in a similar way and fulfils a similar role. (Shroff et al, 2004; Lydall and Whitehall, 2005). The functions of MacroH2A and H2A.Bbd are not fully understood. However, MacroH2A associates with repressive chromatin (Chakravarthy and Luger, 2006), whereas H2A.Bbd seems to be associated with transcriptionally active chromatin in mammals (Chadwich and Willard, 2001).

1.2.2.3 ATP-dependent chromatin remodeling enzymes

ATP-dependent chromatin remodeling complexes (consisting of between 4 and 17 subunits) render DNA more accessible by weakening DNA-histone contacts, sliding nucleosomes along DNA, or removing H2A-H2B dimers from the nucleosome (Becker and Horz, 2002; Flaus and Owen-Hughes, 2004; Saha et al, 2006). Chromatin remodeling enzymes utilize the energy of ATP hydrolysis to alter the contacts of histones with DNA (van Vugt et al, 2007). ATP-dependent chromatin remodeling enzymes possess a conserved Snf2 helicase domain that is capable of binding and hydrolyzing ATP (Eisen et al, 1995). They can be classified into four main families: Swi/Snf , Iswi, Ino80 and CHD.

SWI/SNF: In addition to the Snf2 helicase domain, The Swi/Snf (mating type switching/sucrose non-fermenting) family proteins possess a bromodomain that binds acetylated histone tails (Marfella et al, 2007; Wang et al, 2007). Drosophila brahma (BRM), mammalian BRG1 (Brahma related gene 1) and yeast SNF2 are examples of proteins that belong to this family. Swi/Snf complexes function in various cellular processes such as DNA replication, repair and transcription (Wang et al, 2007).

Iswi: the Iswi (imitation switch) family proteins possess a SANT (SWI3, ADA2, NCOR, TFIIIB) domain that binds histone tails (Marfella et al, 2007; Wang et al, 2007). The chromatin accessibility complex (CHRAC), nucleosome remodeling factor (NURF) complex and ATP-utilizing chromatin assembly and remodeling factor complex (ACF) are examples of the Iswi family (Tsukiyama(a) et al, 1995; Tsukiyama(b) et al, 1995; Varga-Weisz et al, 1997; Ito et al, 1997).

INO80: The Ino80 complex is reported to facilitate exonucleolytic resection, promote Ku70/80 recruitment and displace nucleosomes during a successful strand invasion event.

It also contributes to the cell-cycle checkpoint response. SRCAP (SNF2-related CREB-activator protein) and p400 are examples of Ino80 (inositol requiring 80) family proteins in mammals.
CHD: Like all ATP-dependent remodeling enzymes, CHD (Chromodomain helicase DNA binding) family proteins possess a conserved Snf2 helicase domain, and also a chromodomain that binds methylated lysines in the N-terminal tail of histone H3.

1.2.2.4 Histone chaperone

Histone chaperones deliver histones to the DNA during chromatin assembly, as well as remove histones from the DNA to facilitate chromatin disassembly, through binding to the positively charged histones and shielding their charge from the highly negatively charged DNA (Tyler et al, 2002). In budding yeast, several histone chaperones have been identified (Eitoku et al, 2008). Histone chaperones that bind preferentially to histones H3/H4 include Asf1, CAF-1 (chromatin assembly factor 1), HIR (histone regulator), Spt6 and Rtt106 (Emili et al, 2001; English et al, 2005; English et al, 2006; Green et al, 2005; Verreau et al, 1996; Tagami et al, 2004; Bortvin and Winston, 1996; Huang et al, 2005). Furthermore, FACT (facilitates chromatin transcription) (Orphanides et al, 1999), Nap1 and Vps75 can associate with all four core histones (Park et al, 2008; Andrew et al, 2008; Selth et al, 2009).

1.3 Asf1

CIA/Asf1 (cell cycle gene 1 (CCG1)-interacting factor A or antisilencing function 1) was first identified in a genetic screen based on its ability to disrupt transcriptional silencing in budding yeast when overexpressed (Le et al, 1997). Later, it was shown that Asf1 was a histone chaperone involved in both replication-coupled and replication-independent nucleosome assembly (Green et al, 2005; Tagami et al, 2004; Tyler et al, 1999). Asf1 is a highly conserved histone chaperone among eukaryotes that assembles and disassembles chromatin during transcription, replication and repair (Le et al, 1997; Tyler et al, 1999; Munakata et al, 2000; English et al, 2006). Although Asf1 is not required for viability in *S.cerevisiae*, it is essential in *S. pombe, Drosophila*, chicken and humans (Umehara et al, 2002; Moshkin et al, 2002; Sanematsu et al, 2006; Groth et al, 2005). In mammals, there are two forms of Asf1, Asf1a and Asf1b, which appear to have common functions, as both proteins are present in the complexes co-purified with H3.1. However, they appear to have distinct functions in a replication-independent assembly pathway, since Asf1a interacts with HIRA, but Asf1b does not (Tagami et al, 2004).

Asf1 has a wide variety of functions in transcription, DNA replication and DNA repair (De Koning et al, 2007; Eitoku et al, 2008; Park and Luger, 2008; Sharp et al, 2001; Chimura et al, 2002; Adkins (a) et al, 2004; Korber et al, 2004; Schwabish et al, 2006; Williams et al, 2008; Le et al, 1997; Tyler et al, 1999; Tagami et al, 2004; Das et al, 2009; Emili et al, 2001; Hu et al, 2001). Yeast deleted for *ASF1* exhibit spontaneous DNA damage, display increased frequencies of genome rearrangements (Myung et al, 2003; Prado et al, 2004), and are sensitive to a number of genotoxic agents that damage DNA during replication (Tyler et al, 1999; Linger et al, 2005). This is physiologically significant because chromosome rearrangements are an important source of tumourigenic mutations and often arise through replication-linked DNA damage.

1.3.1 Structure of Asf1

The N-terminal domain containing 155 residues is the highly-conserved core region of Asf1. In contrast, the C-terminal tail is variable, unstructured and flexible (Daganzo et al, 2003; Mousson et al, 2005). In *S.cerevisiae* and *S.pombe*, the Asf1 C-terminal sequence is extremely rich in asparatates and glutamates and this type of tail is common in histone chaperones. In vertebrates, the Asf1 C-terminal sequences are not as rich in acidic residues, but they are phosphorylated by Tousled-like kinases. The major Tlks (Tousled-like kinases) phosphorylation sites are located in the C-terminal part of Drosophila and human Asf1 within a (D/E)-N-S-(L/M) consensus motif, and both proteins cooperate in control of chromatin dynamics and cell cycle progression (Carrera et al, 2003; Sillje and Nigg, 2001; Mello et al, 2002). This phosphorylation by Tlk is inhibited by ATM/ATR/Chk1 kinases in response to DNA damage (Silje and Nigg, 2001; Groth et al, 2003). The loss of Tlk activity or mutation of phosphorylation sites for Asf1 results in degradation of Asf1 by both proteasome-dependent and independent pathways (Pilyugin et al, 2009).

The N-terminal domain of Asf1 consists of three helical linkers on top of a compact immunoglobulin-like β-sandwich fold. This domain is sufficient for all currently known functions of the full-length protein (Daganzo et al, 2003). Asf1 has a large electro-negative surface potential surrounding one side, and a highly conserved hydrophobic groove that interacts with histone proteins (Daganzo et al, 2003; Mousson et al, 2005).

The 3D structure of the functional N-terminal domain of budding yeast was determined by X-ray crystallography (Figure 3a)(Daganzo et al, 2003). Florence Mousson and Françoise Ochsenbein determined the structure of the human Asf1a N-terminal domain by nuclear magnetic resonance spectroscopy (NMR) (Mousson et al, 2005). The structures of yeast and human Asf1 N-terminal domains are quite similar. Recently, the YEATS domain of yeast Yaf9 was shown to have a highly similar structure to Asf1. Yaf9 is a subunit of both

the NuA4 histone H4 acetyltransferase complex and the SWR1 remodeling complex (Wang et al, 2009). The authors suggested that Yaf9 may have a similar histone-binding capacity as Asf1.

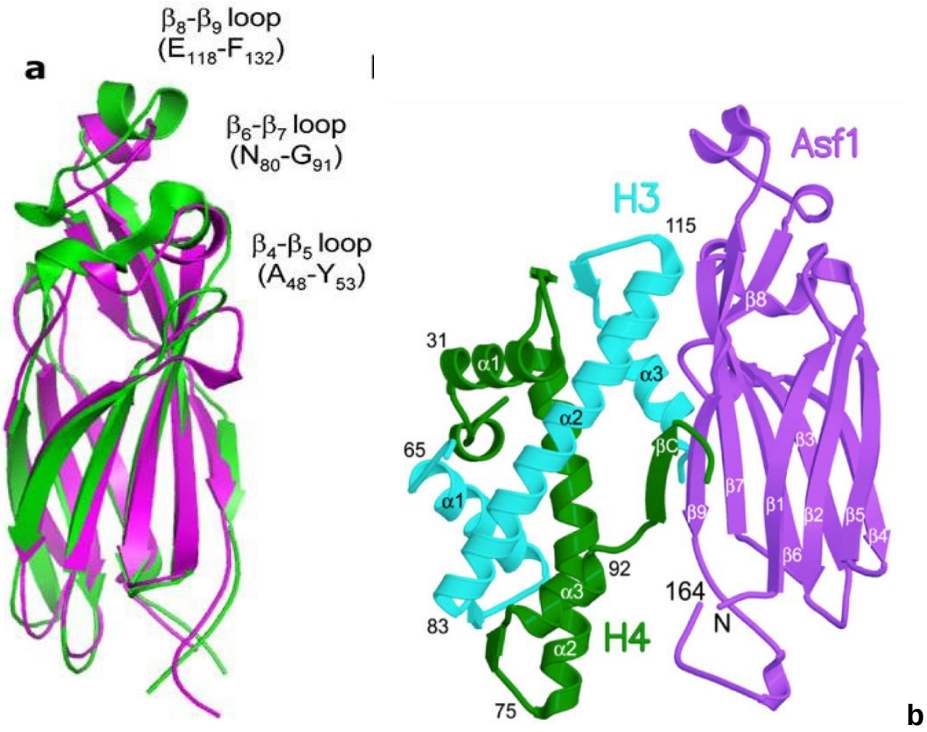

Figure 3. (a) Structure of the Asf1 N-terminal domain is well conserved. The superposition between hAsf1a (1-156) (purple) and *S.cerevisiae* Asf1(green) (Mousson et al, 2005; Daganzo et al, 2003).
(b) Ribbon diagram model of the Asf1p N-terminal domain bound to heterodimer histone H3 (cyano) and H4 (green) (English et al, 2006).

Structure of the Asf1-H3/H4 complex

This structure shows that Asf1 binds to a histone H3/H4 heterodimer (Fig 3b) (English et al, 2006; Natsume et al, 2007). The hydrophobic groove of Asf1 binds the histone H3-H4 heterodimer by enveloping the C-terminus helix of histone H3, thereby blocking the formation of a $(H3\text{-}H4)_2$ heterotetramer. Furthermore, the C-terminus of histone H4, that forms a mini-β sheet with histone H2A in the nucleosome, undergoes a major conformational change upon binding to Asf1 and adds a β strand to the Asf1 β sheet sandwich (English et al, 2006; Natsume et al, 2007). Additionally, the non-conserved acidic C-terminal tail of yeast Asf1 may strengthen the interaction between Asf1 and H3/H4 (English et al, 2006; Daganzo et al, 2003).

1.3.2 Asf1 at the crossroads of chromatin and DNA checkpoint pathways

Chromatin assembly occurs in a stepwise manner: a tetramer of histones H3/H4 is deposited first followed by two dimers of H2A/H2B on the outside of the tetramer (Verreault et al, 1996). Asf1 interacts with both CAF-1 and HIR and hands off histones to CAF-1 and HIRA facilitating replication-dependent and replication-independent chromatin assembly respectively (Krawitz et al, 2002; Nakatani et al, 2004; Green et al, 2005, Mousson et al, 2007).

1.3.2.1 Role for Asf1 in chromatin assembly/disassembly

Replication-dependent chromatin assembly/disassembly

The association of DNA with the histones in the nucleosome makes it difficult to access the DNA by protein molecules. The nucleosome is disassembled into two H2A-H2B dimers and a $(H3\text{-}H4)_2$ tetramer ahead of the moving fork during DNA replication, transcription and repair. Then the parental histones are relocated behind the replication fork and the full nucleosome density is completed by the deposition of newly synthesized histones. (Tagami et al, 2004; Falbo and Shen, 2006; Groth et al, 2007). In *S.cerevisiae*, passage through S phase in the absence of core histone synthesis results in a loss of viability that cannot be rescued by re-expression of histones in G2 (Kim et al, 1988).

The H2A-H2B chaperone FACT has been shown to be associated with the MCM (Minichromosome maintenance) helicase that unwinds DNA in front of the replication fork (Tan et al, 2006). Asf1 is also associated with the MCM helicase, suggesting that Asf1 plays a role in disrupting parental nucleosomes and potentially transfering them onto the nascent DNA behind the fork (Groth et al, 2007).

Asf1 acts in both chromatin assembly and disassembly (Adkins et al, 2004a,b; Adkins et al, 2007; Korber et al, 2006). Yeast Asf1 and both human isoforms Asf1a and Asf1b can interact with CAF-1 p60, promoting replication-dependent chromatin assembly synergistically with CAF-1 (Figure 5c) (Verreault, 2000; Sharp et al, 2001; Krawitz et al, 2002; Mello et al, 2002; Loyola and Almouzni, 2004). This pathway ensures that histones are promptly assembled onto newly replicated DNA to minimize the potential for DNA damage, as well as being important for inheritance of epigenetic information during DNA replication and repair (Ye et al, 2003; Groth et al, 2007; Henikoff et al, 2004). CAF-1 associates with the replication forks through an interaction with proliferating cell nuclear antigen (PCNA), a component essential for DNA replication and DNA repair (Shibahara and Stillman, 1999; Zhang et al, 2000; Moggs et al, 2000).

CAF-1 is essential in humans, as depletion of p60 CAF-1 triggers apoptosis in proliferating cells (Nabatiyan and Krude, 2004). In contrast to human cells, Asf1 and CAF-1 are not essential for cell viability in *S.cerevisiae*, probably because of the existence of other chaperones for histone H3-H4, such as Rtt106 (Huang et al, 2005). Besides Asf1, CAF-1 has been shown to mediate histone deposition onto DNA assisted by Rtt106 that binds to CAF-1 as well (Huang et al, 2005; Tyler et al, 2001). Although CAF-I is not essential in S. cerevisiae, its inactivation results in increased sensitivity to UV radiation and reduced silencing of genes adjacent to telomeric DNA (Kaufman et al, 1997).

CAF-1 is an evolutionarily conserved complex. In both yeast and human cells, CAF-1 consists of three subunits: Cac1, Cac2 and Cac3 in yeast ; p150, p60 and p48 in human cells; and p180, p105, p75 and p55 in Drosophila. The smallest subunit p55 binds the N-terminal part of histone H4 via a β-propeller structure (Smith and Stillman 1989; Kaufman et al, 1995; Kaufman et al, 1997; Song et al, 2008).

Asf1N binds a B domain motif found in both the p60 subunit of CAF-1 and HirA (Mello et al, 2002; Sanematsu et al, 2006; Tyler et al, 2001) (Figure 5b). CAF-I and HirA thus compete for binding to the same surface of Asf1N that is distinct from the surface of Asf1N that binds H3/H4 (Malay et al, 2008).

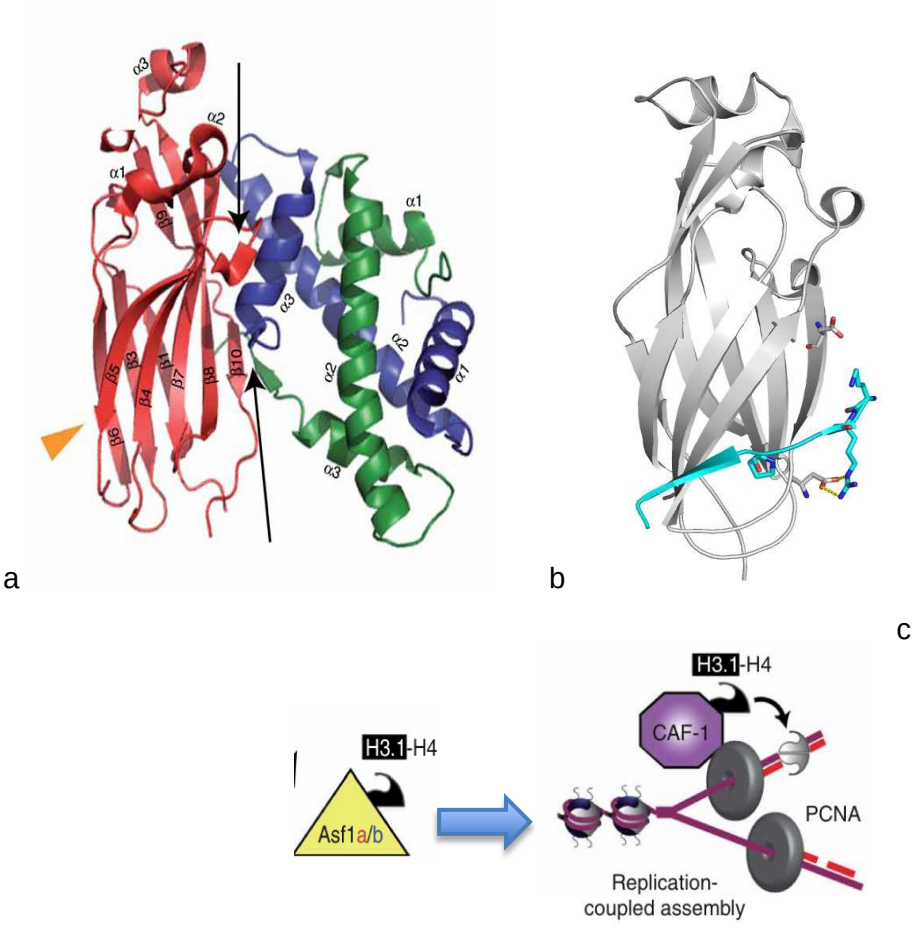

a b c

Figure 4. A view of H3.1-H4 deposition by CAF-1. (a) The structure of Asf1-H3/H4 complex shows two binding sites for human ASFa on the histone dimer. Orange triangle indicates CAF-1-binding site. (b) Interaction of yeast Asf1 (SpAsf1) with a peptide from the p60 subunit of CAF-1, spCac2 (Malay et al, 2008). (c) Both Asf1a and Asf1b act as histone donors for CAF-1, promoting H3.1 deposition (De Koning et al, 2007).

Replication-independent chromatin assembly

Outside the S phase, histones can be deposited onto DNA by HIRA (HIR complex in *S. cerevisiae*) via a replication-independent pathway (Henikoff and Ahmad, 2005). The interaction between Asf1 and Hir was initially found in budding yeast and Asf1 can copurify with all four subunits of HIR (Hir1, Hir2, Hir3 and Hpc2). This interaction is necessary for telomeric silencing (Sharp et al, 2001; Daganzo et al, 2003; Green et al, 2005). Similarly, Asf1 forms complexes with histones H3 and H4 as well as HIRA in humans (Figure 4c). HIRA preferentially deposits the histone replacement variant H3.3 in nucleosomes (Loppin et al, 2005; Nakayama et al, 2007; Tagami et al, 2004; Van der Heijden et al, 2007). Since H3.3 is predominantly incorporated into actively transcribed genes (Mito et al, 2005; Schwartz et al, 2005; Wirbelauer et al, 2005), the HIRA/ASF1a complex is thought to mediate transcription-coupled deposition of histone H3.3 (Henikoff et al, 2008; Nourani et al, 2006; Prather et al, 2005; Ray-Gallet et al, 2002; Tagami et al, 2004). The overexpression of HIRA can also inhibit histone expression and lead to an S-phase arrest (Nelson et al, 2002).

The human Asf1 N-terminal domain has been shown to interact with the B-domain of HIRA (Daganzo et al, 2003; Zhang et al, 2005) in the form of an antiparallel β-hairpin (Tang et al, 2006) (Figure 4b). The evolutionarily conserved B-domain of HIRA (425-472) is located in the central portion of the protein. This surface is located on the opposite side of the H3 binding site of Asf1 (Tang et al, 2006). The ASF1 D37R+E39R double mutant disrupts the ASF1a-HIRA interaction, but does not affect the ASF1a-H3 complex (Daganzo et al, 2003; Tang et al, 2006; Mousson et al, 2005).

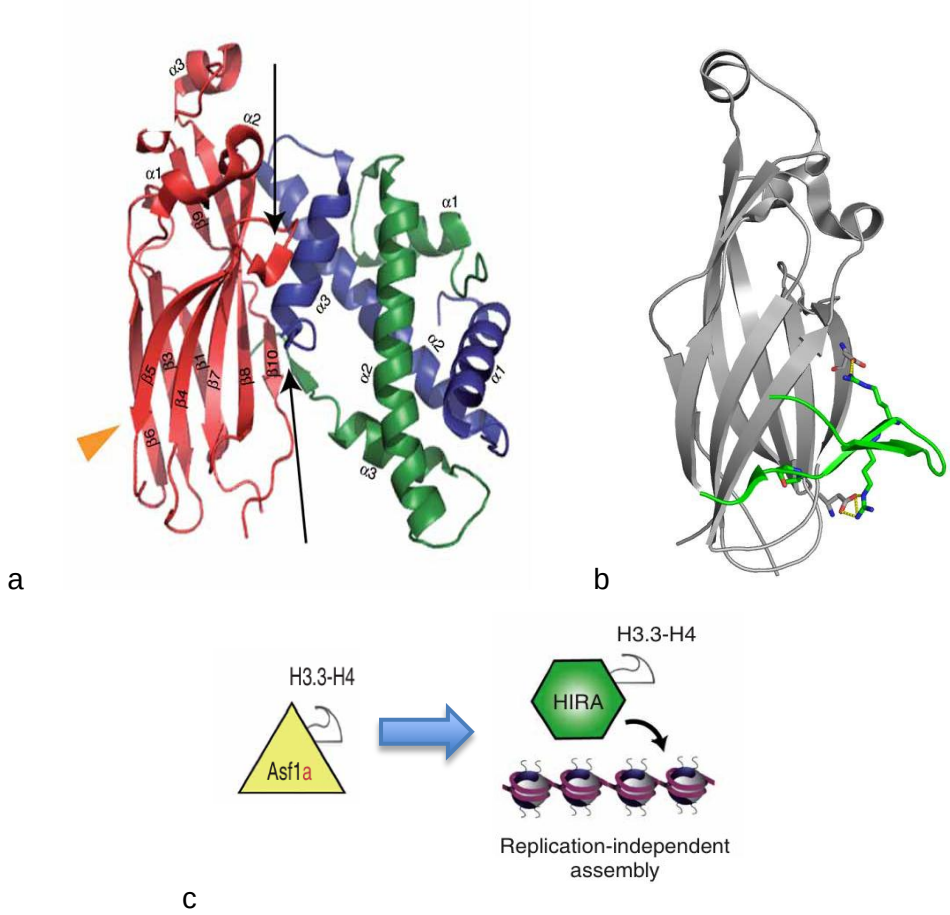

Figure 5. A view of H3.3-H4 deposition by HIRA. (a) The structure of Asf1-H3/H4 complex shows two binding sites for human ASFa on the histone dimer. Orange triangle indicates HIRA-binding site. (b) hAsf1a-HIRA Ribbon diagram of a HIRA B domain peptide (green) bound to hAsf1a N-terminal domain (gray) (Tang et al, 2006). (c) Asf1a cooperate with HIRA to deposit H3.3.

1.3.2.2 Asf1 and DNA damage checkpoint pathway

Asf1 promotes genomic stability and protects against DNA damage and replication stress (Mousson et al, 2007). Asf1 participates in the regulation of the DNA damage checkpoint pathway by interacting with the central checkpoint kinase Rad53. Additionally, Asf1 is required for histone H3K56 acetylation during DNA repair.

Asf1 and Rad53

Asf1 is important for genomic stability, since cells lacking Asf1 are sensitive to agents that cause DNA damage or replication stress, such as methyl methane sulfonate (MMS), hydroxyurea (HU), camptothecin (CPT), bleomycin and cisplatin (Emili et al, 2001; Hu et al,

2001; Mousson et al, 2005; Ramey et al, 2004; Tamburini et al, 2005). HU treatment inhibits the ribonucleotide reductase (RNR) and leads to depletion of dNTPs and stalling of DNA replication (Elledge et al, 1992; Slater et al, 1973). MMS methylates DNA bases and can indirectly lead to the presence of abasic sites as well as single- and double-strand breaks in DNA. CPT is an interfacial inhibitor of DNA topoisomerase I that stabilizes the covalent complex formed by DNA topoisomerase I when it relaxes DNA by cleaving one DNA strand. DSBs are formed when the replication machinery collides with the CPT-stabilized complex of DNA topoisomerase I bound to the DNA (Pommier et al, 2003).

Yeast Asf1 forms a complex with Rad53 in the absence of genotoxic stress. A part of the Rad53-Asf1 interaction is mediated by the FHA1 domain of Rad53 binding to a phsophorylated form of Asf1 (Schwartz et al, 2003). The Asf1-Rad53 complex was reportedly dissociated when yeast cells were subjected to genotoxic stress in a Mec1-dependent manner (Emilie et al, 2001; Hu et al, 2001). It was suggested that the phosphorylation sites of Rad53 induced by DNA damage could inhibit the Asf1-Rad53 interaction. These observations suggested that activation of Rad53 and liberation of Asf1 may be an important cellular response to DNA damage acting perhaps at the level of chromatin assembly (Emili et al, 2001; Hu et al, 2001). However, in mammalian cells, Asf1 does not interact with Chk2 (homologue of Rad53), but rather with Tlk kinases that are not conserved in yeast (Shillje and Nigg, 2001). The Tlk kinases phosphorylate C-terminal sequences of Asf1 during S phase, and this phosphorylation is inhibited in response to genotoxic stress. The functional significance of this phosphorylation is poorly understood, although there is some data suggesting that phosphorylation can affect the half-life of Asf1 isoforms.

Asf1 and H3K56Ac

Acetylation of H3K56 is an abundant modification of all newly synthesized H3 in budding yeast, fission yeasts and in *Tetrahymena thermophilus* (Masumoto et al, 2005; Garcia et al, 2007; Xhemalce et al, 2007), but is much less abundant in mammalian cells (Jasencakova et al, 2010). H3K56 is located at the DNA entry/exit point on the nucleosome core (Davey et al, 2002). Although H3K56 acetylation does not appear to greatly alter the overall structure of the nucleosome, acetylation at this residue increases the plasticity of nucleosomes, which may facilitate access of necessary protein factors to the DNA (Neumann et al, 2009; Watanabe et al, 2010).

H3K56Ac is involved in the response to DNA damage during replication (Collins et al, 2007; Driscoll et al, 2007; Han et al, 2007a,b,c; Masumoto et al, 2005; Tsubota et al, 2007). In yeast, H3K56ac peaks during S phase where it plays a role in the DNA damage response

and is largely deacetylated by the Sir2-related HDACs Hst3 and Hst4 during the G2/M phase of the cell cycle (Masumoto et al, 2005; Han et al, 2007a,b,c; Chen et al, 2008; Zhou et al, 2006; Celic et al, 2006; Maas et al, 2006).

H3K56 acetylation is catalyzed by Rtt109 (also known as KAT11) in *S.cerevisiae* and *Schizosaccharomyces pombe* (Xhemalce et al, 2007; Schneider et al, 2006; Tsubota et al, 2007; Han et al, 2007a,b,c; Driscoll et al, 2007; Allis et al, 2007), and by CBP/p300 and/or Gcn5 in mammalian cells (Das et al, 2009; Tjeertes et al, 2009). In addition to sensitivity to genotoxic stress, cells lacking the H3K56 acetyltransferase Rtt109 or cells expressing H3 with K56 mutated to arginine (H3K56R) exhibit an increased frequency of spontaneous chromosome breaks (Allis et al, 2007; Driscoll et al, 2007; Han et al, 2007a,b,c). Rtt109 harbors very low acetyltransferase activity on its own (Driscoll et al, 2007; Tsubota et al, 2007), but its activity is strongly stimulated by either Asf1 or Vps75 (Albaugh et al, 2010; Berndsen et al, 2008; Han et al, 2007c; Collins et al, 2007). Asf1 physically interacts with Rtt109 and is absolutely required for H3K56 acetylation. Vps75 also interacts with Rtt109 to promote H3K56ac. However, the accumulation of H3K56ac *in vivo* is dependent on Rtt109 and Asf1, but not Vps75. The ***asf1Δ*** or ***rtt109Δ*** mutants lack H3K56 acetylation, but no decrease was observed in cells lacking Vps75 (Tsubota et al, 2007; Schneider et al, 2006; Recht et al, 2006; Selth and Svejstrup, 2007).

H3K56 acetylation is required for S-phase chromatin assembly and was proposed to be a critical signal for turning off the DNA damage checkpoint following DNA repair followed (Chen et al, 2008), although this latter claim is controversial (Kim and Haber, 2009). H3K56 acetylation can increase the binding affinity between H3-H4 with CAF-1 and Rtt106 to promote efficient deposition of H3-H4 onto replicating DNA by these two histone chaperones (Li et al, 2008).

H3K56Ac is also involved in DSB repair. The mutations affecting H3K56Ac lead to increased sensitivity to agents that cause DSBs. The persistence of K56 acetylation when DSBs are present is due to the presence of DNA damage checkpoint proteins, and may be important for replication fork progression in the presence of DNA damage. (Chen et al, 2008).

Asf1 is thought to maintain the integrity of the replisome through H3K56 acetylation. Asf1 has been shown to directly interact with origins of replications and can also associate with components of the replisome (Groth et al, 2007; Han et al, 2007c). Indeed, in absence of Asf1 or H3K56 acetylation, components of the replisome are lost upon HU treatment (Franco et al, 2005; Han et al, 2007c). It appears that Asf1 and H3K56 acetylation promote the stability of stalled replications forks, contributing to cellular survival upon replication stress.

1.3.2.3 Transcriptional regulation by Asf1

In yeast, Asf1 facilitates chromatin disassembly at the *PHO5* promoter to promote transcriptional activation, suggesting that it acts as a histone acceptor (Adkins and Tyler, 2004). Asf1 travels with the transcription machinery and/or rapidly fills in gaps left in nucleosome arrays following passage of RNA polymerase (Schwabish et al, 2006). The nature of Asf1 as an interactor with the TFIID subunit Bdf1 also suggests its participation in transcription control at various RNA polymerase II-dependent gene loci (Chimura et al, 2002; Zabaronick and Tyler, 2005). Asf1 is also involved in developmental gene expression control by mediating transcriptional repression of NOTCH target genes in Drosophila (Goodfellow et al, 2007).

In yeast, the loss of Asf1 results in impaired cell proliferation and minor defects of gene silencing at telomere and silent mating loci *HMR* and *HML*. These effects are greatly enhanced by inactivation of CAF-1, but not Hir (Tyler et al, 1999; Sharp et al, 2001; Krawitz et al, 2002). Asf1 and Hir participate together in a pathway for telomeric silencing that is independent of a pathway dependent on CAF-I (Daganzo et al, 2003).

In addition, Asf1 was found to mediate histone H3 eviction and deposition during transcriptional elongation. Furthermore, Asf1 has been implicated in transcription-dependent, replication-independent histone H3 exchange at promoters, another process which can deposit K56-acetylated H3.

1.3.2.4 Asf1 and histone modification

Asf1 can affect the PTM state of histones. In addition to its role in promoting H3-K56-acetylation described above, Asf1 also contributes to the acetylation of H3K9 and can promote trimethylation of H3K36 by Set2 in yeast (Adkins et al, 2007b; Lin et al, 2010). In human U2OS cells, histones bound to Asf1 showed two typical chromatin marks: H4K16Ac and H3K9Me3, giving rise to the hypothesis that Asf1 handles both new and parental histones during DNA replication (Groth et al, 2007).

1.4. DNA damage Checkpoints

Checkpoints were defined as molecular signaling cascades that trigger cell-cycle delay or arrest in response to DNA damage, providing sufficient time for repair from the damage (Hartwell et al. 1989). The DNA damage checkpoints control all the cell cycle phases in response to DNA damage. This damage results from the effect of exogenous mutagens, such as UV light, ionizing irradiation or chemical compounds, as well as spontaneous

damage that can arise from endogenous reactive oxygen species, or due to difficultes encountered during genomic DNA replication. If not repaired by continuously active repair pathways, DNA damage will lead to base mutations or single and double-strand chain breaks (Sancar et al, 2004). The DNA damage checkpoint cascades are evolutionarily conserved in eukaryotic organisms (Paulovich and Hartwell, 1995; Zhou and Elledge, 2000).

1.4.1 DNA damage checkpoint proteins and checkpoint pathway

	Budding yeast	Fission yeast	Human
PIKK	Mec1	Rad3	ATR
PIKK	Tel1	Tel1	ATM
Adaptor	Rad9	Crb2	53BP1, MDC1, BRCA1?
Rfc1 homolog	Rad24	Rad17	Rad17
9-1-1 clamp	Rad17	Rad9	Rad9
	Mec3	Hus1	Hus1
	Ddc1	Rad1	Rad1
MRX complex	Mre11	Mre11	Mre11
	Rad50	Rad50	Rad50
	Xrs2	Nbs1	Nbs1
BRCT domain adaptor?	Dpb11	Rad4/Cut5	TopBP1
Signaling kinase	Rad53	Cds1	Chk2
Signaling kinase	Chk1	Chk1	Chk1
Polo kinase	Cdc5	Plo1	Plk1
Securin	Pds1	Cut2	Securin
Separase	Esp1	Cut1	Separase
APC-targeting subunit	Cdc20	Slp1	$p55^{CDC}$/CDC20

Table 1. The proteins involved in the DNA-damage checkpoints and their orthologues (Harrison et al, 2006).

Checkpoint signaling consists of damage sensors, transducers and effectors (Ellege 1996). The sensors recognize the damaged DNA and initiate the signaling response. Transducers can be activated by the DNA damage signal passed from the sensors, then amplify the damage signal by phosphorylating downstream effectors. Finally, the effectors excute the regulation of different cellular processes.

DNA checkpoint pathways are conserved in eukaryotes and require a family of serine/threonine protein kinases which show strong similarity to the lipid kinase phosphatidyl-inositol-3-kinase (PI3K). Mec1 and Tel1 in budding yeast and their homologues Ataxia-Telangectasia Mutated (ATM), Ataxia-Telangectasia Related (ATR) and DNA-PK in humans are members of this family (Harrison and Haber, 2006). Other downstream kinases are also conserved and consist of Chk1 and Rad53 in budding yeast, Chk1 & Chk2 in vertebrates, Chk1 & Cds1 in fission yeast (Harrison, 2006).

In the presence of exogenous DNA-damaging agents or replication inhibitors, the exposure

of ssDNA at DSBs or at stalled replication forks is essential for activation of the DNA damage checkpoint. Single-strand DNA may be generated at stalled forks by the continued unwinding of DNA by MCM helicases ahead of the stalled replication fork (Sogo et al. 2002; Byun et al. 2005; Nedelcheva et al. 2005). The ssDNA is subsequently bound by RPA. The RPA-coated ssDNA, a structure commonly found after replicative stress or as a DNA repair intermediate, is critical for Mec1-Ddc2 recruitment. (Rouse and Jackson 2002; Zou and Elledge, 2003; Harrison and Harber, 2006; Branzei and Foiani, 2008).

Activation of PIKK family members also depends on other DNA damage sensors, such as the PCNA-like Ddc1-Mec3-Rad17 complex and the Rad24-Rfc2-5 alternative replication (RFC) complex. The budding yeast Ddc1-Mec3-Rad17 complex is a PCNA-like checkpoint clamp (orthologous to the human 9-1-1 complex) that was shown to be loaded onto the single- and double-stranded DNA junction of stalled replication forks by the clamp loader Rad24-RFC complex (Kondo et al, 2001; Melo et al, 2001; Majka et al. 2003). The Ddc1-Mec3-Rad17 complex stimulates the kinase activity of Mec1 (Majka et al, 2006), and Mec1 phosphorylates the Rad24 subunit of the clamp loader and the Ddc1 and Mec3 subunits of the clamp. Interestingly, it was shown that the co-localization of the Ddc1-Mec3-Rad17 complex and Mec1-Ddc2, is sufficient to activate Mec1 even without induced DNA damage (Bonilla et al, 2008).

Mec1 is an essential phosphatidylinositol 3-kinase-like kinase (PIKK) that associates with the DNA binding protein Ddc2 to form a checkpoint sensor complex (Paciotti et al, 2000). The phosphorylation of RPA may be required for later steps in the checkpoint cascade through interaction with other checkpoint proteins, or maybe required for the dissociation from DNA (Bartrand et al, 2004; Harrison and Haber, 2006). After binding to ssDNA, Mec1 functions in activating the checkpoint signal cascade via phosphorylation of the tranducer proteins Rad9 and Mrc1, and subsequent phosphorylation of the essential checkpoint effector kinase Rad53 (Branzei and Foiani, 2006). Rad53 is hyperphosphorylated and activated in response to DNA damage or DNA replication stress (Sun et al. 1996; Sanchez et al. 1996). Rad53 mutants are hypersensitive to genotoxic stress (Allen et al. 1994; Sun et al. 1996; Pellicioli et al. 1999). Activated Rad53 is critical for cellular processes through its downstream targets.

Another pathway involves the PIKK kinase Tel1 (ATM). Compared to Mec1 (ATR), Tel1 plays a minor role in response to DSBs in yeast. Deletion of *TEL1* results in telomere shortening (Smogorzewska and de Lange, 2004), but does not show obvious checkpoint signalling defects or increased sensitivity towards DNA damage agents (Morrow et al, 1995). Instead of using Ddc2, Tel1 binds to DNA through its association with the MRX complex (Mre11-Rad50-Xrs2). In the presense of DSBs, Tel1 can activate the DNA

damage checkpoint pathway when Mec1 is absent (Nakada et al, 2003). Tel1 can respond to DSBs in a Mec1-dependent and –independent manner. In the Mec1 dependent manner, Tel1 is considered to contribute to DNA resection and produce ssDNA by activating an exonuclease that may correspond to MRX (Mantiero et al, 2007).

In contrast to budding yeast, both ATM and ATR have important functions in the checkpoint response in mammalian cells and are thought to be activated by different kinds of DNA damage. ATM is specially involved in the reponse to unprocessed DSBs, whereas ATR apprears to be activated by processed DSB ends, replicative stress and intermediates of DNA repair pathway (Jazayeri et al, 2006; Longhese et al, 2006).

Chk1 primarily contributes to the cell cycle arrest response to DNA damage in budding yeast, while Rad53 is more widely responsible response to DNA damage and replication stress. Chk1 has a major role in metazoan checkpoints, but a minor role in budding yeast.

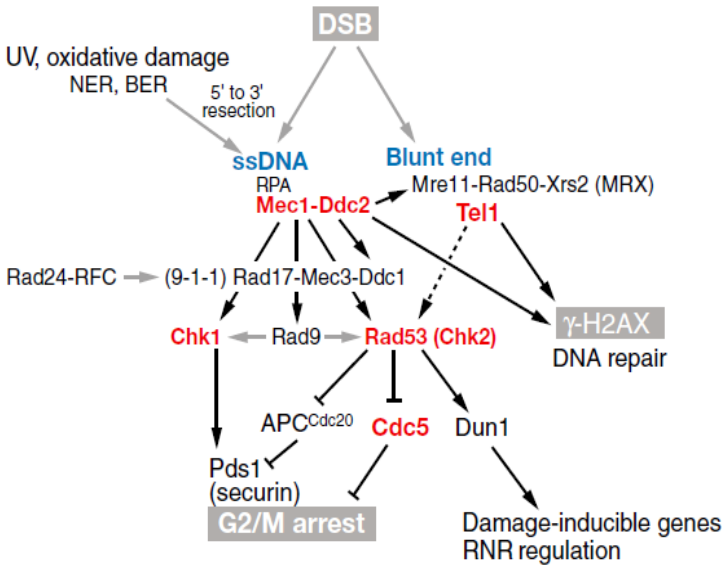

Figure 6. DNA damage checkpoint pathways in *S.cerevisiae* (Harrison et al. 2006). Black arrows indicate protein kinase phosphorylations of several target proteins that activate downstream events, whereas a black line terminated in a bar indicates an inhibitory modifications. Grey arrows indicate protein interactions that facilitate checkpoint activation.

1.4.2 Downstream targets

The DNA checkpoint pathways are involved in cell cycle progression, DNA repair, DNA replication fork stabilization, DNA replication origin firing, chromatin remodeling, transcription of DNA damage response genes, and induced apoptosis and senescence (Zhou et al. 2000; Shiloh Y 2003; Abraham RT 2001; Bartek and Lukas, 2001; Santocanale

and Diffley 1998; Shirahige et al. 1998; Foiani et al. 2000; Nyberg et al. 2002; Tercero et al. 2003).

1.4.2.1 Cell cycle arrest

In response to DNA damage, checkpoints delay or arrest the cell cycle to provide sufficient time for repair. The phase of the cell cycle where the damage occurs determines the specific response. DNA damage checkpoints include G1/S checkpoints that delay or block cells before entry into S phase and S-phase and G2/M checkpoints that delay or block cells before the entry into mitosis (G2 in most organisms, but pre-anaphase in budding yeast). The G1/S checkpoint recognizes DNA damage during G1 phase and inhibits entry into S phase. The S-phase checkpoint/replication checkpoint, which is activated by DNA damage or impeded replication forks during S-phase, is crucial for stabilizing stalled replication forks and regulating late origin firing. The G2/M checkpoint prevents cells from initiating mitosis in the presence of damage to ensure that damaged chromosomes do not undergo chromosomal segregation during mitosis (Nyberg et al, 2002).
Pds1, a yeast securin, is required for normal cell cycle arrest in response to DNA damage (Cohen-Fix et al, 1997; Yamamoto et al, 1996). After DNA damage, Pds1 is hyperphosphorylated in a Mec-1, Rad9-, Chk1-dependent, but Rad53-independent manner (Cohen-Fix et al, 1997). At the entry into mitosis, this checkpoint-dependent phosphorylation prevents its degradation by ubiquitination by Cdc20/ APC (Anaphase Promoting Complex) (Agarwal et al, 2003; Sanchez et al, 1999). However, Rad53 inhibits mitotic exit. Rad53 is required to maintain CDK activity during the checkpoint arrest likely through inhibition of Cdc5 (Cheng et al, 1998; Sanchez et al, 1999). Cdc5 inhibits the Bub2/Bfa1 complex which in turn inhibits the mitotic exit network (MEN) (Geymonat et al, 2003; Hu et al, 2002; de Bettignies and Johnston, 2003). Rad53-dependent inhibition of Cdc5 could therefore inhibit progression through mitosis and help maintain the checkpoint arrest.

1.4.2.2 Transcriptional response and regulation of RNR

Dun1, a kinase downstream of Mec1/Rad53, was originally identified as a mutant deficient in the transcriptional induction of genes after DNA damage (Zhou and Elledge, 1993). Dun1 is recruited to activated Rad53 through the Dun1 FHA domain (Bashkirov et al, 2003), and then activated by Rad53 dependent phosphorylation of the Dun1 activation loop (Chen et al, 2007). Dun1 inhibits the transcriptional repressor Crt1 by phophorylation to prevent Crt1 binding to DNA, resulting in the up-regulation of several genes involved in DNA repair or

dNTP biosynthesis, including the *RNR3* gene encoding a large subunit of the ribonucleotide reductase and the *HUG1* gene encoding a small protein of unknown function (Elledge et al, 1992; Basrai et al,1999). DNA damage induced activation of Dun1 increases RNR activity by derepressing *RNR* gene transcription and by targeting by phosphorylation the RNR inhibitor Sml1 for proteolytic degradation (Zhao and Rothstein, 2002). Dun1 thus controls both the abundance and the activity of ribonucleotide reductase. The lethality of both *MEC1* and *RAD53* deletion can be suppressed either by deletion of *SML1* or by overexpression of *RNR* large subunit genes (Zhao et al, 1998; Desany et al, 1998). These results indicate that Mec1 and Rad53 are important for increasing the synthesis of dNTPs. Additionally, Rad53 phosphorylates Swi6 that is a subunit of transcription factor SBF/MBF (Sidorova et al. 1997). This phosphorylation is thought to contribute to the delay in G1 after DNA damage.

1.4.2.3 Histone modification

As highlighted above, the rapid phosphorylation of serine 129 on histone H2A (γH2AX) is induced by DNA damage in a Mec1 and Tel1-dependent manner. γH2A is important for amplifying the checkpoint response in mammalian cells via recruitment of the checkpoint mediator Mdc1 (Su, 2006) and maintaining high checkpoint activity in yeast (Keogh et al, 2006). γH2A is also required for the recruitment of both the INO80 and SWR1 ATP-dependent chromatin remodeling complexes, as well as cohesins to DSBs. Mec1/Tel1 also phosphorylates Ino80.

When cells are exposed to genotoxic stress, Mec1-dependent downregulation of the Hst3 and Hst4 deacetylases lengthens the persistence of H3K56ac in chromatin (Maas et al, 2006, Thaminy et al, 2007, Masumoto et al, 2005). In addition, Rad9 binds H3K79-me3 in budding yeast. Removal of Rad9 from methylated histone leads to increased resection activity and partially bypasses the requirement for CDK activation of DSB processing (Lazzaro et al, 2008).

1.4.2.4 Activation of DNA repair

Different kinds of lesions require different repair pathways. The checkpoint pathway facilitates and induces DNA repair mechanisms (Harrison and Haber, 2006; Nyberg et al, 2002). So far, the data are not sufficient to define specific mechanisms. However, the activities of at least some DNA repair proteins are modified after DNA damage in *S.cerevisiae*. Several DNA damage checkpoint proteins contain tandem BRCT (BRCA1 carboxyl terminus) domains, a known phosphopeptide binding motif that is common among checkpoint and repair proteins (Glover et al, 2004). These proteins, such as BRCA1 and

BRCA2 in mammalian cells, are involved in DSB repair, and deficiencies in these proteins result in increased genomic instability (Hoeijmakers, 2001).

DSBs are potentially lethal lesions because segregation of chromosomes in the presence of un-repaired DSBs can result in the loss of large amounts of genetic information. DSBs can be induced by endogenous free oxygen radicals, collapsed replication forks, or by the physical force generated when dicentric or catenated chromosomes are pulled to opposite poles during mitosis (Acilan et al, 2007). DSBs are also produced exogenously when cells are exposed to DNA damaging agents, such as ionizing radiation (IR), chemical agents such as chemotherapeutics that poison topoisomerase I or topoisomerase II (Degrassi et al, 2004), or UV light that creates pyrimidine dimers and crosslinks (Limoli et al, 2002; Bosco et al, 2004).

DSB repair is carried out by two major pathways: non-homologous end joining (NHEJ) and homologous recombination (HR) (Haber et al, 2000). HR can be further subdivided into gene conversion and single strand annealing (SSA). HR, which occurs mainly during late S-G2 phase, takes advantage of sequence homology from an undamaged sister chromatid or homologous chromosome to repair the lesion with high fidelity. NHEJ, that involves processing and ligation of broken DNA ends, is the major pathway for repairing non-replication-associated breaks and occurs predominantly in the G1 phase of the cell cycle (Daley et al, 2005). The tightly packaged chromatin structure impedes DNA repair and the current DNA repair model on chromatin is: access-repair-restore (Smerdon et al, 1991).

The phosphorylation of various repair factors is dependent on DNA damage checkpoints. In budding yeast, the checkpoint kinases have been shown to phosphorylate and regulate the recombination factors Srs2, Rad55 and Slx4 (Liberi et al, 2000; Bashkirov et al, 2000; Flott et al, 2007). Srs2, a DNA helicase/translocase, influences various steps of the recombination process by removing Rad51 from DNA. It is not known whether checkpoint-dependent Srs2 phosphorylation influences its role in recombination, however, it was proposed that Srs2 might be involved in removing checkpoint proteins from DBSs after repair to resume cell cycle progression (Vaze et al, 2002). The recombination protein Rad55, a Rad51 paralog, is phosphorylated by Mec1 upon DNA damage and this modification may play a role in activating recombinational repair (Bashkirov et al, 2000; Herzberg et al, 2006). Mec1/Tel1-dependent phosphorylation of Slx4 also controls the single-strand annealing (SSA) sub-pathway of DSB repair (Flott et al, 2007). Rtt107 is implicated in Mms2-dependent DNA repair during S phase, and its phosphorylation by Mec1 requires Slx4 (Rouse, 2004; Roberts et al, 2006). Nej1 phosphorylated by Dun1 has been shown to effect NHEJ (Ahnesorg and Jackson, 2007).

In *S.cerevisiae*, a mutation in Rad24 that affects activation of the Mec1-dependent pathway slowed down the kinetics of DSB resection and promoted ectopic recombination with short

homologous donor sequences (Aylon ad Kupiec, 2003). In fission yeast, the phosphorylation of Crb2 (a putative Rad9 ortholog) by CDK1 is important to mediate later steps of HR implicating the RecQ helicase Rqh1 and the Top3 topoisomerase (Caspari et al, 2002).

1.4.2.5 S-phase specific downsteam targets

During DNA replication, a DNA lesion caused by stresses such as UV damage, oxidative damage, genotoxic drugs or growth medium deprivation may slow down or even arrest progression of the replication fork. HU depletes the cellular dNTP pool and causes replication fork stalling. MMS also slows fork progression (Tercero and Diffley, 2001). MMS was found to inhibit replication fork progression independently of checkpoint kinases, but the inhibition of late origin firing is dependent on Mec1 and Rad53 activation.

Role of replication checkpoint in stabilizing stalled replication forks

The replication checkpoint is required to stabilize stalled replication forks to prevent their collapse and promote their restart (Longhese et al, 2003). Fork collapse can often result in DSBs, chromosomal rearragements and genomic instability (Branzei and Foiani, 2005). Cells lacking *MEC1* or *RAD53* are subject to irreversible collapse of stalled replication forks (Tercero et al. 2001). Many replication proteins dissociate from the stalled replication forks in the absence of the replication checkpoints (Blow et al. 2005; Cobb et al. 2003; Lucca et al. 2004). The replication checkpoints may stabilize the stalled replication fork by phosphorylating components of the replication fork, such as RPA, DNA polymerase α, Mcm2-7, Exo1 and Esc4/Rtt107 (Brush et al, 1996; Pellicioli et al, 1999; Cobb et al. 2003; Cobb et al, 2005; Cotta-Ramusino et al, 2005; Segurado and Diffley, 2008; Chin et al, 2006). These phosphorylations may prevent the collapse of arrested forks and the formation of abnormal replication intermediates, including DSBs. However, the targets of Rad53 and Mec1 that are important in preventing replication fork collapse have not yet been identified. MMS also slows fork progression as mentioned above. Cells lacking Mec1 are more sensitive to MMS than cells lacking Rad53, which suggests that Mec1 can stabilize stalled forks at least partly independently of Rad53 (Tercero et al. 2001).
Rad53 inhibits the exonuclease Exo1 by phosphorylation. Deletion of *EXO1* can rescue the MMS, UV and IR, but not HU, sensitivity of *rad53* mutants (Segurado et al, 2008). Thus, Exo1 is an important target of Rad53 in the cellular response to MMS, UV, and IR.
Additionally, Mrc1 is phosphorylated in a checkpoint-dependent manner. Mrc1 is associated with the replication fork and is required for normal replication fork progression, but also is

involved in preventing continued replisome progression at stalled forks. Mrc1 binds to the Tof1-Csm3 complex at stalled replication forks to prevent the uncoupling of the replication machinery components such as polymerases, MCMs and Cdc45 (Nedelcheva et al. 2005). Mrc1, Csm3 and Tof1 are presumed to act as a bridge to regulate the progression of DNA unwinding with DNA synthesis. Mrc1 can bind to Pol2, which is a catalytic subunit of the leading strand polymerase. This binding is regulated by checkpoint-dependent phosphorylation of Mrc1 (Lou et al. 2008). Mrc1 also interacts with the Mcm6 helicase when cells are treated by MMS (Komata et al. 2009). Decreasing the amount of Mcm2-7 complex available for loading at dormant origins results in slower replication rates and decreased viability (Ge et al, 2007).

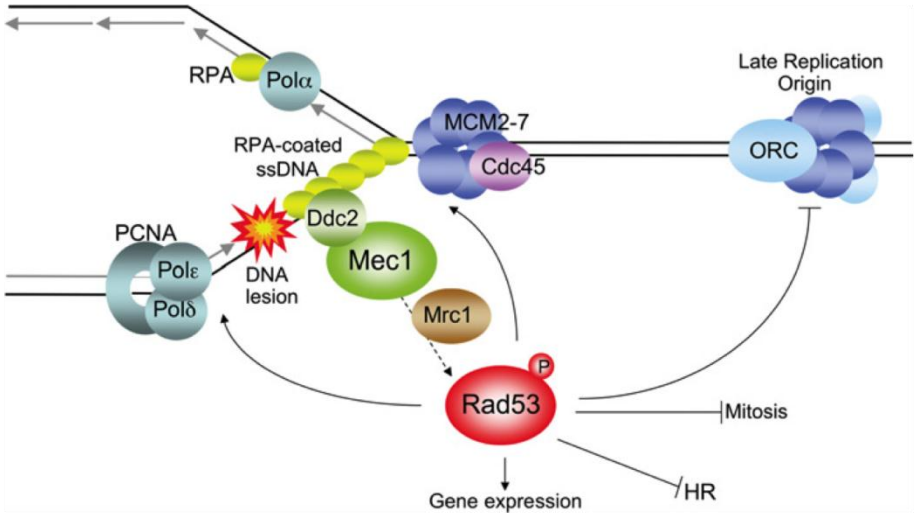

Figure 7. Replication checkpoint response at the replication fork (Segurado et al, 2009). When replication forks hit DNA lesions or stall because of dNTP deprivation, the effector kinase Rad53 is phosphorylated and activated. Rad53 maintains stable, functional DNA replication forks, inhibits firing of late origins, activates gene expression and prevents entry into mitosis and unscheduled recombination.

Control of late origin firing

On each eukaryotic chromosome, DNA synthesis begins at origins of replication found at hundreds or thousands of sites. The first origins of replication were identified in budding yeast. The regulation of origin initiation or “firing” is strongly conserved across evolution (Bell and Dutta 2002). Most cell types have a temporal programme of origin activation whereby origins fire in a continuum throughout S-phase, such as early and late firing origins. The replication checkpoints regulate DNA synthesis by inhibiting late origin firing. The early origins must fire to elicit the checkpoint response and the checkpoints inhibit the firing of

late or dormant origins in response to DNA damage (Santocanale et al. 1998, Santocanale et al. 1999, Shirahige et al. 1998). The checkpoint blocks origin firing by inhibiting the transition of the pre-replicative complex (preRC) to the preinitiation complex (preIC). The preRC contains an inactive form of the Mcm2-7 helicase loaded at origins through the action of the ORC complex, Cdt1, and the Cdc6 ATPase. At the G1/S transition, CDKs (cyclin-dependent kinases) and DDK (Dbf4-dependent kinase) must be activated to promote the transition to the preIC containing Mcm10, Cdc45, GINS, Sld2, Sld3, and Dpb11. In budding yeast, recent studies have shown that Rad53 phosphorylates directly Sld3 and Dbf4 to inhibit the CDK and DDK pathway respectively to block late origin firing. Sld3 and the Cdc7-Dbf4 kinase complex are required for DNA replication initiation (Tanaka et al. 2007; Bousset et al. 1998; Zegerman et al. 2010; Lopez-Mosqueda et al. 2010). The DNA damage checkpoints (ATM, ATR, Chk2, Chk1) also inhibit late origin firing in mammalian cells (Santocanale and Diffley, 1998; Shirahige et al, 1998; Dimitrova and Gilbert, 2000; Zachos et al, 2003; Bartek et al, 2004). ATM/Chk2 phosphorylates and destabilises Cdc25A, which prevents Cdk2 phospho-tyrosine dephosphorylation, thereby preventing Cdk2 activation and blocking DNA synthesis (Falck et al, 2001). Replication stress activates ATR and Chk1, which regulate initiation by controlling Cdc45 assembly at replication origins (Apricio et al, 1999; Costanzo et al, 2000; Liu et al, 2006). The frequency of origin usage in clusters of early origins might also be negatively regulated by the ATR pathway, through a lateral inhibition of activated origins on the potential neighbouring origins (Mechali 2010).

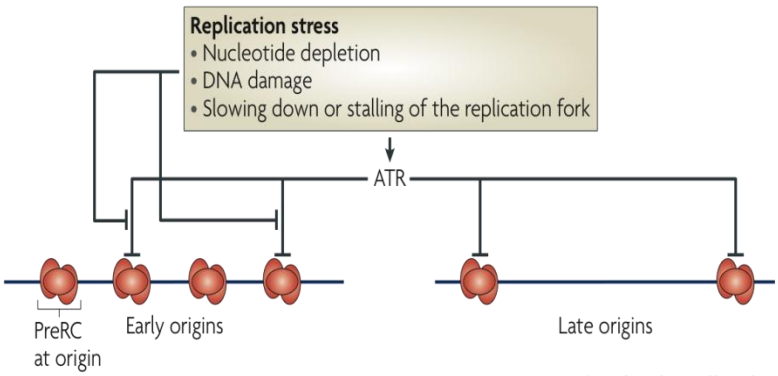

Figure 8. Checkpoint control of replication origins firing (Mechali 2010). The checkpoint signalling through ATR results in the inhibition of late origins. The frequency of origin usage in clusters of early origins might also be negatively regulated by the ATR pathway, through a lateral inhibition of activated origins on the potential neighbouring origins.

1.4.3 DNA damage checkpoint inactivation: recovery and adaptation

Recovery and adaptation correlate with the disappearance of phosphorylated Rad53, largely due to the function of Ser/Thr phosphatases (Heideker et al, 2007). Once DSB repair is complete, the DNA damage checkpoints are reversed so that cells can resume cell cycle progression by «checkpoint recovery» (Bartek and Lukas, 2007). The mechanism of checkpoint recovery is unknown, although several proteins have been identified to play a role in this process so far, including Rad51 and the DNA helicase Srs2 (Vaze et al, 2002; Krejci et al, 2003).

Cells can also turn off the DNA damage checkpoint in the absence of DNA repair by «adaptation» (Bartek and Lukas, 2007). Although the pathway is not fully elucidated, it was shown to involve several several proteins including Cdc5, the phosphatases Ptc2/3 as well as casein kinase 2 (CK2) and the NHEJ protein Ku complex (Lee et al, 1998).

Ptc2/3 and CK2 play a role in adaptation and recovery. Ptc2/3 phosphatases are required for the DNA checkpoint inactivation, but only in response to DSBs such as that induced by the HO endonuclease (Leroy et al, 2003). Ptc2/3 binds to the FHA1 domain of Rad53 and dephosphorylates Rad53. Ptc2 binding to FHA1 is dependent on its phosphorylation by CK2.

The endonuclease Sae2 is involved in meiotic and mitotic DSB processing and in subsets of recombination pathways together with the MRX complex (Keeney & Kleckner, 1995; Rattray et al, 2001; Lobachev et al, 2002; Neale et al, 2002; Clerici et al, 2005) Sae2 undergoes Mec1- and Tel1- dependent phosphorylation. The *sae2Δmec1Δ* or *sae2Δtel1Δ* mutants fail to adapt and maintain Rad53 phosphorylation. Overexpression of Sae2 can override the checkpoint arrest following UV irradiation in the presence or absence of Tel1 (Baroni et al, 2004; Clerici et al, 2006). These results suggest that Sae2 may regulate Mec1/Tel1 to promote adaptation.

1.5. Rad53

Rad53 is a central protein kinase in the checkpoint pathway in the budding yeast *S.cerevisiae* (Allen et al. 1994). Rad53 is homologous to *S.pombe* Cds1 and mammalian Chk2. Because of its robust hyperphosphorylation after checkpoint activation, modified Rad53 is widely used as an experimental marker for checkpoint activation. Rad53 is essential for cell viability even in the absence of DNA damage. This lethality of *rad53*Δ cell can be suppressed by over-expressing the largest subunits of ribonucleotide reductase (*RNR*), or by deletion of *SML1* encoding a peptide inhibitor of RNR (Zhao et al. 1998), but the checkpoint functions cannot be rescued by these manipulations (Desany et al. 1998).

The Rad53 protein (821 aa) has a poly-SQ/TQ motif at the N-terminus, two FHA domains, a kinase domain and the C-terminal region.

1.5.1 Structure of Rad53

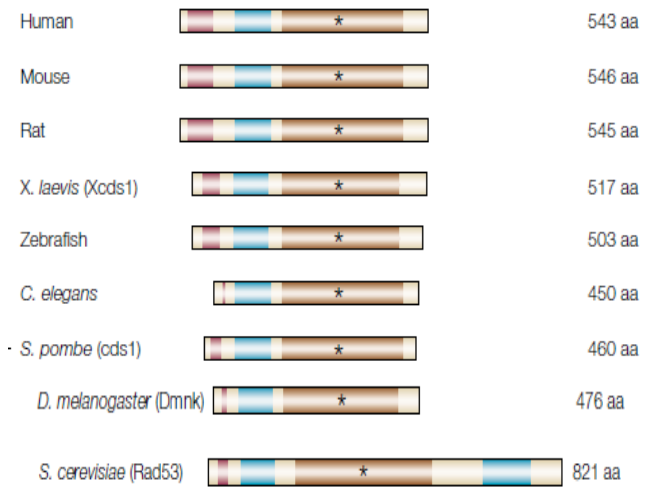

Figure 9. Rad53 and its homologues in different species. The alignment of conserved domains: The SQ/TQ-rich domain in maroon, the FHA domain in blue and the kinase domain in brown. The highly conserved activation loop is marked by an asterisk.

The SQ/TQ motif

Rad53 contains sixteen SQ/TQ motifs, eight of which are concentrated into two cluster domains (SCD1 and SCD2, in which there are four SQ/TQ motifs). These SQ/TQ motifs, which are typical consensus sites for PIKKs, are the putative Mec1/Tel1 (ATM/ATR) target sites for transducing the DNA damage signal (Traven and Heierhorst, 2005; Kim et al. 1999). The Rad53-SCD1-4AQ mutant can reduce significantly Rad53 activation in response to DNA damage, which can be fully restored by reversion of any single threonine residue in this motif (Lee et al. 2003a). SCD1 interacts with the FHA domain of Dun1 and also binds the FHA1 domain of Rad53 itself, promoting oligomerization and activation of Rad53 (Lee et al, 2003a,b; Harrison 2006).

Figure 10. Schematic representation of the domain structure of Rad53: The SQ/TQ-rich domain in purple, the FHA domains in green and the kinase domain in blue.

FHA domain (forkhead-associated domain)

Structurally intact FHA domains contain approximately 150 residues (Liao et al. 1999; Hammet et al. 2000). Rad53 is a unique kinase containing two FHA domains: an N-terminal FHA1 domain and a C-terminal FHA2 domain (Durocher et al. 1999). These two FHA domains play a role in recruiting Rad53 to sites of DNA damage for activation (Durocher and Jackson, 2002). The two FHA domains are partially redundant for its activation. The loss of either FHA domain in presence of DNA damage shortens the normal arrest time. The checkpoint defect of the FHA1/FHA2 double mutant is similar to that of the *rad53-kinase dead* mutant (Pike et al. 2003; Schwartz et al. 2003).

In response to DNA damage, Rad53 binds to hyperphosphorylated Rad9, which is mediated by both FHA1 and FHA2 domains of Rad53 (Sun et al. 1998; Schwartz et al. 2002). Mutation of FHA2 reduces Rad53 phosphorylation and the Rad53-Rad9 interaction in the presence of MMS, but not HU (Schwartz et al. 2003; Sun et al. 1998). FHA1 binds to Rad53 itself, and to Mrc1, the histone chaperone Asf1, the S-phase regulator kinase Dbf4, the phosphatase Ptc2, and many other proteins involved in trancription, morphogenesis and cytokinesis (Emili et al. 2001; Hu et al. 2001; Duncker et al. 2002; Leroy et al. 2003; Schwartz et al. 2003; Sun et al. 1998; Gilbert et al. 2001; Smolka et al. 2006).

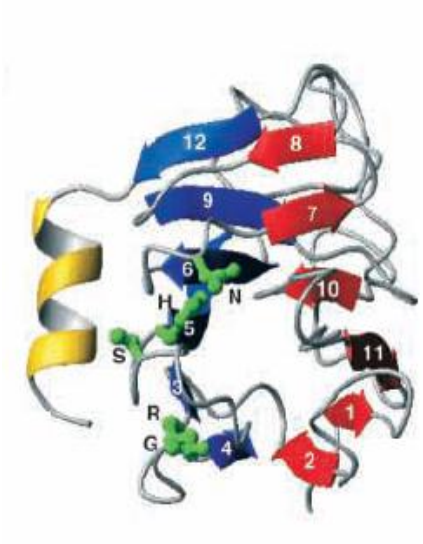

Figure 11. The three-dimensional structure of the Rad53 FHA domain consists of a β-sandwich (Li et al, 2000). One β-sheet has been highlighted in blue, and the other in red.

The FHA2 domain (573-730) structure showed the presence of two antiparallel beta-sheets making a beta-sandwich. There are 11 β-strands that interact with each other through strong hydrophobic interactions and a small C-terminal β-helix.
Similar to FHA2, the FHA1 domain comprises of a 11-strand β-sandwich with a small C-terminal helix (Durocher and Jackson, 2002).
The FHA1 domain of Rad53 recognizes preferentially the peptide pTXXD, and the FHA2 domain of Rad53 recognizes pTXXL and pYXL (Byeon et al. 2001; Wang et al. 2000). However, three-dimensional structures of Rad53-FHA1 bound to the pTXXIY peptide of Mdt1, and Ki67-FHA domain binding of the β strand of hNIFK, have shown that FHA domains may have more than one type of binding mode (Byeon et al. 2005; Mahajan et al. 2005). The structure of the Chk2-FHA domain was published in 2002 and was shown to recognize the peptide pTXXI (Li et al. 2002; Qin et al. 2003).

Rad53 kinase domain

The structure of the Rad53 kinase domain has not yet been determinated. However, this domain contains key functional elements including an activation loop identified by homology with other serine/threonine kinases. The phosphorylation of the activation loop at residues T354 and T358 is required for Rad53 kinase activity (Fiorani et al, 2008). Other conserved residues in the kinase domain such as K227 and D339 are also required for catalytic activity. The *rad53-K227A* single mutant and *rad53-K227A+D339A* double mutants show little or no kinase activity and are checkpoint deficient (Sweeney et al, 2005).

Structure and activation mechanism of the CHK2 DNA damage checkpoint kinase

The protein kinase Chk2 (checkpoint kinase 2), the mammalian homolog of the budding yeast Rad53, is phosphorylated and activated in response to DNA damage. It consists of an N-terminal SQ/TQ cluster domain (SCD), a middle FHA domain, and a C-terminal serine/threonine kinase domain (KD) (Ahn et al, 2004). The SCD consists of multiple SQ/TQ motifs that contain ATM phosphorylation sites, with Thr68 being the primary site that gets phosphorylated in response to DNA damage (Ahn et al, 2000; Matsuoka et al, 2000; Melchionna et al, 2000). Once phosphorylated, the pThr68 of Chk2 can bind *in trans* to the FHA domain of another molecule promoting dimerization (Ahn et al, 2002, Li 2002). The activation of the Chk2 KD requires phosphorylation of Thr383 on the activation loop (T-loop) (Lee and Chung, 2001; Schwarz et al, 2003). The Chk2 dimer is thought to be disassociated into monomers after activation (Ahn et al, 2002). The crystal structure of an inactive Chk2 dimer has been recently solved (Cai et al, 2009). The protein Chk2 crystallizes as a dimer in a SCD-independent manner through FHA-KD and FHA-FHA

interactions between two monomers. The FHA-KD interactions are centered on Ile157, a residue mutated in the Li-Fraumeni syndrome. Once activated, the kinase domain was proposed to change conformation in a way that disrupts either or both the FHA-KD and FHA-FHA interfaces, contributing to the dissociation of the dimer.

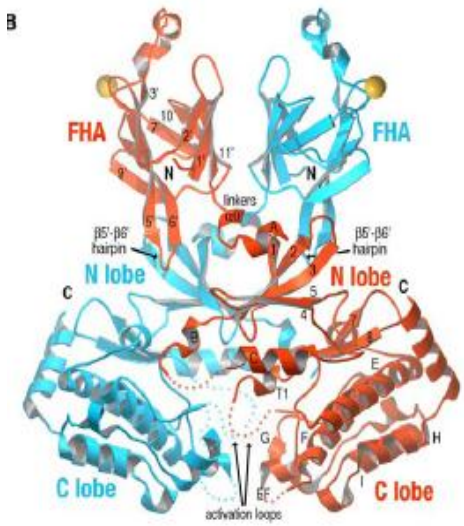

Figure 12. Structure of Chk2^{K249R} dimer (Cai et al, 2009). To avoid heterogeneous phosphorylation, they used the kinase-dead Chk2 mutant Chk2^{K249R}. The FHA domains and the N and C lobes of the bilobal kinase domain are labeled. The yellow spheres indicate the approximate positions of the phospho Thr phosphate group. Dotted lines indicate disordered regions, including the activation loops.

The C-terminal region

A bipartite nuclear localization signal (NLS) is located in the C-terminal region of Rad53. This NLS is required for efficient translocation of Rad53 into the nucleus, where it exerts its checkpoint functions as a guardian of the genome. The C-terminal truncation mutant perturbs the nuclear localization of Rad53 (Smolka et al. 2006; Sun et al. 1996). The C-terminal tagging of Rad53 with a 3HA epitope was reported to decrease the levels of Rad53 in cells, leading to increased sensitivity to HU, but increased resistance to MMS relative to the wild type (Cordon-Preciado et al. 2006). Increased resistance of this mutant to MMS was correlated with lower levels of Rad53 kinase activity and more rapid recovery from cell cycle arrest after transient MMS exposure, but with increased levels of mutagenesis. In our study, this C-terminal domain of Rad53 is important for the Asf1-Rad53 interaction. More details will be discussed later in this chapter.

1.5.2 Rad53 activation model

As discussed above, transducers act to amplify the damage signal that will later activate the effector proteins. In response to DNA damage, Rad53 is recruited to Mec1 by Rad9, whereas upon replication stress, Mec1 requires Mrc1 for Rad53 activation.

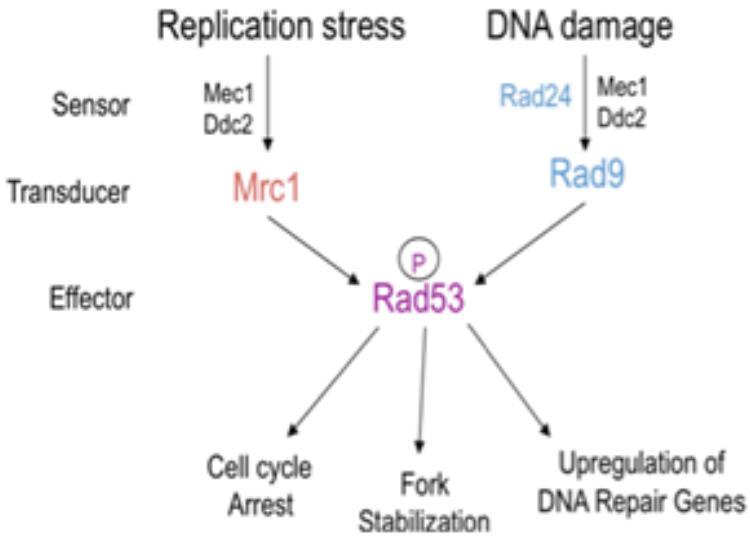

Figure 13. Two main pathways for Rad53 activation involving Rad9 and Mrc1.

Mec1 activates Rad53 via Rad9

In response to DNA damage, the RPA-coated ssDNA recruits independently the Mec1-Ddc2 and the clamp loader complex Rad24-RFC (You et al. 2002; Zou et al. 2003; Lucca et al. 2004, Kanoh et al. 2006; Branzei et al. 2009). Once loaded by Rad24-RFC, the PCNA-like Ddc1-Mec3-Rad17 clamp complex can facilitate Mec1 activation (Majka et al. 2006). The mediator Rad9 co-localizes with Mec1 at sites of DNA damage where it is phosphorylated by Mec1 (Naiki et al, 2004). Phosphorylated Rad9 recruits Rad53 to the damage site where it is then also phosphorylated by Mec1 (Emili 1998; Schwartz et al. 2002; Sweeney et al. 2005). Mec1-dependent phosphorylation of Rad9 allows Rad9 dimerization via its C-terminal BRCT-repeats, and facilitates Rad53 autophosphorylation *in trans*, perhaps by increasing the local Rad53 concentration on the Rad9 surface (Soulier and Lowndes, 1999; Gilbert et al. 2001; Lisby et al, 2004). After phosphorylation, Rad53 is released from Rad9, most likely because the modified protein has a lower affinity for the adaptor, and Rad53 then mediates the phosphorylation of its downstream substrates (Gilbert et al, 2001).

Mec1 activates Rad53 through the mediator Mrc1 in response to replicative stress

Mrc1 is a component of the DNA replisome and travels with the replication forks during DNA synthesis (Szyjka et al. 2005; Gambus et al. 2006; Lou et al. 2008; Alcasabas et al. 2001; Osborn and Elledge. 2003; Tanaka et al. 2001). Mrc1 is the counterpart of Rad9 for activating the DNA checkpoints in response to replicative stress (Pellicioli and Foiani, 2005; Sweeney et al. 2005; Toh and Lowndes, 2003). Mec1 phosphorylates Mrc1 which is required for its binding to Rad53 and for subsequent phosphorylation of Rad53 by Mec1 at stalled replication forks (Alcasabas et al. 2001, Chen et al. 2009).

Phosphorylation sites of Rad53

Two studies have characterized by mass spectrometry 32 Rad53 phophorylation sites in response to DNA damage induced by 4-NQO (4-nitroquinolineoxide) and MMS (Smolka et al. 2005; Sweeney et al. 2005). Thirteen potential autophosphorylation sites and 14 potential sites phosphorylated by other kinases, such as Mec1 and CDK, were identified in response to the UV-mimetic drug 4-NQO by Sweeney et al., whereas Smolka et al. identified seven phosphorylated sites in the absence of DNA damage and eight additional sites that become phosphorylated in response to MMS. These studies suggest that different drugs have different mechanisms to activate Rad53.

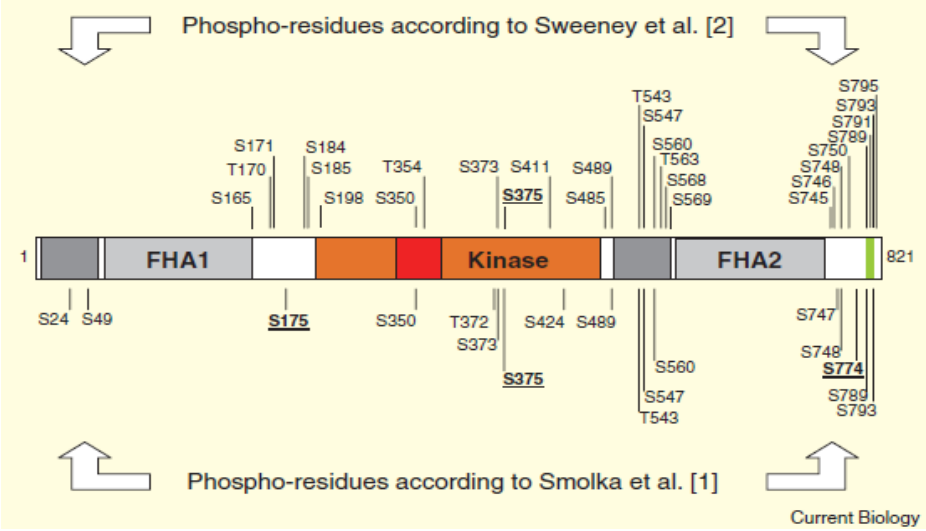

Figure 14. Rad53 phosphorylation sites upon 4-NQO (top) and MMS (bottom) (Pellicio and Foiani, 2005).

1.5.3 Rad53 and histone degradation

Rad53 is also involved in the degradation of excess, non-nucleosomal (soluble) histones (Gunjan and Verreault, 2003). Rad53 regulates histone protein levels in a kinase-dependent surveillance mechanism. Consistently, *rad53Δ* but not *mec1Δ* mutants are extremely sensitive to histone H3 overexpression, and deleting the major H3-H4 gene partially suppresses the DNA damage sensitivity, chromosome loss and slow growth phenotypes of *rad53Δ* cells (Gunjan and Verreault, 2003; Singh et al, 2009). These results suggest that the housekeeping function of Rad53 is independent of its functions in the DNA damage checkpoints. Rad53 maintains cellular histone levels by phosphorylating excess non-nucleosomal histones, which are then ubiquitylated and degraded by the proteasome (Gunjan and Verreault, 2003; Singh et al, 2009).

1.6 Aim of this thesis

Asf1 is important for genomic stability since *asf1* mutants show indications of increased endogenous DNA damage and are sensitive to various genotoxic stresses (Tyler et al, 1999). Rad53 forms a complex with Asf1 that is dissociated after some types of genotoxic stress. The importance of these key proteins in DNA checkpoint and chromatin pathways, and the modulation of their interaction in response to genotoxic stress, strongly suggests that their interaction plays a role in the response to DNA damage. However, evidence for such a role is lacking nearly ten years after the initial description of this complex. The aim of this thesis is to contribute to our knowledge of the structural basis for the Asf1-Rad53 interaction and to determine the functional role of its modulation in response to genotoxic stress.

Results I

Manuscript submitted for publication:

In this manuscrit, my work contributed to these 3 parts of the results:
"-Mutations in the H3, H4, and HirA/CAF-1 binding surfaces of Asf1N affect the stability of the Asf1-Rad53 complex;
-Phosphorylation of C-terminal Rad53 serine and threonine residues cannot explain dissociation of the Rad53-Asf1 complex upon treatment of yeast cells with hydroxyurea;
-The *rad53-ALRR* mutation destabilizes the Asf1-Rd53 complex and increases the resistance of rad9 and rad24 mutants to genotoxic stress."

Surprising complexity of the Asf1 histone chaperone-Rad53 kinase interaction

Yue Jiao[a,1], Karsten Seeger[b,1,2], Aurelie Lautrette[b], Albane Gaubert[b], Florence Mousson[b], Raphael Guerois[b], Carl Mann[a,3], and Françoise Ochsenbein[b,3]

[a]CEA, iBiTec-S, Service de Biologie Intégrative et de Génétique Moléculaire, Gif-sur-Yvette, F-91191, France.

[b]CEA, iBiTec-S, SB2SM, Laboratoire de Biologie Structurale et Radiobiologie, Gif-sur- Yvette, F-91191, France.

[1]Y.J. and K.S. contributed equally to this work.

[2]Present address: Institut für Chemie. Universität zu Lübeck. 23562 Lübeck. Germany.

[3]To whom correspondence may be addressed. E-mail: carl.mann@cea.fr or francoise.ochsenbein@cea.fr

Author contributions: C.M. and F.O. designed research and wrote the paper with contributions from the other authors; Y.J. and C.M. performed biochemical and genetic experiments; A. L., K. S., F. M., and A. G. performed biochemical experiments, crystallogenesis and calorimetry; K.S. and F.O. performed structural analyses (NMR and crystallography); R.G. performed bio-informatic analyses; all authors contributed to data analysis.

The authors declare no conflicts of interest.

This article is a PNAS Direct Submission.

BIOLOGICAL SCIENCES: Biochemistry.

Abstract

The histone chaperone Asf1 and the checkpoint kinase Rad53 are found in a complex in budding yeast cells in the absence of genotoxic stress. Our data suggest that this complex involves at least three interaction sites. One site involves the H3-binding surface of Asf11 with an as yet undefined surface of Rad53. A second site is formed by the Rad53-FHA1 domain binding to Asf1-T270 phosphorylated by casein kinase II. The third site involves the C-terminal 21 amino acids of Rad53 bound to the conserved Asf1 N-terminal domain. The structure of this site showed that the Rad53 C-terminus binds Asf1 in a remarkably similar manner to peptides derived from the histone co-chaperones HirA and CAF-I. Furthermore, C-terminal Rad53-F820 binds the same pocket of Asf1 as does histone H4-F100. Thus Rad53 competes with histones H3-H4 and co-chaperones HirA/CAF-I for binding to Asf1. Rad53 is phosphorylated and activated upon genotoxic stress. The Asf1-Rad53 complex dissociated when cells were treated with hydroxyurea but not methyl methane sulfonate, suggesting a regulation of the complex as a function of the stress. We identified a *rad53* mutation that destabilized the Asf1-Rad53 complex and increased the viability of *rad9* and *rad24* mutants in conditions of genotoxic stress, suggesting that complex stability impacts the DNA damage response.

\body

Introduction

Asf1 is a highly conserved chaperone of histones H3 and H4 that has been implicated in histone modification and nucleosome assembly/disassembly during DNA transcription, replication, recombination, and repair (1). In addition to H3-H4, Asf1 interacts with several other chromatin associated proteins in a conserved manner, including the HirA and CAF-I histone co-chaperones (2) and the Bdf transcription factors (3). In budding yeast, Asf1 also forms a complex with the DNA damage checkpoint kinase Rad53 (4, 5). Curiously, in mammalian cells, Asf1 does not appear to interact with Chk2 (6), the mammalian ortholog of Rad53, but rather with Tousled-like kinases that are also implicated in DNA damage responses but that are not conserved in yeast (7). The Asf1-Rad53 complex was reportedly dissociated when yeast cells were subjected to genotoxic stress in a Mec1-dependent manner (4, 5). Mec1 activates Rad53 by phosphorylation in response to genotoxic stress. It was suggested that Rad53 could target Asf1 to sites of DNA damage where Rad53 activating phosphorylation would then liberate Asf1 to facilitate DNA repair (4, 5). This model is compelling, but no experimental verification has yet appeared. Rad53 binding to Asf1 was also suggested to inhibit the ability of Asf1 to promote transcriptional silencing on the basis of genetic data (8). To test the functional importance of the Asf1-Rad53 complex, we mapped the interaction surfaces and solved the X-ray structure between the conserved Asf1 N-terminal domain (Asf1N) and the C-terminal peptide of Rad53. These structural data allowed us to identify a mutation destabilizing the complex. Interestingly, this mutant increased the resistance to genotoxic stress of *rad9* and *rad24* mutants that are partially defective in Rad53 activation.

Results

Rad53 and Asf1 interact through at least two binding sites. We used GST pull-down experiments to characterize the Asf1-Rad53 interaction *in vitro*. Different constructs of Asf1 (full-length and N-terminal domain) and Rad53 (full-length, and fragments containing the FHA1 domain, the kinase domain, the FHA2 domain, or C-terminal peptides) were expressed and purified from *E. coli* with a GST or a 6His tag respectively (Fig. 1A). Full-length Rad53 undergoes extensive autophosphorylation when it is expressed in *E. coli* (9) and this form of the protein was unable to bind Asf1 (Fig. 1B). *In vitro*, dephosphorylation of Rad53 allowed its binding to both GST-Asf1 and GST-Asf1N, but not to GST alone (Fig. 1B and Fig. S1A). Thus, Rad53 autophosphorylation blocks its binding to Asf1. We further analyzed binding of Rad53 domains to the GST-Asf1 constructs. Interestingly, both GST-Asf1 and GST-Asf1N specifically bound C-terminal peptides of Rad53, but not the FHA1, kinase, or FHA2 domains (Fig. 1B). Schwartz et al. previously showed that the Rad53 FHA1 domain could pull down Asf1 in yeast extracts, but treatment of such extracts with protein phosphatase prevented binding (10). We confirmed this observation, and we further verified that GST-Rad53-Cter peptides (aa 734-821 and 781-821) could pull down Asf1 from yeast extracts treated with protein phosphatase (Fig. 1C and Fig. S1B). These results suggest that Rad53 and Asf1 interact through at least two binding sites: Rad53-FHA1 binds a phosphorylated site of Asf1, and the C-terminal peptide of Rad53 binds Asf1N.

The Rad53 FHA1 domain binds Asf1 phosphorylated on T_{270}. The Rad53 FHA1 domain was previously shown to bind pTxxD phospho-threonine peptides (11, 12). We sought Asf1 phospho-threonines recognized by FHA1. Rad53-FHA1 could pull down full-length Asf1, but not Asf1N from yeast extracts, indicating that the phospho-peptide bound by FHA1 is within the acidic C-terminal tail of Asf1 that contains two pairs of threonines nearby acidic residues (Fig. 1D and S2A). We created two mutants in which threonines were changed to alanine in a pairwise fashion ($T_{215}A+T_{220}A$ and $T_{265}A+T_{270}A$) and expressed them in yeast. The Rad53-FHA1 domain could pull-down the $T_{215}A+T_{220}A$ mutant, but not the $T_{265}A+T_{270}A$ mutant (Fig. 1D). Interestingly, of these 4 threonine residues, only T_{270} is conserved in the Asf1 sequence from different yeast species (Fig. S2A), and was the only site predicted to bind FHA1 by the STRIP program that we developed for the prediction of phospho-binding sites (13). Importantly, phospho-T_{270} was found on Asf1 that co-purified with Rad53 from yeast extracts (14). Finally, a synthetic Asf1 peptide phosphorylated solely on T_{270} interacted with the FHA1 domain as determined by NMR chemical shift perturbation experiments (Fig. S2B, S2C). The FHA1 binding mode was similar to that of other FHA1 partners (see Supplementary results) (11, 12, 15). Isothermal titration calorimetry (ITC) indicated that FHA1 bound the phospho-T_{270} peptide with a dissociation constant of 5.3 μM (Fig. S2D). The Rad53-FHA1 domain was previously shown to interact with peptides that had been phosphorylated by casein kinase II (15) whose catalytic subunits are encoded by the yeast *CKA1* and *CKA2* genes (16). We thus examined if this was also the case for Asf1. We found that FHA1 could not pull-down Asf1

from a thermosensitive yeast *cka1! cka2-ts* mutant (16) (Fig. 1D). Furthermore, yeast Cka1 and Cka2 were found to co-purify with Asf1 in a high-throughput screen (17). Altogether, these results suggest that CKA2 phosphorylates at least T270 in Asf1 and that this creates a binding site for the Rad53-FHA1 domain.

The Rad53 C-terminal peptide (aa 800-821) binds to Asf1N on the HirA/CAF-I and histone H4 binding surfaces. We used ITC to define more precisely the minimal Rad53 C-terminal fragment sufficient for Asf1N binding. Peptides from 8-40 residues were synthesized and tested for their binding affinity to Asf1N (Table 1). The fragment containing the last 21 aa of Rad53 (800-821) was the minimum fragment retaining the maximum binding affinity to Asf1N. The dissociation constant was 0.08 (±0.03) µM, which is 2 orders of magnitude lower than for the Rad53 FHA1-phospho-Asf1 interaction (Fig. S3A). We then solved the structure of the complex between Asf1N (1-156) and the Rad53 C-terminal peptide (800-821) by X-ray crystallography at 2.9 Å resolution (see Table S1 for statistics). The peptide contacts Asf1 in two distinct regions defining two binding epitopes (Fig. 2A). The first binding epitope corresponds to Rad53 K804-T811 that lies in an extended conformation on the hydrophobic surface of Asf1 between the fourth and the fifth beta strands (residues D58 to F72). Three Rad53 residues (K804 CO, A806 NH, and D809 NH, CO), establish backbone pairing hydrogen bonds with Asf1 L61 NH, CO and K71 NH, CO respectively. The side chains of two Rad53 residues, A806 and L808, point towards the Asf1 conserved hydrophobic surface composed of I60, L61, V62 and F72 side chains. In addition, the side chains of two basic residues, K804 and R805 form salt bridges with Asf1-D58 and D37 respectively (Fig. 2B). Interestingly, despite a low sequence identity, this binding epitope overlaps that of the B domain-like peptides of HirA/p60-CAF-I (2, 18) with a similar binding mode (Fig. 2C). Thus, Rad53 binding to Asf1 is competitive with HirA and CAF-I. Based on the alignment of HirA, CAF-I and Rad53 C-terminal peptides, we defined an Asf1 binding motif that is less stringent than previously proposed (2, 18). We call this motif, (R/K)R(I/A/V)x(L/P), the AIP box for Asf1-Interacting Protein box. The motif is centered on one strictly conserved arginine residue, corresponding to R805 in the case of Rad53, preceded by a basic residue and followed by a hydrophobic residue (I/A/V) in position i+1, and (L/P) in position i+3 with respect to the conserved arginine (Fig. S3B). Interestingly, the AIP box is present in a subset of proteins that interact with Asf1 in an unknown manner, and may thus potentially bind to the same surface of Asf1 as HirA, p60-CAF-I, and Rad53 (Table S2). These proteins include yeast Kap123, Spt15 and human codanin-1.

The second Asf1-binding epitope of the Rad53 C-terminal peptide involves its last three residues (819-821), and in particular F820 that burrows in the hydrophobic cavity formed by the first and last Asf1 beta strands (residues L6, I9 and P144) (Fig. 2B). The position of this aromatic residue overlaps that of histone H4-F100 (Fig. 2C), suggesting that this interaction competes with binding of histone H4 to Asf1.

In the crystal structure, the Rad53(800-821) peptide swaps between two Asf1 molecules

(Supplementary results and Fig. S4). Analysis of the dynamic behaviour of the complex using NMR spectroscopy showed that bridging of Asf1 dimers by the Rad53 peptide is an artefact of the crystal packing (Supplementary data and Fig S5). Furthermore, the second epitope is highly dynamic, consistent with its ability to swap with a second Asf1 molecule in the crystal.

We analysed by ITC the relative importance of residues found in contact with Asf1 in the structure (Table 1). Consistent with the dynamic analysis, deletion of the second binding epitope or mutation of the aromatic F820 residue had a minor impact on the binding affinity, while deletion or mutation of hydrophobic or charged residues inside the first epitope (the AIP box) prevented binding or dramatically decreased the affinity (Table 1). Thus, the AIP box predominates in Asf1-Rad53 binding.

Mutations in the H3, H4, and HirA/CAF-I binding surfaces of Asf1N affect the stability of the Asf1-Rad53 complex. We mutagenized Asf1 at a series of residues dispersed over the surface of the N-terminal domain (Fig. 3A). Immunoprecipitation of wild-type and mutant Asf1 from yeast cell extracts showed that specific residues located in the histone H3, histone H4, and HirA/CAF-I binding surfaces of Asf1 were important for its binding to Rad53, whereas other sites had no effect (Fig. 3B). The D37R+E39R and the T147A mutants are located in the HirA/CAF-I (2, 18) and histone H4 (19, 20) binding surfaces of Asf1 respectively, and both mutants showed reduced affinity for Rad53 as predicted by the structure of the Rad53 C-terminal peptide bound to Asf1. Interestingly, the V94R mutant that blocks binding to histone H3 (21) is also defective in binding to Rad53. This residue is too far from the Rad53 C-terminal peptide to be able to affect its binding directly. Furthermore, NMR experiments showed that the V94R mutation has little effect on the overall Asf1N tertiary structure (21), so it is unlikely that this mutation affects Rad53 binding through indirect conformational changes. We considered two explanations for these results. One possibility was that histone H3 bound to Asf1 contributes to the binding of Rad53. To test this possibility, we immunoprecipitated Asf1 from yeast cell extracts containing the histone H3-R129E mutant in place of the wild type. We previously showed that this mutant is unable to bind Asf1 (22, 23). We found that Rad53 was still immunoprecipitated with Asf1 in these extracts in which H3-R129E was not associated with Asf1 (Fig. 3C). This result suggests that Rad53 binding to Asf1 does not require bridging by histone H3. The second possibility is that Asf1 may directly interact with Rad53 through a third binding site overlapping the histone H3 binding surface of Asf1N. Schwartz et al. showed that a Rad53-K227A+D339A kinase dead mutant co-immunoprecipitated weakly with Asf1 in yeast extracts compared to wild-type Rad53 (10). We confirmed this result and showed that the Rad53-K227A single mutant was also affected in its interaction with Asf1 (Fig. S6A). These observations suggest that the Rad53 kinase domain might be able to interact with Asf1, although we did not observe an obvious interaction of the Rad53 kinase domain with GST-Asf1 or GST-Asf1N when all proteins were purified from *E. coli* (Fig. 1B). Alternatively, Rad53 kinase activity may be indirectly required for this putative third interaction site. Our current working model is that Asf1 and Rad53

interact at 3 three distinct surfaces to form a complex that precludes binding of histones and histone co-chaperones to Asf1 (Fig. 3D).

Phosphorylation of C-terminal Rad53 serine and threonine residues cannot explain dissociation of the Rad53-Asf1 complex upon treatment of yeast cells with hydroxyurea. Some previous work suggested that Rad53 and Asf1 are found in a complex in yeast cells in the absence of genotoxic stress, but the complex was dissociated upon treatment of cells with hydroxyurea (HU) or methyl-methane-sulfonate (MMS) (4, 5). We confirmed that Rad53 was no longer immunoprecipitated with Asf1 when cells were treated with HU (Fig. 4A, left). However, we found that phosphorylated forms of Rad53 still co-immunoprecipitated with Asf1 when cells were treated with MMS (Fig. 4A, middle), although the most highly phosphorylated species were not co-immunoprecipitated. These results are consistent with a mass spectroscopy study showing that Asf1 remained associated with Rad53 after treating cells with MMS (14). It is possible that earlier work showing a dissociation of the complex after MMS treatment of cells used immunoprecipitation conditions that were overly stringent. Our results suggest that the complex is differentially regulated in response to HU or MMS treatment, presumably to allow a tailored cellular response to these distinct genotoxic stresses.

Rad53 is phosphorylated at more than 20 serine or threonine residues, some of which are phosphorylated differentially depending on the type of genotoxic stress (9, 14). Dissociation of the Rad53-Asf1 complex may be induced by phosphorylation of Rad53 on specific sites after treatment of cells with HU. We noticed that there are three serine/threonine residues in the Rad53 C-terminal peptide (T_{811}, S_{812} and S_{821}) that binds Asf1N. Relative to the Asf1N binding epitopes in the Rad53 C-terminal sequence (Fig. 2A), T_{811} and S_{812} are located at the very end of the first binding epitope, and S_{821} is in the second binding epitope. We mutated each of these serines/threonine to acidic residues to produce a phospho-mimetic mutant (Rad53-T_{811}D+S_{812}D+S_{821}E, abbreviated as Rad53-TSSDEE). If phosphorylation of one or more of these residues is sufficient to induce dissociation of the complex in response to HU, we would expect that the phosphomimetic Rad53-TSSDEE mutant would not be associated with Asf1 even in the absence of genotoxic stress. However, we found that Rad53-TSSDEE co-precipitated with Asf1 in the absence of genotoxic stress, even in the context of the non-phosphorylatable Asf1-T_{265}A+$_{270}$A mutant that is defective in binding Rad53-FHA1 (Fig. 4A, right). Thus, phosphorylation of C-terminal Rad53 T_{811}, S_{812} or S_{821} residues may potentially contribute to destabilizing the complex, but is not sufficient to explain dissociation of the complex in response to HU treatment.

The *rad53-ALRR* mutation destabilizes the Asf1-Rad53 complex and increases the resistance of *rad9* and *rad24* mutants to genotoxic stress. Rad53 A_{806} and L_{808} contribute to a hydrophobic surface that is important in the binding affinity of the Rad53-C-terminal peptide with Asf1N (Fig. 2B). Mutation of these residues to arginine greatly decreased the affinity of the Rad53 C-terminal peptide for Asf1N (Table 1). Consistently, the yeast Rad53-A_{808}R+L_{808}R (abbreviated *Rad53-ALRR*)

mutant did not co-immunoprecipitate with Asf1 from yeast extracts (Fig. 4B). These observations are consistent with a destabilization of the Asf1-Rad53 complex in the *rad53-ALRR* mutant. In contrast, Asf1-T$_{265}$A+T$_{270}$A was still bound to Rad53 despite its defective interaction with Rad53-FHA1 (Fig. 4A, right). Thus, the interaction of the Rad53-C-terminal peptide with Asf1 makes a more important contribution to the stability of the complex than does the FHA1 interaction, consistent with the ITC data. We tested the *rad53-ALRR* and *asf1-T$_{265}$A+T$_{270}$A* mutants for sensitivity to HU, MMS, and camptothecin, but found no obvious differences with the wild type (Fig. 4C and data not shown). Rad53 is activated in response to genotoxic stress by two parallel pathways. One pathway is mediated by Mrc1 in response to blocked replication forks (24), and the other depends on Rad9, the Rad24 clamp loader complex, and a PCNA-like clamp complex (25). Strikingly, we found that *Rad53-ALRR* increased the resistance of *rad9, rad24*, and *rad9 rad24* double mutants to MMS (Fig. 4C). It also increased the resistance of the *rad9 rad24* double mutant to HU. In contrast, *Rad53-ALRR* did not modify the resistance of the *mrc1* mutant to HU or to MMS. We compared activating phosphorylation of Rad53 in response to HU and MMS in the wild type, the *rad53-ALRR* mutant, the *rad9 rad24* double mutant, and the *rad53-ALRR rad9 rad24* triple mutant. We found no dramatic differences in Rad53 levels or phosphorylation in any of these contexts, but a modest decrease in Rad53 phosphorylation was observed in the *rad9 rad24* double mutant, the *rad53-ALRR* mutant, and *the rad53-ALRR rad9 rad24* triple mutant compared to the wild type in response to HU and MMS (Fig. 4D). This slight difference in phosphorylation was not correlated with sensitivity of these strains to HU or MMS exposure. Since defects in Rad53 dephosphorylation have also been implicated in sensitivity to genotoxic stress, we compared Rad53 dephosphorylation in wild type and *rad53-ALRR* mutant cells after a transient exposure to MMS, but found no obvious difference between the two strains (Fig. S6B). Thus, the ability of the *Rad53-ALRR* mutant to increase the resistance of *rad9* and *rad24* mutants to genotoxic stress does not appear to be due to obvious differences in Rad53 activation or inactivation.

Discussion

We discovered a remarkable complexity to the Asf1-Rad53 interaction that appears to involve three distinct interaction surfaces. First, we show that the Rad53-FHA1 domain binds Asf1 phosphorylated at T270 in its C-terminal acidic tail domain in a casein kinase II-dependent manner. Rad53-FHA1 binds multiple phospho-proteins (13), so there is likely to be dynamic competitive interactions that contribute to the functions of Rad53 in DNA replication and repair. The affinity of the pT$_{270}$ Asf1 phosphopeptide is modest (5 μM) compared to other known FHA1 partners like Ptc2 and Cdc45 (~0.5 μM) (13). Mutation of Asf1-T265 and T270 to alanine prevented binding of Asf1 to Rad53-FHA1, but this mutant had no apparent phenotype and still co-immunoprecipitated with Rad53. We defined a second interaction surface comprised of the C-terminal 21 aa of Rad53 that binds the same surfaces of the conserved Asf1 N-terminal domain as do the histone co-chaperones HirA/CAF-I and

histone H4. Indeed, the Rad53 C-terminal peptide has a strikingly similar binding mode to the HirA and p60-CAF-I B-domain peptides (2, 18), and it is clear that the three proteins must compete for binding to the same surface of Asf1N. Considering the relative affinity of the corresponding peptides for Asf1, the *S. cerevisiae* Rad53 C-terminal peptide presents the highest affinity (~100 nM, Table 1) compared to the FHA1 binding site and also compared to that of human and *S. pombe* HirA/p60-CAF-I B-domain peptides for Asf1 (~2 μM) (2, 18). Based on the structure of Rad53, HirA, and p60-CAF-I B-domain peptides in complex with Asf1, we derived a new minimal sequence motif (R/K)R(I/A/V)x(L/P) that we call the AIP box (Asf1-Interacting Protein box), for peptides potentially able to bind this same surface of Asf1 (Fig. S3B). In the three founding members of the AIP box family, namely Rad53, HirA and p60-CAF-I, mutation of the central arginine residue or the two hydrophobic residues in positions i+1 and i+3 abolishes the binding of the peptide to Asf1 (Table 1) (2, 18). This small degenerate binding motif could be compared to the well-characterized PCNA PIP box that is found in many proteins associated with the replication fork with binding affinities to PNCA in the same range as the AIP-box to Asf1 (100 nM to 50 μM) (26). The AIP-box is too degenerate to identify novel Asf1 binding partners by searching in the large database of non-redundant protein sequences. However, we found this motif in a subset of proteins that bind Asf1 in an unknown manner (Table S2). It is now possible to mutate these potential AIP boxes to assess their functional importance. Interestingly, the Rad53 AIP box is conserved only in yeast species, consistent with the fact that the human Chk2 ortholog was not found in a complex with Asf1 (6).

Phe-820 of Rad53 also competes with Phe-100 of histone H4 for binding to a distinct surface of Asf1N. It is unlikely that the Rad53 C-terminal peptide is able to compete with binding of the heterodimeric H3-H4 to Asf1N that occupies a much greater surface than that of the F_{820} binding pocket. However, the Asf1-V_{94}R mutant is defective in both histone H3 and Rad53 binding. Since Asf1-V_{94} is distal to the surface bound by the Rad53 C-terminus, an additional region of Rad53 likely interacts with the H3 binding epitope on Asf1N. Similarly, it was suggested that in addition to its AIP box, other regions of HirA must contribute to its interaction with Asf1 and impart a specificity for binding to the mammalian Asf1a isoform (2).

Rad53 and Asf1 are found in a complex in yeast cells in the absence of genotoxic stress. Our data indicate that Rad53 competes with histones H3-H4 and the co-chaperones HirA and CAF-I for binding to Asf1. We found that the Asf1-Rad53 complex was dissociated when cells were treated with hydroxyurea, a ribonucleotide reductase inhibitor, but not when cells were treated with the methylating agent MMS. Rad53 is activated by phosphorylation at multiple sites in response to genotoxic stress. Some sites, such as a T-loop phosphorylation, are probably necessary for Rad53 activation in all situations. However, other phosphorylations are specific to cells treated with the UV-mimetic 4-nitro-quinoline 1-oxide or with MMS (9, 14). Some phosphorylation sites specific to HU treatment may explain the dissociation of the Asf1-Rad53 complex in this condition relative to MMS. A phospho-mimetic mutant at putative phosphorylation sites in the C-terminus of Rad53 did

not lead to dissociation of Asf1. Thus, we suggest that phosphorylation within the putative third interaction surface in the Asf1-Rad53 complex is required for dissociation of the complex in presence of HU. Dissociation of the Asf1-Rad53 complex would increase the pool of Asf1 competent for binding histones and other partners, and could also modify the ability of Rad53 to phosphorylate specific substrates. The identification of Rad53 phosphorylation sites that are specific to HU-treated cells would allow further testing of this model.

Our structure of Asf1N in association with the Rad53 C-terminal peptide allowed us to identify residues important for the stability of the complex. The *rad53-ALRR* mutation disrupts an important hydrophobic contact and destabilizes the Asf1-Rad53 complex in yeast cells. Although this mutant did not have an obvious phenotype on its own, we found that it increased the resistance to genotoxic stress of *rad9* and *rad24* mutants. Rad9 and Rad24 are implicated in activation of Rad53 in response to DNA double-strand breaks (25). In asynchronously growing cells, we observed only modest decreases in Rad53 phosphorylation in the *rad9 rad24* mutant treated with HU or MMS compared to wild type cells, presumably because Rad53 is still efficiently activated by Mrc1 at stalled replication forks in these cells (24). The *rad53-ALRR* mutation did not significantly modify the profile of Rad53 phosphorylation, so the increased viability of *rad53-ALRR rad9 rad24* mutants exposed to MMS or HU may not be through effects on Rad53 activity. We favor the hypothesis that the decreased stability of the Rad53-Asf1 interaction in the *rad53-ALRR* mutant increases cell viability through increased tolerance or repair of lesions (including reconstitution of chromatin structure) provoked by HU or MMS in the *rad9 rad24* mutants. This could presumably occur by the increased availability of Rad53 or Asf1 to interact with its multiple alternative partners at the levels of DNA metabolism and chromatin.

Materials and Methods

Detailed information is provided in the Supplementary Methods.

Data deposition: The atomic coordinates and structure factors have been deposited in the Protein Data Bank in Europe (PDBe), www.ebi.ac.uk/pdbe (PDB ID code ###).

Acknowledgements

We thank John Diffley for the generous gift of anti-Rad53 serum, and Oscar Aparicio, Paul Kaufman, Robert Sclafani, Katsunori Sugimoto for plasmids, and Steve Elledge, Claiborne Glover, Maria Pia Longhese, and Neal Lowndes for yeast strains. We thank the Imagif platform for access to the crystallization robot. We thank Pierre Legrand for useful advice at the PROXIMA1 beamline of the SOLEIL synchrotron. We thank the SOLEIL synchrotron and ESRF (beamlines ID29 and ID23) for beam time for recording preliminary diffraction data. We thank the TIGR for providing NMR time at 800MHz and we thank Carine van Heijennort for her help for setting up NMR filtered experiments. We thank Brice Murciano, Marie-Helene LeDu and Jean-Baptiste Charbonnier for their

help in crystallogenesis and crystallography, and Othman Rechiche and Simona Miron for their help in calorimetry. We are grateful to Jean-Yves Thuret and Armelle Lengronne for comments on this manuscript. Y.J. was supported by the CEA International doctoral program. K. S was supported by the CEA. This work was supported by grants from the French National Research Agency ANR- 07-BLAN-0098-01 to C.M and ANR-07-JCJC-0126 to F. O. and the French Association for Research on Cancer ARC 4916 to C.M. and ARC 8006 to F. O.

References

1. Mousson F, *et al.* (2007) The histone chaperone Asf1 at the crossroads of chromatin and DNA checkpoint pathways. *Chromosoma* 116(2):79-93.
2. Tang Y, *et al.* (2006) Structure of a human ASF1a-HIRA complex and insights into specificity of histone chaperone complex assembly. *Nat Struct Mol Biol* 13(10):921-929.
3. Akai Y, *et al.* (2010) Structure of the histone chaperone CIA/ASF1-double bromodomain complex linking histone modifications and site-specific histone eviction. *Proc Natl Acad Sci U S A* 107(18):8153-8158.
4. Emili A, *et al.* (2001) Dynamic interaction of DNA damage checkpoint protein Rad53 with chromatin assembly factor Asf1. *Mol Cell* 7(1):13-20.
5. Hu F, *et al.* (2001) Asf1 links Rad53 to control of chromatin assembly. *Genes Dev* 15(9):1061-1066.
6. Groth A, *et al.* (2005) Human Asf1 regulates the flow of S phase histones during replicational stress. *Mol Cell* 17(2):301-311.
7. Sillje HH & Nigg EA (2001) Identification of human Asf1 chromatin assembly factors as substrates of Tousled-like kinases. *Curr Biol* 11(13):1068-1073.
8. Sharp JA, *et al.* (2005) Regulation of histone deposition proteins Asf1/Hir1 by multiple DNA damage checkpoint kinases in S. cerevisiae. *Genetics* 171(3):885-899.
9. Sweeney FD, *et al.* (2005) Saccharomyces cerevisiae Rad9 acts as a Mec1 adaptor to allow Rad53 activation. *Curr Biol* 15(15):1364-1375.
10. Schwartz MF, *et al.* (2003) FHA domain-mediated DNA checkpoint regulation of Rad53. *Cell Cycle* 2(4):384-396.
11. Liao H, *et al.* (2000) Structure of the FHA1 domain of yeast Rad53 and identification of binding sites for both FHA1 and its target protein Rad9. *J Mol Biol* 304(5):941-951.
12. Durocher D, *et al.* (2000) The molecular basis of FHA domain:phosphopeptide binding specificity and implications for phospho-dependent signaling mechanisms. *Mol Cell* 6(5):1169-1182.
13. Aucher W, *et al.* (2010) A strategy for interaction site prediction between phospho-binding modules and their partners identified from proteomic data. *Mol Cell Proteomics* 9(12):2745-2759.
14. Smolka MB, *et al.* (2005) Dynamic changes in protein-protein interaction and protein phosphorylation probed with amine-reactive isotope tag. *Mol Cell Proteomics* 4(9):1358-1369.
15. Guillemain G, *et al.* (2007) Mechanisms of checkpoint kinase Rad53 inactivation after a double-strand break in Saccharomyces cerevisiae. *Mol Cell Biol* 27(9):3378-3389.
16. Zhang R, *et al.* (2007) Molecular dissection of formation of senescence-associated heterochromatin foci. *Mol Cell Biol* 27(6):2343-2358.
17. Krogan NJ, *et al.* (2006) Global landscape of protein complexes in the yeast Saccharomyces cerevisiae. *Nature* 440(7084):637-643.
18. Malay AD, *et al.* (2008) Crystal structures of fission yeast histone chaperone Asf1 complexed with the Hip1 B-domain or the Cac2 C terminus. *J Biol Chem* 283(20):14022-14031.
19. Natsume R, *et al.* (2007) Structure and function of the histone chaperone CIA/ASF1 complexed with histones H3 and H4. *Nature* 446(7133):338-341.
20. English CM, *et al.* (2006) Structural basis for the histone chaperone activity of Asf1. *Cell* 127(3):495-508.
21. Mousson F, *et al.* (2005) Structural basis for the interaction of Asf1 with histone H3 and its functional implications. *Proc Natl Acad Sci U S A* 102(17):5975-5980.
22. Agez M, *et al.* (2007) Structure of the histone chaperone ASF1 bound to the histone H3 C-terminal helix and functional insights. *Structure* 15(2):191-199.

23. Galvani A, *et al.* (2008) In vivo study of the nucleosome assembly functions of ASF1 histone chaperones in human cells. *Mol Cell Biol* 28(11):3672-3685.
24. Alcasabas AA, *et al.* (2001) Mrc1 transduces signals of DNA replication stress to activate Rad53. *Nat Cell Biol* 3(11):958-965.
25. Navadgi-Patil VM & Burgers PM (2009) A tale of two tails: activation of DNA damage checkpoint kinase Mec1/ATR by the 9-1-1 clamp and by Dpb11/TopBP1. *DNA Repair (Amst)* 8(9):996-1003.
26. Bruning JB & Shamoo Y (2004) Structural and thermodynamic analysis of human PCNA with peptides derived from DNA polymerase-delta p66 subunit and flap endonuclease-1. *Structure* 12(12):2209-2219.

Figure Legends

Fig. 1. Rad53 and Asf1 interact through at least two binding sites. *(A)* Schematic representation of the different constructs of Asf1 and Rad53 produced in *E. coli* for pull-down assays. *(B)* GST pull-down assays with GST, GST-Asf1, GST-Asf1N and different 6His-tagged fragments of Rad53. The asterisk indicated a dimeric form of GST and the double asterisk indicates a GST-Asf1 degradation product. *(C)* GST-pull-down assays with GST, GST-FHA1, GST-Rad53-C-ter, and yeast extracts expressing Asf1-myc. The asterisk corresponds to a degradation product of GST-C-ter. *(D)* GST pull-down assay with GST (control) and GST-FHA1 (Pull-down) of yeast extracts expressing Asf1-myc full length, Asf1N-myc, or Asf1-myc mutated on threonine residues of the C-terminal tail as indicated. The pull-down was performed with extracts from the wild-type or *cka1! cka2-ts* (thermosensitive mutant of *CKA2*) mutants expressing or not WT *CKA2* from a plasmid, and with the addition of calf intestinal phosphatase to cell extracts where indicated (*CKA2* + CIP).

Fig. 2. Crystal structure of Asf1N in complex with the C-terminus of Rad53(800-821). *(A)* Cartoon representation of Asf1 (in grey) bound to Rad53(800-821) in orange. Dashed lines are used to materialize the peptide chain between the two binding epitopes. Important Rad53 residues are labeled. *(B)* Detail of the interface delineated in panel A. In the crystal structure, the peptide bridges epitopes on two different Asf1 molecules, but NMR solution analyses indicate that the peptide normally binds a single Asf1 molecule (see Sup. Data and Fig. S4). Hydrophobic side chains are shown as spheres, polar and charged residues as sticks. Polar contacts are shown as yellow dashed lines. Residue labels are indicated. *(C)* Cartoon representation of Asf1 (in grey) bound to the HirA B domain (in green) and to the H3 (in rose)-H4 (in magenta) complex. Residues overlapping with Rad53 are indicated.

Fig. 3. Putative third interaction surface involving the H3-binding surface of Asf1 and the kinase domain of Rad53. *(A)* Cartoon representation of Asf1 (in grey) bound to the Rad53-K_{804}-S_{812} peptide (in orange) and to the H3 (in rose)-H4 (in magenta) complex. Residues that were mutated to test their effect on Rad53 binding are shown with spherical atoms for N (blue), O (red), and C (grey). *(B)* Co-immunoprecipitation of Rad53 and histone H3 with the indicated mutants of Asf1-myc. Input indicates proteins in total cell extracts. IP indicates proteins co-precipitating with Asf1-myc on anti-myc beads. Asf1 is tagged with a 13-myc epitope, except for the A_{128}D-K_{129}D and

R123E mutants that have fewer repetitions of the myc epitope. *(C)* Rad53 co-precipitates with Asf1 in extracts from a histone H3-R129E (*hht2-R129E*) mutant that cannot bind Asf1. *(D)* Schema of tripartite model for the Asf1-Rad53 interaction. The question mark indicates that the putative interface between Asf1N and
the kinase domain of Rad53 awaits further experimental verification.

Fig. 4. Dissociation of the Asf1-Rad53 complex when cells are treated with HU but not MMS, and destabilization of the complex by the *rad53-ALRR* mutation and its phenotypic consequences. *(A)* Asf1-myc was immunoprecipitated from extracts of control cells and cells treated with 200 mM HU for 2 h at 30 ℃ (left panel) or with increasing MMS (0.05%, 0.1%, 0.15%, 0.2% final concentration) for 1 h at 30 ℃ (middle panel). Right panel: Wild-type Rad53 and the Rad53-TSSDEE (T811D+S812E+S821E) mutant co-precipitate with the Asf1-T265A+T270A-myc non-phosphorylatable mutant that is defective in binding Rad53-FHA1. *(B) Rad53-ALRR* (A806R+L806R) does not co-immunoprecipitate with Asf1-myc in conditions allowing efficient co-immunoprecipitation of wild-type Rad53. *(C) rad53-ALRR* increases the growth of *rad9* and *rad24* mutants in the presence of MMS or HU. *(D)* Only minor differences in Rad53 phosphorylation in W303 wild type, *rad9 rad24*, *rad53-ALRR*, and *rad53-ALRR rad9 rad24* yeast strains during normal growth or after treatment with 200 mM HU for 2 h at 30 ℃ or with 0.05% MMS for 1 h at 30 ℃.

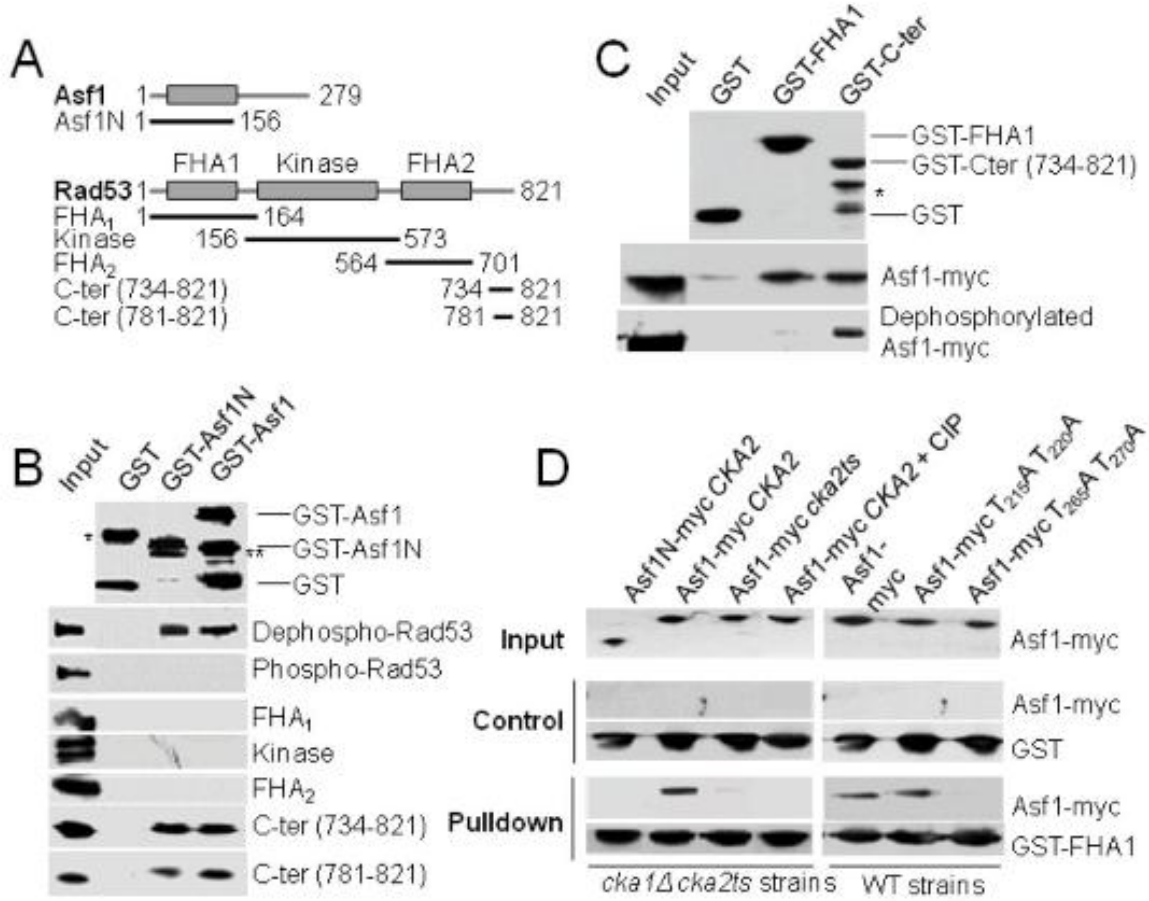

Figure 1.

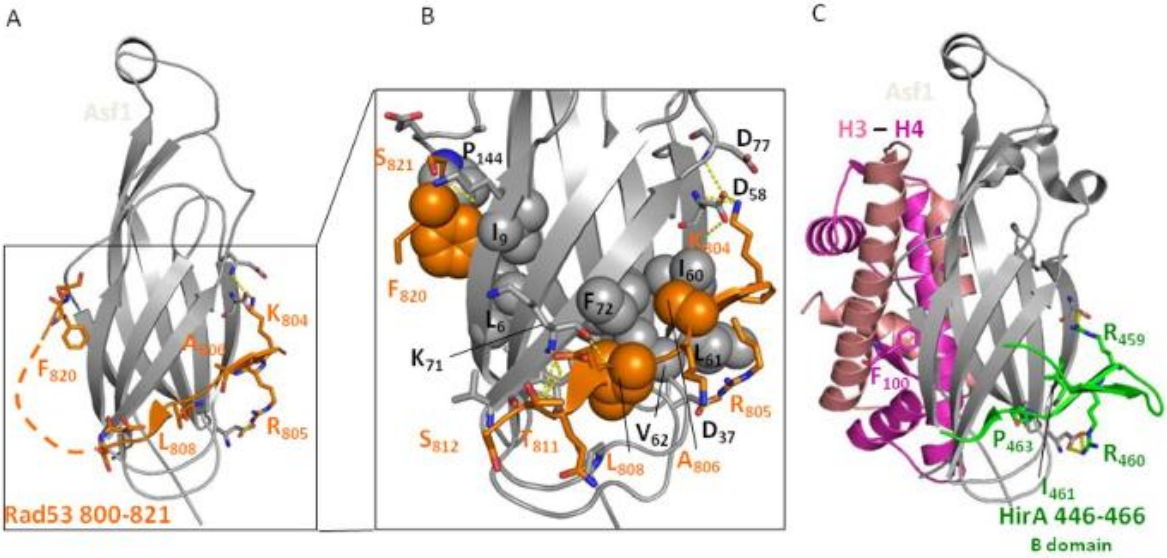

Figure 2.

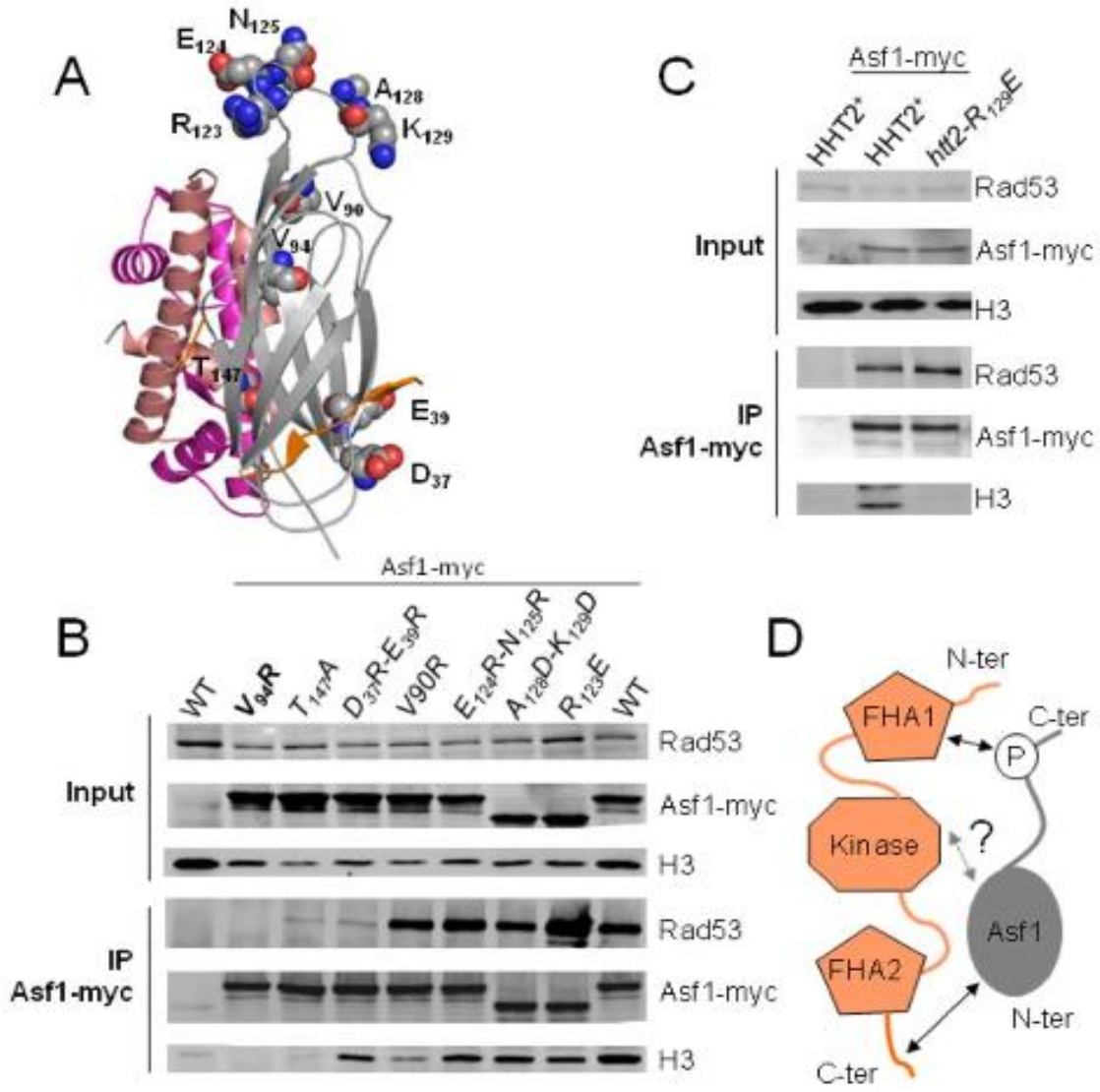
A
N125
E124
A128
R123
K129
V90
V94
T147
E39
D37
B
Asf1-myc
WT
V94R
T147A
D37R-E39R
V90R
E124R-N125R
A128D-K129D
R123E
WT
Input
IP
Asf1-myc
Rad53
Asf1-myc
H3
C
Asf1-myc
HHT2*
HHT2*
hht2-R129E
Input
IP
Asf1-myc
Rad53
Asf1-myc
H3
D
N-ter
FHA1
C-ter
P
Kinase
?
Asf1
FHA2
N-ter
C-ter

Figure 3.

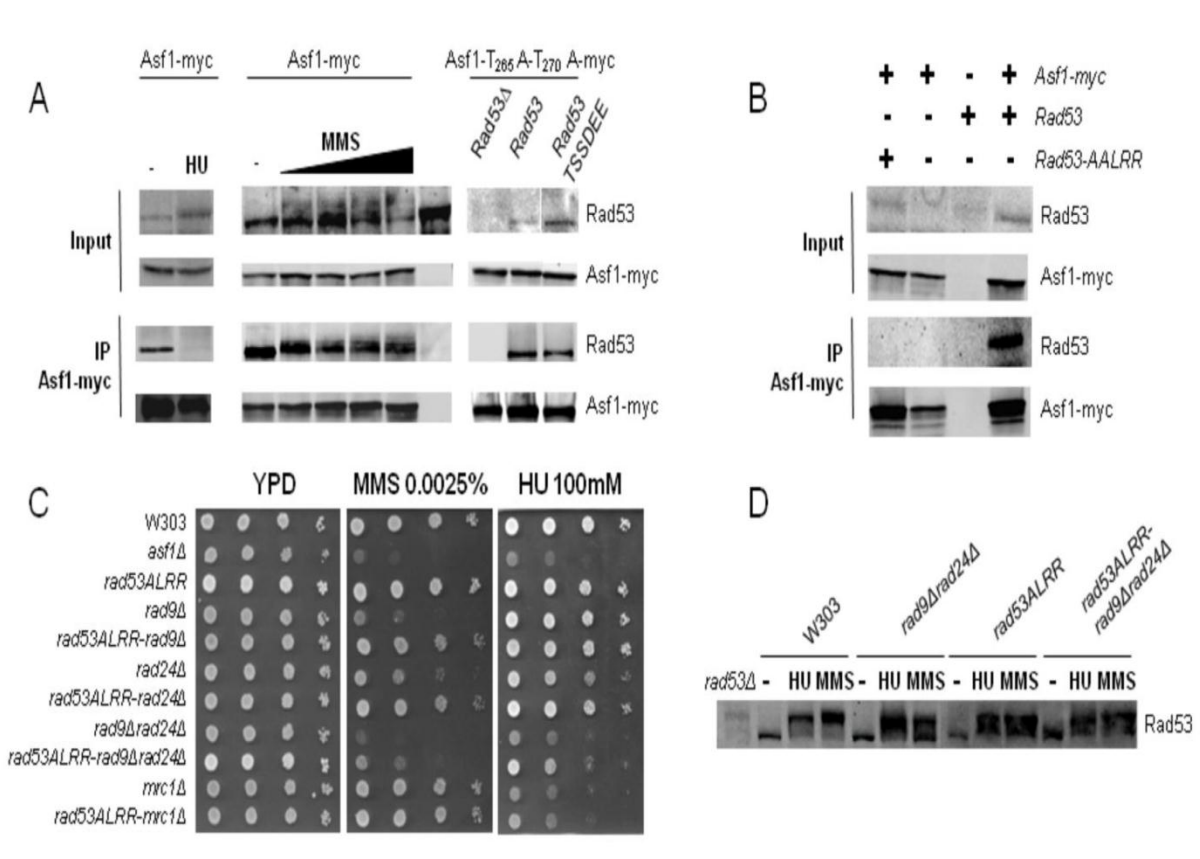

Figure 4.

Table Legends

Table 1. Summary of ITC data for Asf1N binding to C-terminal fragments of Rad53

Table 1

Peptide	Kd (μM) *	Kd ratio +	ΔH (kCal.M^{-1})
Rad53 800-821	0.08(±0.03)	1	-10.8(±0.1)
Rad53 781-821	0.28(±0.05)	3	-9.1(±1.2)
Rad53 800-811	0.42 (±0.06)	5	-3.5(±0.1)
Rad53 811-821	undetectable	ND$	ND$
Rad53 800-821 $A_{806}R$-$L_{808}R$	7.1 (±0.5)	89	-3.1(±0.2)
Rad53 800-821 $R_{805}A$	11.6 (±1)	145	-3.8(±0.9)
Rad53 800-821 $R_{805}D$	undetectable	ND$	ND$
Rad53 800-821 $F_{820}A$	0.58 (±0.4)	7	-2.9(±0.9)

* binding stoichiometry was found N≈1 (±0.1) for all peptides
+ ratio of the Kd with that of the reference peptide Rad53 800-821
$ND = not determined.

Supplementary Results

NMR Characterization of the complex of Rad53 FHA1 (1-164) with Asf1 (266-277)

No chemical shift variation of the FHA1 ^{1}H-^{15}N heteronuclear single-quantum coherence spectrum (HSQC) amide resonances was observed upon addition of the unphosphorylated Asf1 peptide ^{266}DIESTPKDAARS^{277} (Sup. Fig S2B). In contrast, a few FHA1 amide resonances shifted upon the

addition of the phosphorylated Asf1 peptide (pT(Asf1) ^{266}DIES(pT)PKDAARS^{277})(Sup. Fig S2C). The ^{1}H-^{15}N HSQC of the free FHA1 domain was nearly identical to the one published (1), thus allowing the assignment of at least five signals corresponding to R35/NHe, R70/NHe, N86, S85, and G133. The chemical shift variations observed after addition of pT(Asf1) were virtually identical in magnitude and direction to those observed for pT(Rad9) (1) or pT(Ptc2) (2). In particular, S85, N86, and the side chain proton of R70 (involved in the binding of the phosphate group of the phospho-threonine) showed large chemical shift variations, whereas the signal corresponding to NH$ of R35 remained unchanged. These data indicated a similar binding mode for pT(Asf1), pT(Ptc2) and pT(Rad9).

Dynamic analysis of the Rad53 C-terminal peptide (800-821) bound to Asf1N by NMR

In the crystal structure, two Rad53(800-821) peptides were found swapped between two Asf1 molecules (Sup. Fig. S4). We thus asked if the peptide could promote Asf1 dimerization in solution by analyzing the same complex using NMR spectroscopy. The Asf1 amide chemical shift changes upon Rad53(800-821) binding showed that, in solution, the regions of Asf1 perturbed by the peptide are those predicted by the crystal structure of the complex, confirming that the binding mode is similar in solution (Sup. Fig. 5A). In addition, we recorded and assigned some intermolecular nuclear Overhauser effects (NOEs) that were fully compatible with the X-ray structure (data not shown). ^{15}N-^{1}H heteronuclear relaxation parameters (R_1, R_2 and NOEs) of uniformly ^{15}N labeled Asf1N allowed the calculation of the global correlation time of free and bound Asf1 (Sup. Fig. 5B). These were fully compatible with the formation of a heterodimeric Asf1-Rad53 complex (Sup. Fig. 4C). We thus conclude that the swapping of Rad53 (800-821) observed in the crystal structure is an artefact of crystal packing and that the peptide wraps around one Asf1 molecule (Fig. 2A, Sup. Fig. S4B). We were unable to define by NMR spectroscopy the precise conformation of the linker between the two epitopes because of the lack of intermolecular NOE and short range NOE (data not shown). We thus analyzed the dynamic behaviour of the uniformly ^{15}N labelled free and bound Rad53(800-821) peptide (Sup Fig. 5C). ^{1}H-^{15}N heteronuclear relaxation parameters together with the HN chemical shifts clearly show that the free Rad53 peptide is unfolded and folds upon Asf1 binding. Values of R_1, R_2 and ^{15}N-^{1}H heteronuclear NOEs of the bound peptide are compatible with a tight Asf1 binding with a significant exchange contribution (see Lipari Szabo analysis Sup. Fig. 5D). Fluctuating ends corresponding to residues 800-805 and 819-821 are observed, even though the 819-821 segment corresponds to the second Asf1 binding epitope. This epitope is thus highly dynamic, consistent with its ability to swap with a second Asf1 molecule in the crystal packing.

Supplementary Materials and Methods

Protein expression and Purification for crystallization experiments.

Production and purification of recombinant proteins for structural studies, isothermal calorimetry (ITC) and pull-down experiments was performed with the same procedure. Uniformly ^{15}N and ^{15}N-^{13}C labelled Asf1(1-156) and Rad53(800-821) was also performed with the same protocol, except that the cellular culture was performed in minimal mediu(M9) supplemented with ^{15}N ammonium chloride and/or ^{13}C glucose. Recombinant soluble (His)6-tagged GST fusion proteins expressed from pETM30 (gift from G. Stier, EMBL Heidelberg) constructs were immobilized on GSH agarose (Sigma) and then eluted with an excess of glutathione (Sigma). They were cleaved using a (His)6-tagged TEV protease (1% w/w of protease / fusion protein). A Ni-NTA agarose column (Qiagen) was used to trap the (His)$_6$-tagged TEV protease and the (His)6-tagged GST as described (3). For structural biology and ITC experiments, an additional final purification step using either ion exchange chromatography (resource Q, GE Healthcare) or reverse phase chromatography (proRPC 16/10, GE Healthcare) was performed for Asf1 and the Rad53 peptides respectively, as decribed (4, 5)). Unlabeled Rad53 peptides used for ITC, NMR or crystallization trials were obtained by chemical synthesis (Genecust). The peptide and protein concentrations were precisely measured by amino acid analysis.

Crystallization and Data Collection

Purified Asf1 (1-156) was concentrated to 9 mg/mL in a 3 kDa limit concentrator (Millipore) and buffer exchanged to 50 mM Tris 50-pH 7.4. The protein was incubated 1 hour at room temperature with a 1x Protease inhibitor cocktail (Roche). The peptide was solubilized in water, the pH was adjusted to ~7.4, lyophilized and resuspended in water to the final concentration of 10 mg/ml. Concentrated peptide was added to the protein at a final ratio of one Asf1 molecule for three Rad53 peptide molecules. Crystals of the complex were grown by sitting drop vapour diffusion at 20 ℃ against reservoir solution containing 35% PEG 4000, 0.1M Na Acetate-pH 4.6, 0.2 M NH_4 sulphate. Crystals were grown for several days and reached sizes of 100!m x 40!m x 40!m. Crystals were then flash-frozen in liquid nitrogen after cryo-protection with glycerol supplemented reservoir solution. Diffraction data were collected on the Proxima1 beamline at the SOLEIL synchrotron (Gif-sur-Yvette, France). Crystals belonged to space-group C121 and diffracted up to 2.94Å resolution (see Sup. Table 1). All data were processed and integrated using XDS (Sup. Table S1) (6).

X-ray Structure Determination and Refinement

Structure resolution was carried out using molecular replacement using the structure of yeast Asf1 as search model (pdb code 1ROC). Four proteins per asymmetric unit were found. The structure was refined and the peptide model was built using the software Buster with non crystallographic symmetry constrains and TLS (Sup. Table S1) (7) and visualized with the software Coot (8). Structure representations presented in the paper were drawn with Pymol (http://pymol.sourceforge.net/).

NMR characterization of the complex of Asf1 (1-156) with Rad53 (800-821)

NMR samples were prepared in the following buffer: Tris D_{11} 10 mM, pH 7.4, NaN3 0.1%, EDTA 1 mM, DSS 0.1 mM. D_2O 10% or 100%. Several samples were used in this study: uniformly ^{15}N (or $^{15}N/^{13}C$) labeled yeast Asf1 (1-156) alone or in complex with unlabeled Rad53 (800-821), uniformly ^{15}N (or $^{15}N/^{13}C$) labeled Rad53 (800-821) in complex with unlabeled Asf1 (1-156). For these samples, the concentrations of the labeled and unlabeled molecules were 0.1 mM and 0.2 mM respectively. NMR experiments were carried out on Bruker DRX-600 MHz and 700 MHz spectrometers equipped with cryoprobes at 278 ℀K or 303 ℀K. ^{1}H, ^{15}N and ^{13}C backbone resonance assignments of free and Rad53(800-821) bound Asf1 were achieved using standard ^{15}N-^{1}H – HSQC, ^{15}N-edited NOESYHSQC (mixing time of 120 ms), HNCA, HN(CO)CA, CBCA(CO)NH, HNCO, HBHA(CO)NH, CBCACOHA and HNHA experiments. Side chain assignments were achieved using HCCH-TOCSY (mixing time of 10 ms), HCCH-COSY, and ^{13}C edited NOESY-HSQC experiments (mixing time of 120 ms). Proton chemical shifts (in ppm) were referenced relative to internal DSS and ^{15}N and ^{13}C references were set indirectly relative to DSS using frequency ratios (9). All NMR data were processed using Xwinnmr (Bruker) and analyzed using Sparky (T. D. Goddard and D. G. Kneller, University of California, San Francisco). Intermolecular NOEs were obtained by filtered edited experiments described in (10) (mixing time of 150 ms). They are fully compatible with the contacts observed in the crystal structure. Cumulative chemical shift variation of Asf1 amides upon Rad53(800-821) addition was calculated as $\Delta ™ = [(™_{HN^b}-™_{HN^f})^2 + (2.75(™_{H\langle^b}-™_{H\langle^f}))^2 + (0.17(™_{N^b}-™_{N^f}))^2]^{1/2}$, where b and f refer to the bound and free form respectively. The scaling factors normalize the magnitude of the $^{1}H_N$, $^{1}H\langle$ and ^{15}N chemical shift changes (in ppm unit) (11). ^{15}N-^{1}H heteronuclear relaxation data R_1, R_2 and ^{15}N-^{1}H heteronuclear NOEs of free and bound Asf1, and free and bound peptide were measured at 700 Mhz with the standard Bruker pulse scheme in an interleaved 3D experiment using a recycle delay of 4 s. R_1 values were calculated from fits of 12 relaxation delays of 1, 1, 20, 50, 100, 200, 350, 500, 800, 1000 and 1500 ms. R_2 values were calculated from fits of 11 relaxation delays of 16, 16, 32, 49, 65, 81, 98, 130, 228 and 326 ms. Data were analysed with a macro of the Sparky software (T. D. Goddard and D. G. Kneller, SPARKY 3, University of California, San Francisco). The Lipari and Szabo analysis was performed with the in house Matlab macro as described (12).

NMR Characterization of the complex of Rad53 FHA1 (1-164) with Asf1 (266-277)

NMR sample was prepared in the following buffer: phosphate 10 mM, pH 6.5, DTT 1 mM, NaN_3

0.1%, EDTA 1 mM, DSS 0.1 mM. D_2O 10%. The concentration of uniformly ^{15}N labeled FHA1 domain was 163 ∝M. Phosphorylated or unphophorylated ^{266}DIES(pT)PKDAARS^{277} peptide derived from Asf1 sequence pT(Asf1), obtained by chemical synthesis (Genecust), was progressively added with a molar ratio at the end of the titration of 1:3.4. NMR experiments were carried out on a Bruker Advance-700 spectrometer equipped with a cryoprobe at 293 ℃K. Experimental conditions were identical to those used for the structure determination by NMR spectroscopy of FHA1 in complex with a tight binding peptide from Rad9 in (1, 2).

Isothermal Titration Calorimetry (ITC) experiments.
ITC experiments were performed using a MicroCal VP-ITC instrument (GE Healthcare) at 5 ℃ for the interaction with the C-terminal peptides of Rad53 and 303 ℃K for the interaction of FHA1 with the phosphorylated Asf1 peptide. A 15 µM solution of the FHA1 or Asf1(1-156) domains in buffer Tris 50 mM, pH 8 and Tris 50mM, pH 7.4 respectively was introduced in the calorimeter cell (1.337 mL) and was titrated by a 200 µM and 250 µM respectively solution of Asf1 or Rad53 C-terminal peptides respectively using automatic injections of 6 µL. Integration of the peaks corresponding to each injection and correction for the baseline were done using Origin-based software provided by the manufacturer. Fitting of the data to an interaction model results in the stoichiometry (N), equilibrium binding constant (K_a) and enthalpy of complex formation (ΔH). The experimental data allow calculation of the free energy change (ΔG) and of the entropy term (TΔS) according to the classical thermodynamic formulae: $\Delta G = -RT \times \ln K_a$; $\Delta G = \Delta H - T\Delta S$, where R is the universal gas constant and T is the absolute temperature. All experiments were repeated twice with similar results.

GST pull-down assays.
40 ∝g of purified $(His)_6$-GST-fusion proteins were immobilized on GSH agarose and equilibrated with 200 ∝l of buffer H150 (20 mM Hepes-NaOH, pH 7.4, 150 mM NaCl, 0.5% NP40, 1 mM EDTA, 1mM DTT). *E. coli* (1 mg) or *S. cerevisiae* (1 mg) cellular extracts solubilized in the same buffer were added to beads. Beads were washed successively with buffers identical to buffer H150 with increasing NaCl concentration up to 300mM. The beads were collected by centrifugation, washed twice in 20 mM Hepes and two times in 20 mM Hepes, 50mM NaCl, 0.5% NP40. Bound proteins were analyzed by SDS-PAGE and revealed by a polyclonal antibody against the $(His)_6$ tag (Santa Cruz Biotech 8036-HRP) or by polyclonal antibody against the myc tag (Santa Cruz Biotech 9E10). Bound (His)6-tagged GST fusion proteins were also revealed by a polyclonal antibody against the $(His)_6$ tag.

Construction of mutants.
A 3.5 kb genomic *Eco*RI fragment containing the *RAD53* gene and flanking sequences was transferred from Yeplac195-*RAD53 (13)* to the pRS306 Integrating-*URA3* vector (14). This plasmid was then used as template for mutagenesis using the Stratagene QuikChange kit. pRS-*rad53-ALRR* was linearized within the *RAD53* promoter sequence by digestion with *Pac*I to target integration of the plasmid at the *rad53!::HIS3* locus of CMY1227. Transformants were then screened for loss of the pBAD70 (2µ-*TRP1*) plasmid. Construction of Asf1 mutants was described previously (5), as was the construction of the *hht2-R129E* mutant (4).

Yeast strains.
All strains were in the W303 background, except for CMY1389 and CMY1520 in the S288C background and CMY1357 and 1360 in the YPH250 background.

W303-1a *MATa ade2-1 his3-11,15 leu2-3, 112 trp1-1 ura3-1*
CMY1139 W303-1a ***rad53::HIS3 sml1-1***
CMY1155 W303-1a ***rad24::URA3***
CMY1156 W303-1a ***rad9::HIS3 rad24::URA3***
CMY1158 W303-1a ***rad9::HIS3***
CMY1227 W303-1a ***rad53::HIS3***/pBAD70 (2µ,*TRP1*)-*RNR1* Ref. (15)
CMY1396 W303-1a ***ASF1-3HA-kanMX6*** *bar1::LEU2 his3-11 leu2-3,112 lys2 trp1-1 ura3-1*
CMY1501 SEY1127 W303-1a ***mrc1!-3::his5+*** Ref. (16)

CMY1558 W303-1a ***rad53-TSSDEE::URA3::rad53!::HIS3***
CMY1561 W303-1a ***rad53-K227A::kanMX***
CMY1562 W303-1a ***rad53-ALRR::URA3::rad53!::HIS3***
CMY1563 W303-1a ***RAD53::URA3::rad53!::HIS3***
CMY1564 W303-1b ***rad53-ALRR::URA3::rad53!::HIS3***
CMY1565 W303-1 ***rad53-ALRR::URA3::rad53!::HIS3 mrc1!-3::his5+***
CMY1566 W303-1a ***rad53-ALRR::URA3::rad53!::HIS3 rad24::kanMX***
CMY1567 W303-1a ***rad53-ALRR::URA3::rad53!::HIS3 rad9::LEU2***
CMY1568 W303-1a ***rad53-ALRR::URA3::rad53!::HIS3 rad24::kanMX rad9::LEU2***
CMY1569 W303-1a ***rad9::LEU2***
CMY1570 W303-1a ***rad24::kanMX***
CMY1571 W303-1a ***rad24::kanMX rad9::LEU2***
CMY1364 W303-1b ***asf1!::kanMX***
CMY1389 FY2162 *MATa his3"200 leu2"1 ura3-52 trp1"63 lys2-128# Ty912.35-lacZ::his4* ***(hht1-hhf1)"::LEU2 (hht2-hhf2)"::HIS3***/pDM9=pRS416(CEN URA3)-***HHT1+HHF1*** Ref. (17)
CMY1520 MATa *his3"200 leu2"1 ura3-52 trp1"63 lys2-128# Ty912.35-lacZ::his4* ***(hht1-hhf1)"::LEU2 (hht2-hhf2)"::HIS3***/ pDM18 (CEN *TRP1*)-***hht2-R129E+HHF2***
CMY1357 YDH6 *ade2–101 his3-200 leu2-1 lys2–801 trp1-1 ura3–52* ***cka1-1::HIS3 cka2-1::TRP1***/ pCEN6-*LEU2*-***CKA2*** Ref. (18)
CMY1360 YDH13 *ade2–101 his3-200 leu2-1 lys2–801 trp1-1 ura3–52* ***cka1-1::HIS3 cka2-1::TRP1***/ pCEN6-*LEU2*-***cka2-13ts*** Ref. (18)

Co-immunoprecipitation experiments.

Figure 3B: W303-1a transformed by plasmids pRS314 (CEN-*TRP1*) containing *ASF1-myc*, or *asf1-V$_{94}$R-myc*, or *asf1-T$_{147}$A-myc*, or *asf1-D$_{37}$R+E$_{39}$R-myc*, or *asf1-V$_{90}$R-myc*, or *asf1-E$_{124}$R+N$_{125}$R-myc*, or *asf1-A$_{128}$D+K$_{129}$D-myc*, or *asf1-R$_{123}$E-myc* were grown in synthetic medium containing casamino acids, adenine, and uracil in order to maintain selection for plasmid pRS314, and harvested at an O.D. 600nm of 0.8. Cells were resuspended in 4 ml extraction buffer (50mM Tris pH 7.5, 100 mM NaCl, 10% glycerol, Roche protease inhibitor cocktail w/o EDTA) and broken in an Eaton press. Extracts were transferred to 50 Ti tubes and centrifuged (40 krpm, 1h, 4℃), and the protein concentration in the supernatant was determined with the Bradford reagent (Bio-Rad). Extracts (5 to 10 mg of protein for anti-myc IP in a final volume of 1 ml) were incubated with anti-myc beads that had been washed with extraction buffer on a rotating wheel O/N at 4℃. The beads were washed two times with 1 ml extraction buffer + 0.1% Tween-20 and immunoprecipitated proteins were solubilized by heating in the presence of sodium dodecyl sulfate-polyacrylamide gel electrophoresis (SDS-PAGE) sample buffer. Total cell extracts (40 μg) and immunoprecipitated proteins were seperated by SDS-PAGE, transferred to nitrocellulose membranes, incubated with goat anti-Rad53 yC-19 (Santa Cruz Biotechnology sc-6749) or mouse monoclonal 9E10 (anti-myc) antibodies followed by anti-goat or anti-mouse secondary antibodies. Proteins were detected using a Li-Cor Odyssey Imager.

Fig. 3C: CMY1389, CMY1389/pRS314-*ASF1-myc* and CMY1520/pRS316-*ASF1-myc* were grown in synthetic medium selecting for plasmids. Protein extracts and immunoprecipitates were prepared as described above. Membranes were incubated with rabbit anti-H3 antibody (Abcam ab-1791) followed by anti-rabbit secondary antibody.

Fig. 4A and Fig. S8: left and middle panels: W303-1a/pRS314-*ASF1-myc* was grown in 250 ml synthetic medium containing casamino acids, adenine, and uracil till an OD600 of 0.8. Cells were then incubated with MMS (0.05%, 0.1%, 0.15%, 0.2% final concentration) for 1h or 200 mM HU for 2h. Protein extracts and immunoprecipitates were prepared as described above.

Fig. 4A-right: CMY1227/pRS316-*asf1-T265/270A-myc*, W303-1a/pRS314- *asf1-T265/270A*-myc, CMY1558/ pRS314- *asf1-T265/270A* -myc were grown in synthetic medium selecting for plasmids where necessary, and protein extracts and immunoprecipitates were prepared as described above.

Fig. 4B: W303-1a, W303-1a/pRS314-*ASF1-myc*, CMY1562/pRS314-*ASF1-myc* and CMY1227/pRS314-*ASF1-myc* were grown in 250 ml medium selecting for plasmids where necessary, and protein extracts and immunoprecipitates were prepared as described above.

Fig. S6A: W303-1a, W303-1a/pRS316-*ASF1-myc*, CMY1139 *rad53Δ*/pRS316-*ASF1-myc*,

CMY1561 *rad53-K227A*/pRS314-*ASF1-myc*, CMY1139 *rad53Δ*/pRS314-*ASF1-myc*+pRS316-*rad53-K227A+D339A*, CMY1227/pRS314-*ASF1-myc* were grown in synthetic medium selecting for plasmids where necessary, and protein extracts and immunoprecipitates were prepared as described above.

Analysis of Rad53 Phosphorylation.
W303-1a, CMY1156, CMY1562, and CMY1568 were grown in YPD to an OD600 of 0.8. Cells were then incubated with MMS (0.05% final concentration) for 1h or with 200 mM HU for 2h. Yeast extracts were prepared by glass bead beating in 20% trichloroacetic acid (TCA), washing the glass beads in 5% TCA, and combining the wash with the lysate. The protein suspension was then pelleted, resuspended in 1x Laemmli loading buffer (pH8.8), boiled for 5 min, pelleted and the supernatant was retained as a whole-cell extract. Excess acid was neutralized with Tris buffer (pH8.8) when necessary. Protein extracts were resolved on 8% SDS-PAGE gels, and Rad53 was detected with an anti-Rad53 rabbit polyclonal antibody at 1 :10000 dilution. This antibody was initially generously provided by John Diffley (Cancer UK). We later obtained additional antiserum by immunizing rabbits with Rad53-6His protein purified from *E. coli*.

Analysis of Rad53 Dephosphorylation.
W303-1a and CMY1562 were grown in YPD. Cells were treated with %-factor (30 μM final) for 2h at 30 ℃ and then with 0.005% MMS for 30 min at 30 ℃. Pellets were washed two times with YPD and then released into fresh YPD. Cells were harvested at 0', 30', 60', 120' after release. Protein extracts were prepared by TCA precipitation as described above.

Phenotypic analysis.
For spotting analyses, cells were resuspended at 10^7/ml, subjected to 10-fold serial dilutions and 3 μl of each dilution was spotted on plates of YPD, YPD + 100 mM HU, and YPD + 0.0025% MMS. Growth was assayed at 72h.

Supplementary References
1. Yuan C, *et al.* (2001) Solution structures of two FHA1-phosphothreonine peptide complexes provide insight into the structural basis of the ligand specificity of FHA1 from yeast Rad53. *J Mol Biol* 314(3):563-575.
2. Guillemain G, *et al.* (2007) Mechanisms of checkpoint kinase Rad53 inactivation after a double-strand break in Saccharomyces cerevisiae. *Mol Cell Biol* 27(9):3378-3389. 3. Mousson F, *et al.* (2004) 1H, 13C and 15N resonance assignments of the conserved core of hAsf1 A. *J Biomol NMR* 29(3):413-414.
4. Agez M, *et al.* (2007) Structure of the histone chaperone ASF1 bound to the histone H3 C-terminal helix and functional insights. *Structure* 15(2):191-199.
5. Mousson F, *et al.* (2005) Structural basis for the interaction of Asf1 with histone H3 and its functional implications. *Proc Natl Acad Sci U S A* 102(17):5975-5980.
6. Kabsch W (1993) Automatic Processing of Rotation Diffraction Data from Crystals of Initially Unknown Symmetry and Cell Constants. *J Appl Crystallogr* 26:795-800.
7. Bricogne G, *et al.* (2010) BUSTER version 2.9Cambridge, United Kingdom). 8. Emsley P & Cowtan K (2004) Coot: model-building tools for molecular graphics. *Acta Crystallogr D Biol Crystallogr* 60(Pt 12 Pt 1):2126-2132.
9. Wishart DS, *et al.* (1995) 1H, 13C and 15N random coil NMR chemical shifts of the common amino acids. I. Investigations of nearest-neighbor effects. *J Biomol NMR* 5(1):67-81.
10. Zwahlen C, *et al.* (1997) Methods for Measurement of Intermolecular NOEs by Multinuclear NMR Spectroscopy: Application to a Bacteriophage lamba N-Peptide/boxB RNA Complex. *J. Am. Chem. Soc.* 119:6711-6721.
11. Farmer BT, 2nd, *et al.* (1996) Localizing the NADP+ binding site on the MurB enzyme by NMR. *Nat Struct Biol* 3(12):995-997.
12. Ochsenbein F, *et al.* (2001) 15N NMR relaxation as a probe for helical intrinsic propensity: the case of the unfolded D2 domain of annexin I. *J Biomol NMR* 19(1):3-18.
13. Sugimoto K, *et al.* (1997) Rfc5, a replication factor C component, is required for regulation of

Rad53 protein kinase in the yeast checkpoint pathway. *Mol Cell Biol* 17(10):5905-5914.
14. Sikorski RS & Hieter P (1989) A system of shuttle vectors and yeast host strains designed for efficient manipulation of DNA in Saccharomyces cerevisiae. *Genetics* 122(1):19-27.
15. Desany BA, *et al.* (1998) Recovery from DNA replicational stress is the essential function of the S-phase checkpoint pathway. *Genes Dev* 12(18):2956-2970.
16. Osborn AJ & Elledge SJ (2003) Mrc1 is a replication fork component whose phosphorylation in response to DNA replication stress activates Rad53. *Genes Dev* 17(14):1755-1767.
17. Duina AA & Winston F (2004) Analysis of a mutant histone H3 that perturbs the association of Swi/Snf with chromatin. *Mol Cell Biol* 24(2):561-572.
18. Rethinaswamy A, *et al.* (1998) Temperature-sensitive mutations of the CKA1 gene reveal a role for casein kinase II in maintenance of cell polarity in Saccharomyces cerevisiae. *J Biol Chem* 273(10):5869-5877.
19. Daragan VA & Mayo KH (1997) Motional model analysis of protein and peptide dynamics using ^{13}C and ^{15}N NMR relaxation. *Progress in NMR Spectroscopy* 31:63-105.
20. Crooks GE, *et al.* (2004) WebLogo: a sequence logo generator. *Genome Res* 14(6):1188-1190.

DATA collection statistics	
space group	*C121*
Cell parameters: *a* (Å), *b* (Å), *c* (Å), α (deg), β (deg), γ (deg)	125.24, 98.18, 86.49, 90.0, 132.49, 90.0
resolution	38.90-2.94 (3.12-2.94)
Nb unique reflections	16378 (2582)
data redundancy	3.96 (3.82)
Average I/sigma(I)	10.59 (2.36)
Overall completeness %	98.7 (97.5)
Rmerge (%)	21.3 (91.8)
Wavelength (Å)	0.90
Diffraction agreement	
Rfact (%)	18.8
Rfree (%)	25.5
Average B factor	54.3
Stereochemistry (rms deviation)	
Bond length rms(Å)	0.010
Bond angle rms (deg.)	1.33
Ramachandran statistics	
Most-favoured regions (%)	91.98
Additionally allowed regions (%)	4.78
Disallowed regions (%)	3.24
PDB accession code	###

Supplementary Table S1 : Summary of data collection and refinement statistics

gi|6325104|	Rad53p [Saccharomyces cerevisiae]	795 SQIDPSKKVKRAKLDQTSKGPENLQFS 821
gi|6319463|	Hir1p [Saccharomyces cerevisiae]	481 AILNKAVTLKSGKKRVAPTLISTSSS 506
gi|24640390|	hira [Drosophila melanogaster]	430 KDGKRRITPMFI 441
gi|45385815|	protein HIRA [Gallus gallus]	458 GRRRITPLCIA 468
		769 RRLLPPII 776
gi|21536485|	protein HIRA [Homo sapiens]	445 LLKKQVETRTADGRRRITPLCIA 467
gi|24652458|	Caf1-105 [Drosophila melanogaster]	729 RRVSLRTISTPKS 741
gi|4885105|	CAF-1 p60 [Homo sapiens]	494 KTTPRRINLTPLKTDT 509
		482 RRVTLNTLQAWS 493
gi|50513245|	CAF 1 subunit A [Homo sapiens]	29 VKKLIQARLPFKRLNL 44
gi|6323534|	Cac2p [Saccharomyces cerevisiae]	456 SKKRRIHPT 464
gi|18858189|	Caf1-180 [Drosophila melanogaster]	1125 KKRATLIM 1132
gi|57222570|	codanin-1 [Homo sapiens]	195 RRINPTPVSEERS 207
		687 RRAVLTV 693
gi|6320956|	Kap123p [Saccharomyces cerevisiae]	372 ERRAILLAISVA 383
gi|6325116|	Ypl141cp [Saccharomyces cerevisiae]	289 LLRRMLVSDPKKRINLKQI 307
gi|187830909|	p53 isoform f [Homo sapiens]	173 KRALPNNTSSS 183
gi|115583683|	MMS22-like [Homo sapiens]	54 KRLILNL 60
gi|6322293|	Set2p [Saccharomyces cerevisiae]	462 INVAASKMIDLRRVRL 477
gi|125490392|	POU dom, cl 5, TF [mus musculus]	148 QKRITL 153
gi|17137132|	mcm 2 [Drosophila melanogaster]	873 KRRIILQIV 881
gi|6320996|	Spt15p [Saccharomyces cerevisiae]	46 IKRAAPE 52
gi|18858131|	CG3815 [Drosophila melanogaster]	263 TRSCKRAPL 271

Supplementary Table S2 : Possible Asf1 binding interaction Epitope within Asf1 partners. Potential Asf1 partners were extracted from the Biogrid data bases (214 sequences). Search of the motif (R/K)R(A/I/V)x(L/P) (x being any residue) according to the extended sequence (sup Fig. S3B) was performed with the software phi blast.

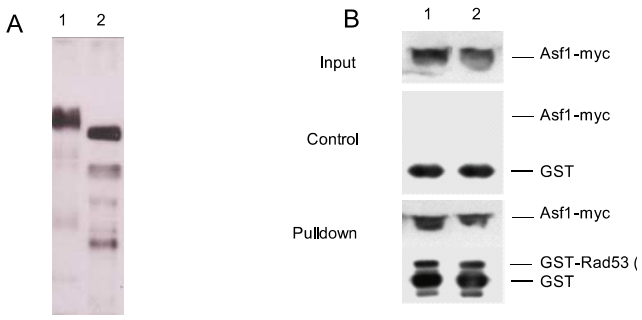

Fig. S1: Further in vitro analysis of the Asf1-Rad53 interaction:

A: Recombinant Rad53 is auto-phosphorylated in *E. coli*. Western blot analysis of *E. coli* extracts overexpressing Rad53 before (lane 1) and after incubation for 30 minutes at 30°C with calf intestinale phosphatase (lane 2). Rad53 was revealed with an anti-Rad53 antibody.

B: GST pulldown experiments with GST-Rad53(781-821) and Asf1-myc from yeast extracts (lane 1) and dephosphorylated yeast extracts (lane 2).

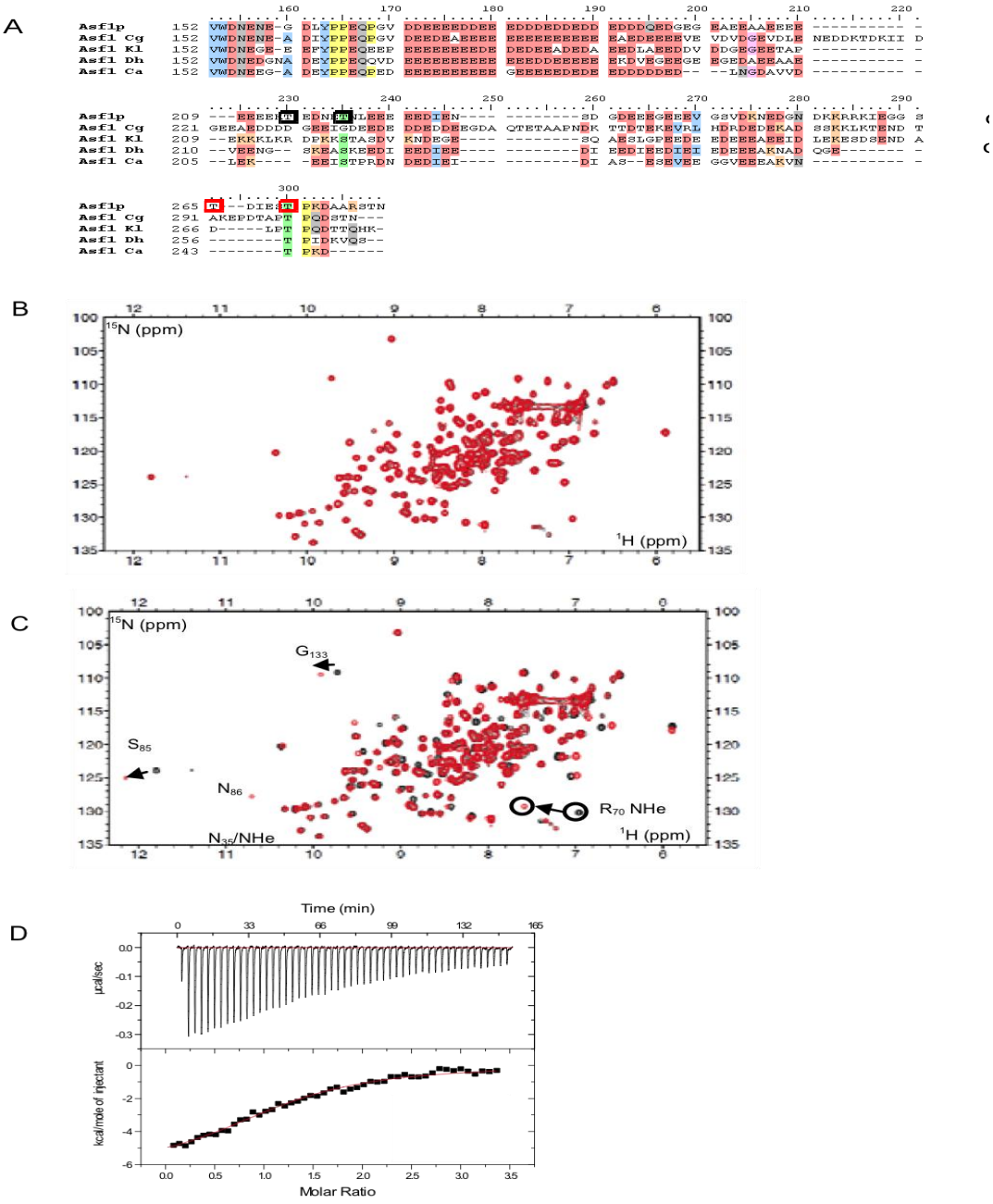

Fig. S2: The Asf1 phospho-T_{270} peptide interacts with the Rad53 FHA1 domain through a standard binding mode.

A: Only T270 is conserved amongst possible FHA1 binding sites in the C-terminal tails of Asf1 in different yeast species. Shown is an alignment of the C-terminal tails of Asf1 in *S. cerevisiae* (Asf1p) and closely related yeast species (*C. glabrata*, Cg, *K. lactis*, Kl, *D. hansenii*, Dh, and *C. albicans*, Ca).

B: ^{1}H-^{15}N heteronuclear single-quantum coherence spectra (HSQC) of uniformly ^{15}N labeled Rad53 before (in black) and after (in red) addition of 1:3.4 peptide ratio of Asf1 ^{266}DIESTPKDAARS^{277} unphosphorylated control peptide.

C: ^{1}H-^{15}N HSQC spectra showing Asf1 ^{266}DIES(pT)PKDAARS^{277} phosphorylated peptide binding. The spectra of the FHA1 domains in free and bound forms (after addition of a 1:3.4 peptide ratio) are represented in black and red, respectively. NH signals of S_{85}, G_{133}, N_{35}/NHe and N_{86} are indicated. Circled peak corresponds to folded NHε resonance signals of arginine residue R_{70}/NHe.

D: Thermogram (upper panel) and the binding isotherm of the titration of the FHA1 domain (15 µM) by the same Asf1 phosphopeptide (200 µM) at 30 °C. The thermogram was fitted to a single site interaction model (Origin) with a stoichiometric value N of 1.2 (±0.1) dissociation constant of 5.2 (±0.8)µM, and reaction enthalpy of -6.3 (±0.4)kCal.M^{-1}.

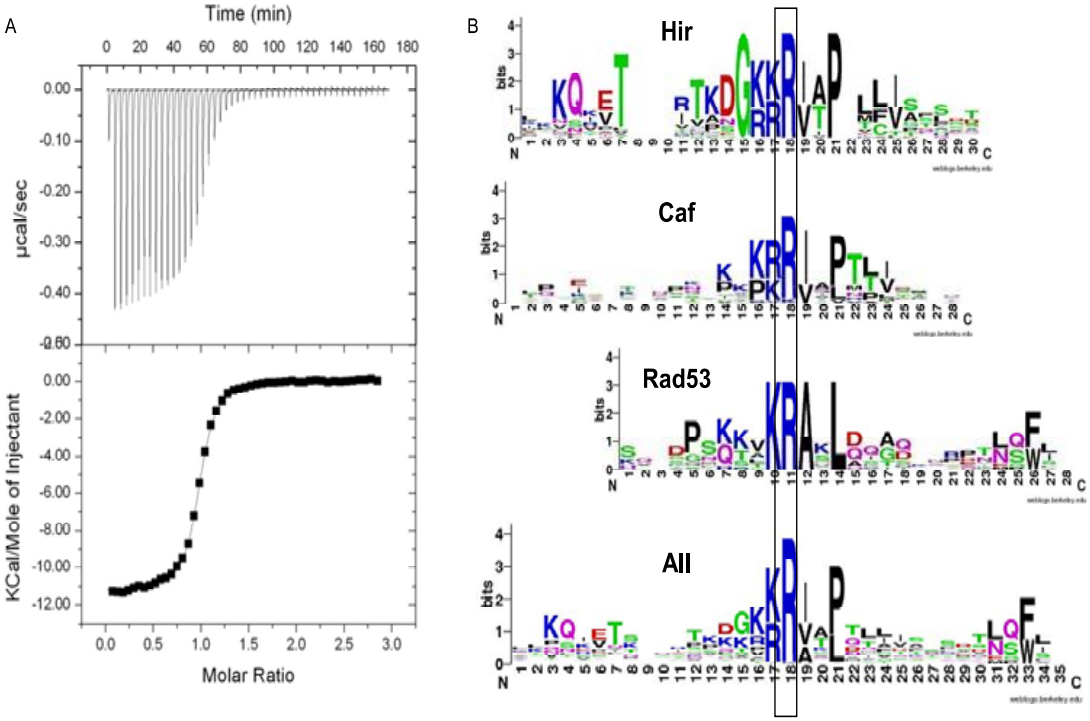

Fig S3: Interaction of Asf1 with Rad53-Cterminal peptide

A: Rad53-Cterminal domain binds Asf1N with a high affinity constant. Thermogram (upper panel) and the binding isotherm of the titration of Asf1N (15 µM) by the Rad53(800-821) peptide (250 µM) at 5 °C. The thermogram was fitted to a single site interaction model (Origin) with a stoichiometric value N of 1.07(±0.06) dissociation constant of 0.08(±0.03) µM, and reaction enthalpy of 10.8(±0.1) kCal.M^{-1} (Table 1).

B: Profile of the peptides binding Asf1N in a similar manner. Graphical representation multiple sequence alignment of Asf1 binding peptides generated using the WebLogo software (20). An alignment of yeast Hir1p (25 sequences), Cac2p (19 sequences) and Rad53 (12 sequences) was obtained with the Blast (NCBI) search program on the non-redundant data base

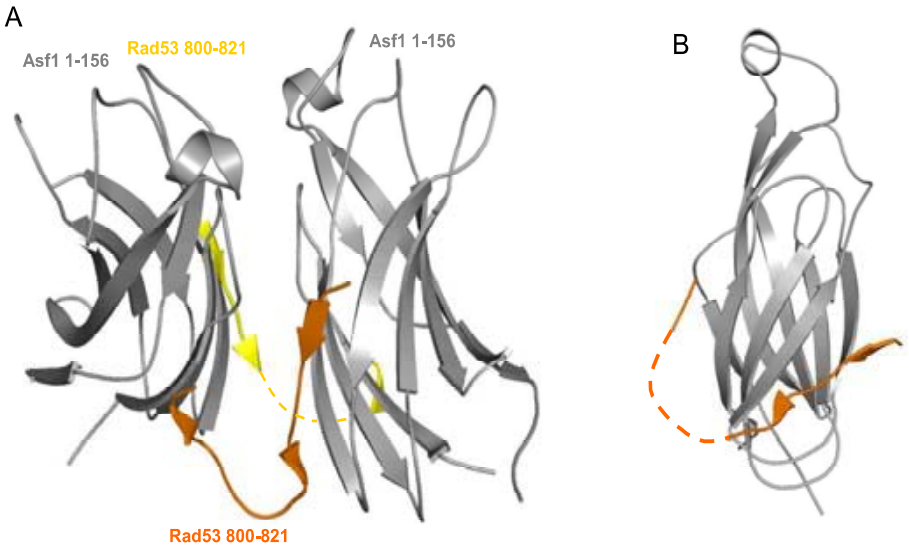

C

	Measured τ_c (ns.rad^{-1})	Calculated τ_c (ns.rad^{-1})* for a monomeric form of Asf1	Calculated τ_c (ns.rad^{-1})* for a dimeric form of Asf1
Asf1 (1-156)	7.7	8.8	16.8
Asf1 (1-156)+Rad53(800-82	9.2	9.9	18.9

* Calculated from the empirical expression given in (19).

Fig. S4: Analysis of the Rad53-C-terminal peptide swapping

A: View of two Asf1(1-156) molecules (in grey) and two Rad53 peptides (in orange and yellow). Only one molecule could be built with a continuous chain (in orange) and was swapped between the two Asf1 molecules. The second Rad53 chain (in yellow) is not continuous. A dashed line was added to follow the chain.

B*:* Model of the complex with one Rad53 peptide (in orange) contacting one Asf1(1-156) (in grey) protein. A dashed line was added to follow Rad53 peptide chain.

C : Correlation time of free and Rad53(800-821) uniformly labelled Asf1(1-156) calculated from heteronuclear ^{15}N-^{1}H relaxation data at 30°C. Experimental are fully compatible with expected values for Asf1 being monomeric in the free and bound states.

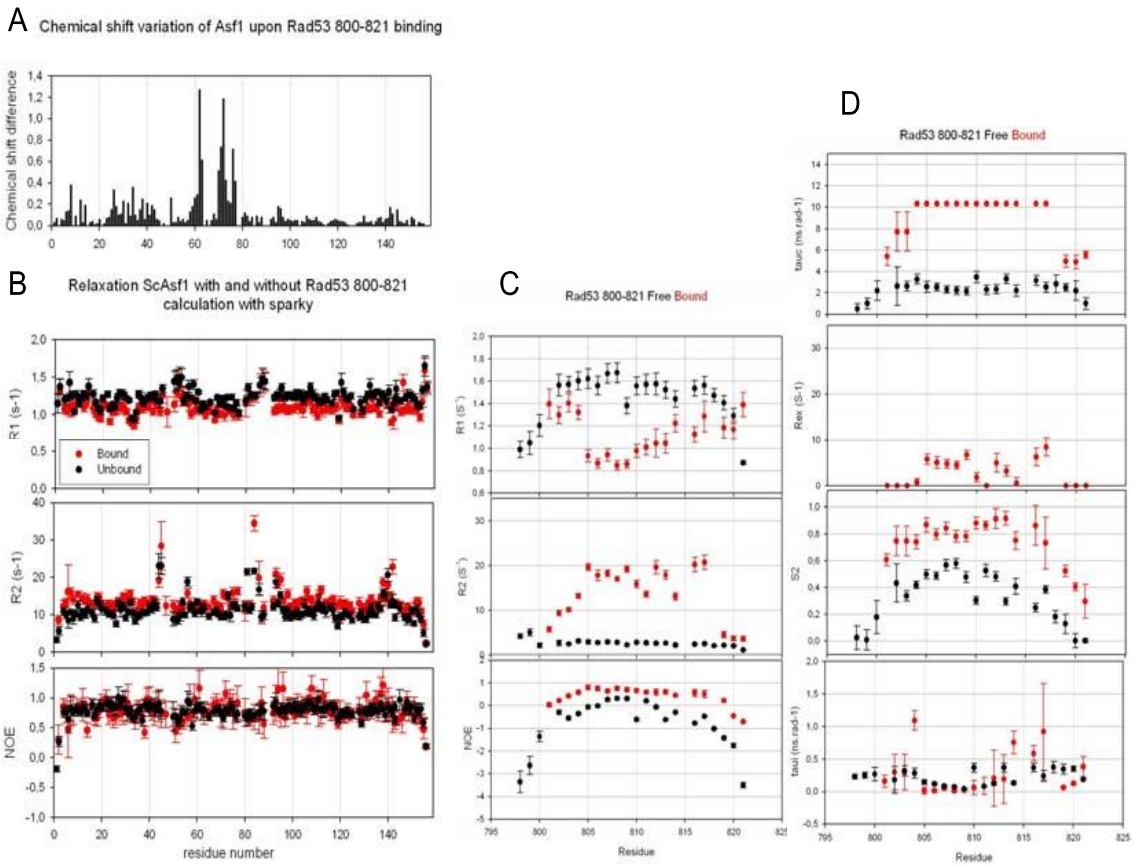

Fig. S5 : NMR 15N-1H relaxation analysis of the Asf1(1-156) Rad53(800-821) complex.

A: Chemical shift variation of Asf1 upon Rad53 (800-821) binding. The chemical shift difference was calculated according to (11).

B: ^{15}N-^{1}H relaxation parameters (R_1, R_2 and nOe) for free (in black) and Rad53(800-821) bound (in red) uniformly labeled Asf1(1-156) at 303°K. Analysis of these parameters allowed the calculation of the global correlation time of free and bound Asf1 (Table S3). These parameters are compatible with a heterodimeric complex and not with a swapped peptide as observed in the crystal structure.

C: ^{15}N-^{1}H relaxation parameters (R_1, R_2 and nOe) for free (in black) and Asf1(1-156) bound (in red) uniformly labeled Rad53(800-821) at 291°K

D: Lipari Szabo analysis of free (in black) and Asf1(1-156) bound (in red) uniformly labeled Rad53(800-821). The free peptide relaxation data were fitted with a model including adjustable τ_c, S^2 and τ_i (internal motion parameter) parameters. No exchange term was needed to correctly fit the data. The bound peptide was fitted with a model including a constant correlation time τ_c= 10.33 ns.rad-1 (estimated from the R_1/R_2 ratio) and adjustable Rex, S^2 and τ_i (internal motion parameter) parameters except for the three first and last residues that were fitted as for the free peptide.

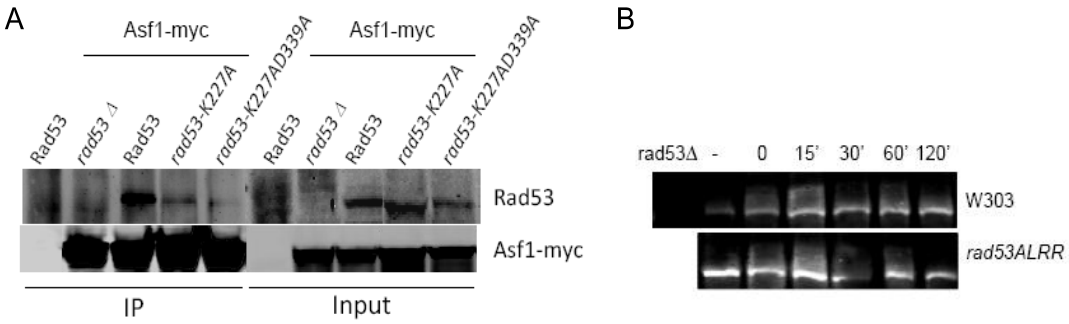

Fig. S6: Rad53 kinase-dead mutants coimmunoprecipitation with Asf1 and Rad53-ALRR dephosphorylation after MMS treatment

A: Rad53-K_{227}A and Rad53-K_{227}A+D_{339}A kinase-dead mutants co-immunoprecipitate less well with Asf1-myc compared to wild-type Rad53. Shown are Western blots with anti-Rad53 and anti-myc antibodies of proteins in cell extracts (Input) and after immunoprecipitation with anti-myc beads (IP).

B: Similar dephosphorylation of Rad53-ALRR and Rad53 wild type after treating cells with MMS and then releasing into YPD. W303-1a wild type and *rad53-ALRR* mutant cells were arrested in G1 by treating with 30 µM alpha factor for 2h at 30°C at which point MMS was added to 0.005% for 30 min. Cells were then washed and released into fresh YPD at 30°C for the indicated time points before preparing TCA protein extracts for SDS-PAGE.

Results II

3. Results not yet submitted for publication

3.1 Mutation of possible phosphorylation sites at the Rad53 C-terminus

In the absence of genotoxic stress, Asf1 forms a stable complex with Rad53. In our submitted article, we showed that the Asf1-Rad53 complex was dissociated when cells were treated with HU, but not MMS. This dissociation of the complex upon HU treatment may be induced by phosphorylation of Rad53 on specific sites. Rad53 has more than 20 serine or threonine residues that are potential phosphorylation sites, some of which are phosphorylated differentially depending on the type of genotoxic stress. We noticed that there are three serine/threonine residues in the Rad53 C-terminal peptide (T811, S812 and S821) that binds Asf1N. We mutated each of these to acidic residues or to alanine to produce a phosphomimetic or a non-phosphorylatable mutant. If phosphorylation of one or more of these residues was sufficient to induce dissociation of the complex in response to HU, we would expect that the phosphomimetic *Rad53-TSSDEE* mutant would not be associated with Asf1 even in the absence of genotoxic stress. However, we found that Rad53, and the *Rad53-TSSDEE* and *Rad53-TSSAAA* mutants all co-precipitated with Asf1-myc or with *Asf1-T265A+270A-myc* in the absence of genotoxic stress (Fig. 15). Thus, phosphorylation of Rad53-TSS residues is probably not sufficient to explain dissociation of the complex in response to HU treatment. Interestingly however, the *Rad53-TSSDEE* mutant co-precipitated less well with Asf1-myc or *Asf1-T265A+270A-myc* after treating cells with MMS. It is thus possible that phosphorylation of the C-terminal TSS residues of Rad53 contribute to destabilization of the Asf1-Rad53 complex in response to HU. Phosphorylation of other Rad53 sites at the putative third interaction surface of the Asf1-Rad53 complex are probably also necessary for destabilization of the complex, and the identification of such sites should aid in better defining the third interaction surface.

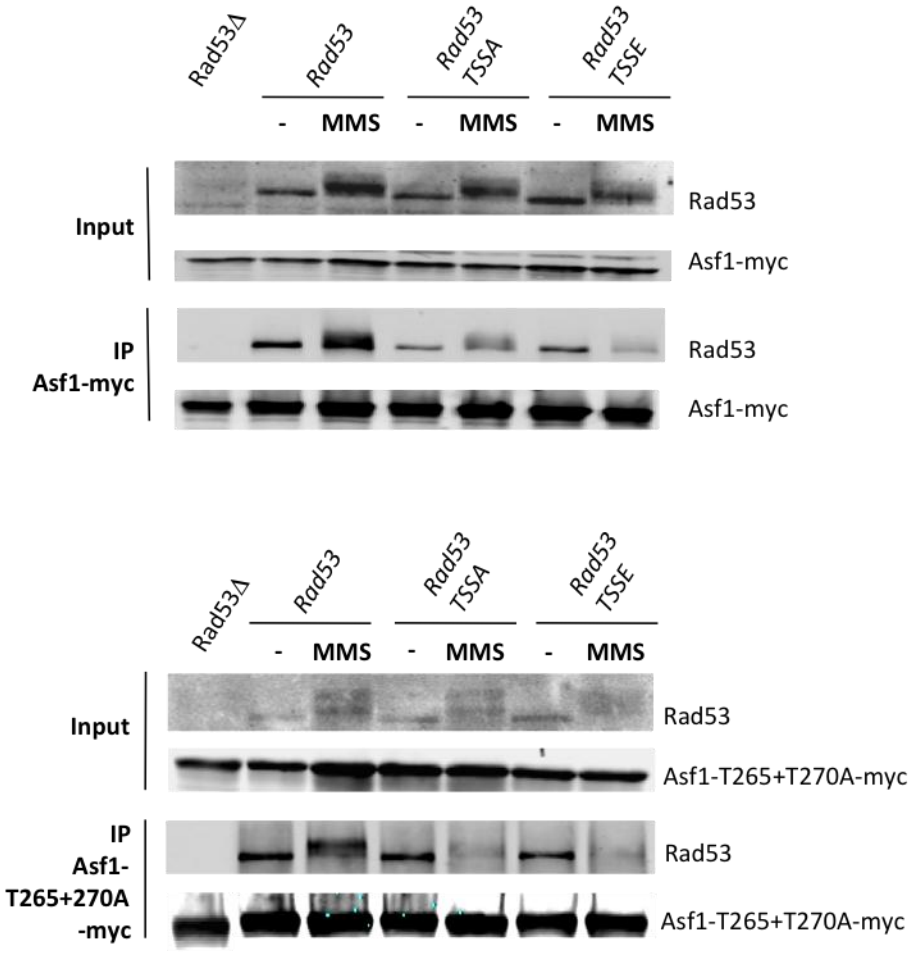

Figure 15. Mutation of possible phosphorylation sites at T811+S812+S821 of Rad53 destabilizes the Asf1-Rad53 interaction. In absence ou presence of MMS, wild-type Rad53, the Rad53-TSSDEE and Rad53-TSSAAA mutant co-precipitate with the Asf1-myc (top) and the Asf1T265A+T270A-myc non-phosphorylatable mutant (bottom).

3.2 Deletion analysis of the Rad53 C-terminus

According to the GST-pull down results, our laboratory identified two important binding sites for the Asf1-Rad53 interaction: the FHA1 domain of Rad53 binds phosphorylated Asf1 at T265 and T270, and the Rad53 C-terminus binds the N-terminal domain of Asf1 (Fig. 1 of our submitted manuscript). Before having determined the structure of the Rad53 C-terminal peptide with Asf1N, we initially sought to test the importance of the Rad53 C-terminus by carrying out a deletion analysis. The C-terminal sequence of Rad53 was truncated at different lengths (from 21aa to 91aa) and fused to a TAP tag or to GFP (Fig. 16A). A putative bipartite nuclear localization signal (NLS) is found

at 785-807 aa of Rad53 (KRIHSVSLSQSQIDPSKKVKRAK). This corresponds to 14-37 aa from the C-terminus of the protein. Indeed, we found that deletion of the last 40 aa of Rad53 led to a partial delocalization of the protein in the cytosol (Fig. 16B), whereas wild-type Rad53 is highly concentrated in the nucleus. In order to compensate for this effect, we also constructed a Rad53-CΔ40 mutant that contained an SV40 NLS (PKKKRKVG) at the junction of the Rad53 truncation with the GFP or the TAP tag. The SV40 NLS restored the nuclear localization of the Rad53-CΔ40 mutant (Fig. 16B). Interestingly, we found that the *Rad53-CΔ40* mutant is sensitive to hyrdoxyurea (HU), but not methyl-methane-sulfonate (MMS) or camptothecin (CPT) (Fig. 16C). The addition of an SV40-NLS suppressed the HU sensitivity of Rad53-CΔ40 (Fig. 16C). These results suggest that resistance to HU requires a higher intranuclear concentration of Rad53 than does resistance to MMS or CPT.

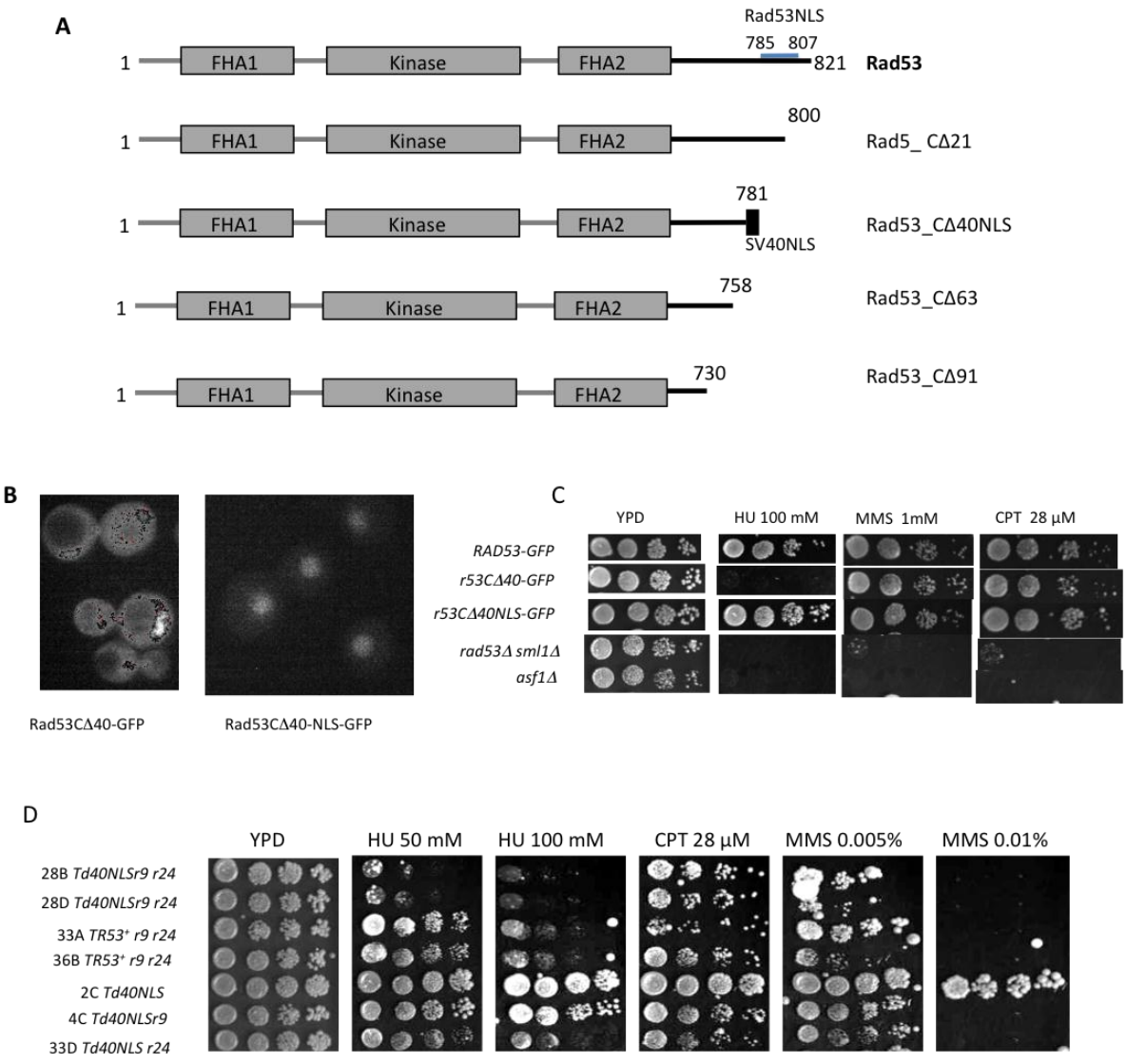

Figure 16. (A) Schematic representation of four different mutants of Rad53 that were truncated from 21 to 91aa at C-terminus of Rad53. (B) *rad53-CΔ40* has a partial localization defect. Addition of an SV40 nuclear localization signal can target Rad53 to the nucleus. (C) *rad53-CΔ40* is mildly sensitive to HU but not to MMS nor CPT, the sensitivity to HU is suppressed by addition of an SV40 NLS. (D) *asf1-T265A+270A rad53-CΔ40NLS rad9 rad24* (28B/28D *Td40NLSr9 r24*) is more sensitive to HU than *rad9 rad24* (*33A/36B TR53*$^{+}$ *r9 r24*). *asf1-T265A+270A rad53-CΔ40NLS* became more sensitive to genotoxic stress when it was combined with *rad9* or *rad24* mutant. T= asf1-T265A+270A allele; d40NLS= rad53CΔ40-NLS allele; r9= rad9 allele; r24= rad24 allele. The number-letter designation refers to tetrad numbers and spore segregants from the genetic cross used to isolate the different mutants (i.e, 28B= spore B of tetrad 28).

We next tested the ability of Asf1-myc to co-precipitate with TAP-tagged Rad53 C-terminal truncation mutants (Fig. 17). All of the Rad53 C-terminal truncation mutants precipitated Asf1-myc less well compared to wild-type Rad53, but there was nevertheless detectable residual interaction for all mutants. Since the loss of the Rad53 NLS in these mutants leads to a partial localization defect, we also tested the ability of the *Rad53-CΔ40-NLS* mutant to precipitate Asf1-myc. This mutant also precipitated less Asf1-myc than wild-type Rad53 despite being properly concentrated in the nucleus. We conclude that loss of Rad53-C-terminal sequences destabilized the Asf1-Rad53 complex, but that residual interaction was detectable due to distinct interaction surfaces. Since we knew that Rad53-FHA1 could bind Asf1 phosphorylated on T270 (see submitted manuscript), we tested the ability of the Rad53 C-terminal truncation mutants to precipitate the *Asf1-T265A+T270A* mutant. Remarkably, the residual interaction of the Rad53 C-terminal truncation mutants with *Asf1-T265A+T270A* was very similar to that of wild-type Asf1. Furthermore, *Rad53-CΔ40* efficiently precipitated the Asf1-N-terminal domain (1-168 aa) when it was overexpressed in yeast (Fig. 17D). We were thus forced to conclude that a third binding site must contribute to the interaction of Rad53 with Asf1. As we show in our submitted manuscript, this third site appears to involve the histone H3 binding surface of Asf1N with an as yet unidentified surface of Rad53 that may lie in its kinase domain (see below).

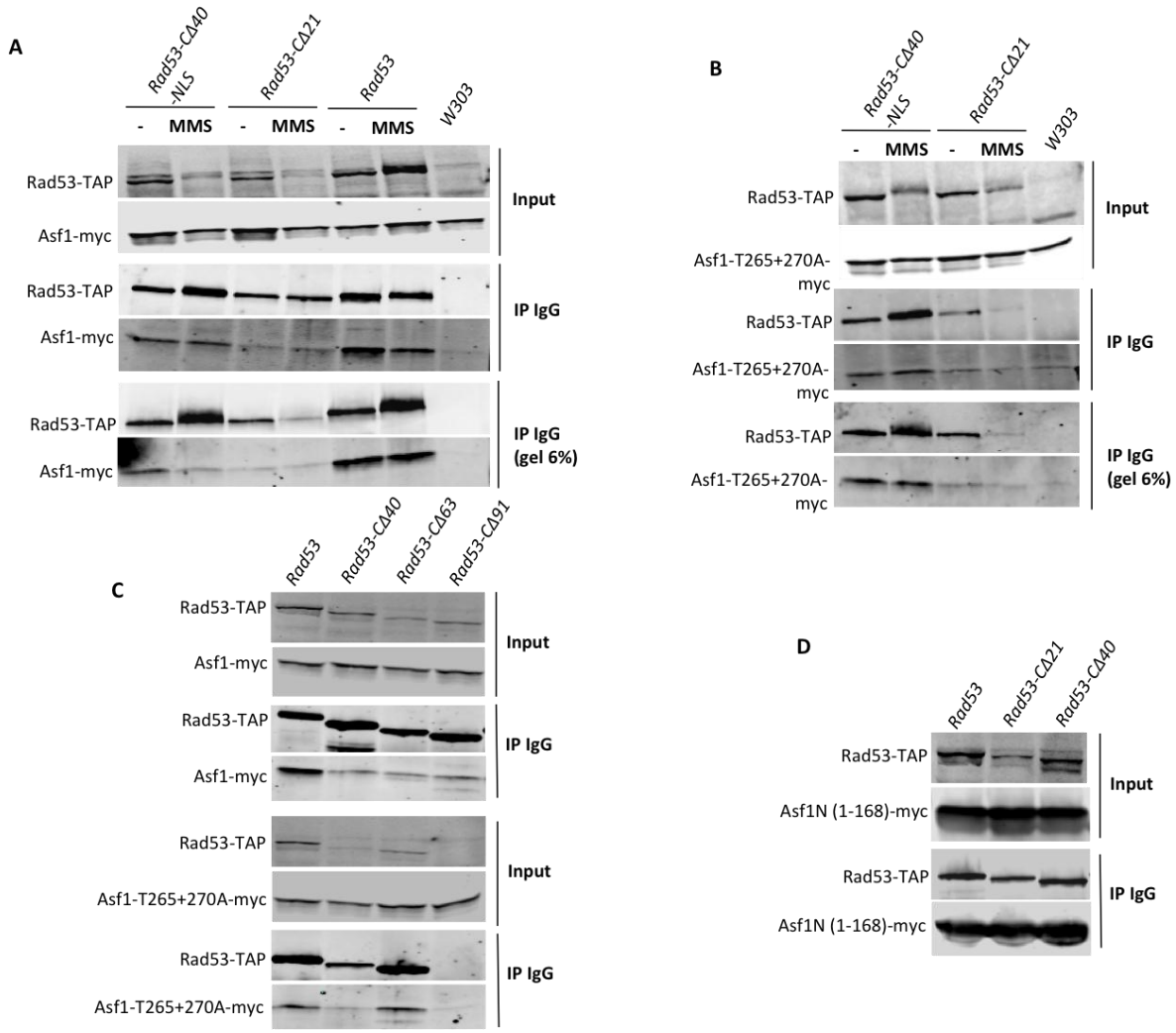

Figure 17. Asf1-myc co-precipitated with TAP-tagged Rad53 C-terminal truncation mutants. Asf1-myc (A) and *Asf1-T265/270A-myc* (B) co-precipitated with Rad53, the *Rad53-CΔ40-NLS-TAP* and *Rad53-CΔ21-TAP* mutant in the absence/presence of MMS. (C) Asf1-myc and Asf1-T265+T270A-myc co-precipitated the *Rad53-CΔ40-TAP, Rad53-CΔ63-TAP* and *Rad53-CΔ91-TAP* mutants. Note however, a problem with the Rad53-CΔ91-TAP precipitation in the context of the Asf1-T265A+270A mutant strain. (D) The overexpressed Asf1-N-terminal domain (1-168 aa) co-precipitated with the Rad53-CΔ21-TAP and *Rad53-CΔ40-TAP* mutants.

Once Françoise Ochsenbein's group had determined the structure of the Rad53 C-terminal peptide with Asf1N, we were able to predict specific residues that were likely to be important in affinity of this interaction. As we describe in our manuscript, the *Rad53-ALRR* (A806R+L808R) mutant disrupts an important hydrophobic surface contributing to this interaction. In the co-immunoprecipitation experiment shown in this paper, we saw no

residual interaction between *Rad53-ALRR* and Asf1-myc. This seems surprising given that we did see a residual interaction between Asf1-myc and Rad53 truncation mutants that were completely missing these C-terminal sequences. These experiments were done at different times under different conditions. The Rad53 C-terminal truncations were fused to the TAP tag and precipitated with IgG beads to test co-precipitation of Asf1-myc. In contrast, Asf1-my was precipitated with anti-myc beads to test co-precipitation of *Rad53-ALRR* and wild-type Rad53 that were not tagged. The TAP Tag sequence does not contain a sequence similar to the KRAXL motif that mediates binding of the Rad53 C-terminus to Asf1N, so we do not think that a fortuitous binding motif in the TAP tag explains the residual interaction. We suggest that the TAP tag precipitations were done under slightly less stringent conditions compared to the Asf1-myc IP, and this allowed us to detect the residual interaction of the Rad53-C-terminal truncations. We feel that the *Rad53-ALRR* mutant also has a residual interaction with Asf1 due to the putative third interaction surface, but we did not detect this residual interaction under the conditions of the Asf1-myc IP.

In our manuscript, we showed that the *Rad53-ALRR* mutant increased the resistance of *rad9* and *rad24* mutants to genotoxic stress. Surprisingly, we found that the *Rad53-CΔ40NLS* decreased the resistance of *rad9 rad24* double mutants to HU, but not MMS or CPT (Fig. 16D). The *Rad53-ALRR* mutant and the *Rad53-CΔ40NLS-TAP* mutant are expected to destabilize the Asf1-Rad53 complex to similar extents. Since the ALRR double point mutant is much more specific than the deletion of the C-terminal 40 aa + fusion of an SV40 NLS + TAP tag, we suggest that the differing phenotype of the Rad53-CΔ40NLS-TAP mutant is due to an effect on another Rad53 partner or substrate. Although we suggest that the phenotype of the *Rad53-ALRR* mutation is due to destabilization of the Asf1-Rad53 complex, we cannot exclude that this double point mutation also affects some other partner or substrate of Rad53.

3.3 Pulldown experiment suggesting that the Rad53 kinase domain can bind Asf1 in yeast extracts.

We suggested that Asf1 may directly interact with Rad53 through a third binding site overlapping the histone H3 binding surface of Asf1N. We also showed that the Rad53-K227A and Rad53-K227A+D339A kinase dead mutants were affected in their interaction with Asf1 (see submitted manuscript Supplementary Fig. 6A). These observations suggest that the Rad53 kinase domain might be able to interact with Asf1, although we did not observe an obvious interaction of the Rad53 kinase domain with GST-Asf1 or GST-Asf1N purified from *E. coli* (see submitted manuscript Fig.1B).

We re-examined this possibility by testing the ability of a GST-Rad53 kinase domain fusion protein produced in *E. coli* to pull down Asf1 in yeast extracts. Since the GST-Rad53 kinase domain appears to undergo autophophosphorylation when expressed in *E. coli*, we also treated cell extracts with lambda protein phosphatase before purifying the fusion protein. The autophosphorylated and the dephosphorylated GST-Rad53 kinase domain fusion protein were both able to pull down Asf1 (Fig. 18A). As expected, GST-FHA1 and GST-Rad53-Cter peptides also pulled down Asf1 whereas GST-FHA2 and GST did not. These results suggest that the Rad53 kinase domain can interact with Asf1, although it is not clear why GST-Asf1 or GST-Asf1N purified from *E. coli* did not bind the Rad53-His6 kinase domain expressed in *E. coli*. Further work is necessary to definitively identify the third interaction surface and to provide a complete description of the Asf1-Rad53 complex.

3.4 Glycerol gradient analysis of Asf1 and Rad53 complexes in yeast extracts

We used glycerol gradient centrifugation of total yeast extracts to further characterize complexes containing Asf1 and Rad53 in the wild type and in the *rad53-ALRR* mutant. Rad53 was detected with anti-Rad53 antbodies, whereas Asf1 was tagged with HA or myc epitopes. Asf1 sedimented in fractions containing Rad53, and in higher molecular weight fractions without Rad53, in glycerol gradients prepared from wild-type extracts (Fig. 18B top). We also observed some apparently free Rad53 (theoretical MW of 95kDa) in the fraction 5, but no free Asf1-HA (50 kDa). In addition to the Asf1-Rad53 complex in fractions 6-7, Asf1 sediments in higher molecular weight fractions that may represent complexes containing histone co-chaperones. Strikingly, in extracts from the *rad53-ALRR* mutant, Asf1 sedimented mainly in low molecular-weight fractions that did not contain *Rad53-ALRR* (Fig 18B bottom). This observation is consistent with a destabilization of the Asf1-Rad53 complex in the *rad53-ALRR* mutant. Curiously, the *Rad53-ALRR* protein itself sediments mainly in fractions 6-7 that correspond to the position of the Asf1-Rad53 complex in wild-type extracts. This result may indicate that the *Rad53-ALRR* mutant binds another protein of the same approximate molecular weight of tagged Asf1, or that the conformation of the *Rad53-ALRR* protein is more compact than wild-type Rad53 and sediments more rapidly for this reason.

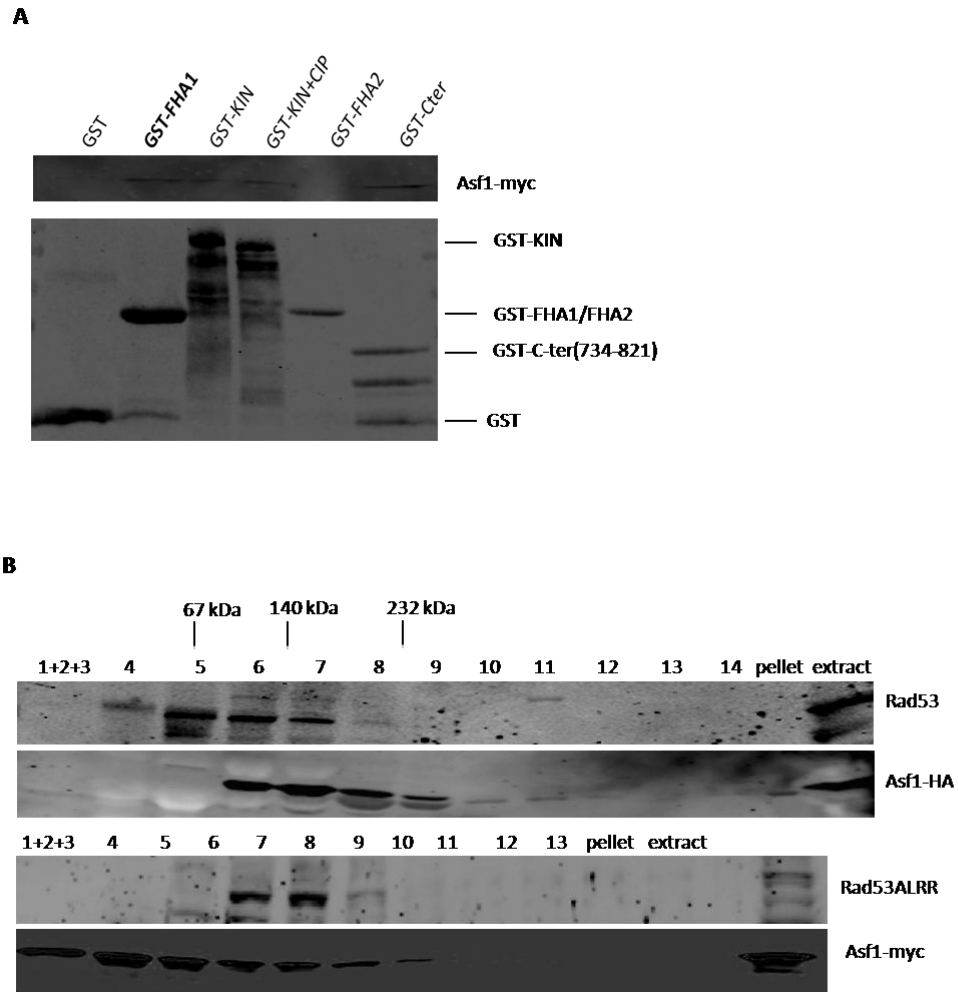

Figure 18. (A) Rad53 interacts with Asf1 through probably three binding sites. GST pull-down assays with GST, GST-Rad53FHA1, GST-Rad53 Kinase domain, dephosphorylated GST-Rad53 Kinase domain with CIP, GST-Rad53FHA2, GST-Rad53 C-terminal domain and yeast extract expressing Asf1-myc. (B) *Rad53-ALRR* sediments mainly at lower molecular weight fractions compared to wild-type Rad53 during glycerol gradient centrifugation of yeast extract. S100 extracts of *RAD53 ASF1-3HA* (top panel) and *rad53-ALRR*/pRS314-ASF1-myc were fractionated on 10-40% glycerol gradients.

Mechanism of the increased resistance of *rad9* and *rad24* mutants to genotoxic stress by the *rad53-ALRR* mutant

3.5 Overexpression of Rad53 or Asf1

The structure of the complex consisting of Asf1N with the Rad53 C-terminal peptide allowed us to identify two residues (A806 and L808) that are important for the stability of the complex. The *Rad53-ALRR* mutant destabilizes the Asf1-Rad53 complex in yeast cells and

increases the resistance to genotoxic stress of *rad9* and *rad24* mutants. It's possible that an increase of free Asf1 or Rad53 is responsible for this increased resistance. We tried testing this possibility by transforming a *rad9*Δ mutant with centromeric or 2µ multi-copy plasmids containing the *ASF1* or *RAD53* genes and testing their resistance to MMS. We did not observe a reproducible increase in the resistance of the *rad9*Δ transformants with these plasmids (data not shown). This result suggests that we cannot reproduce the effect of the *rad53-ALRR* mutation by the simple over-expression of wild-type *ASF1* or *RAD53*.

3.6 Phenotype of the *asf1-T265+270A* mutant

We showed in our submitted m/s that the non-phosphorylatable *Asf1-T265+270A* mutant is unable to bind the Rad53-FHA1 domain. This mutant had no apparent phenotype by itself (Fig. 19A) or when combined with the *rad53-ALRR* (Fig. 19B) or *rad24* mutants (Fig. 19A). Strikingly however, the *asf1-T265+270A rad53-ALRR rad24* triple mutant was less resistant to MMS than the *rad53-ALRR rad24* double mutant (Fig. 19B). Interpreting these results is not simple! The *rad53-ALRR* mutation clearly destabilizes the Asf1-Rad53 complex and increases the resistance of the *rad24* mutant to MMS. The *asf1-T265+270A* mutation prevents binding of Asf1 to the FHA1 domain of Rad53, but had no effect on the efficiency of co-immunoprecipitation of the two proteins from yeast extracts, presumably because this interaction contributes little to the overall affinity of the complex compared to the two other interaction surfaces of the complex. Thus, we suggest that this phenotype of the *asf1-T265+270A* mutant is explained not by further destabilizing the Asf1-Rad53 complex, but rather by increasing the interaction of Rad53 with another binding partner of its FHA1 domain. Rad53 binds multiple proteins through its FHA1 domain and it is possible that in the absence of competition with phospho-Asf1, the increased binding of some other protein might lead to increased MMS sensitivity in the context of the *rad53-ALRR rad24* double mutant. This hypothesis is pure speculation that requires further experimental testing.

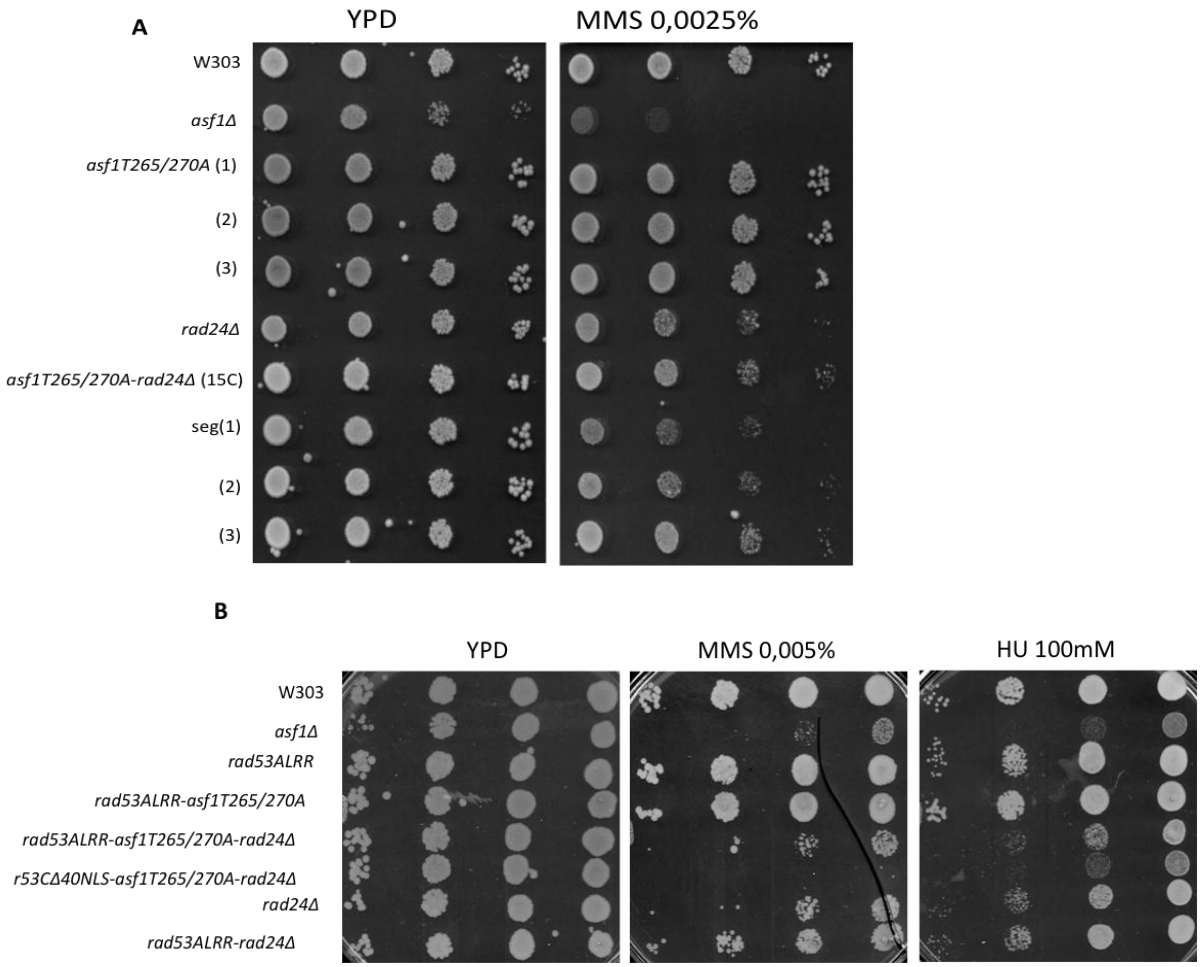

Figure 19. Effect of the *asf1-T265+270A* mutant on HU and MMS sensitivities. (A) *asf1-T265+270A* and *asf1-T265+270A rad24Δ* are not sensitive to genotoxic stress. (B) *asf1-T265+270A rad53-ALRR rad24* exhibit less resistant to MMS than the *rad53-ALRR rad24* mutant.

3.7 Recovery of the *rad53-ALRR* mutant

The *Rad53-ALRR* mutation increased the resistance of *rad9* and *rad24* mutants to MMS (see submitted manuscript Fig. 4). Since Rad53 and Asf1 have both been implicated in S phase progression, we tested the effect of the *rad53-ALRR* mutation on cell cycle progression after synchronizing cells in the G1 phase of the cell cycle in the absence or presence of MMS. Cells were blocked in the G1 phase by treatment with the alpha mating pheromone. Cells were then either released into the cell cycle, or treated with 0.005% MMS for 30 minutes before washing and releasing into the cell cycle. Recovery from G1 arrest and progression through the cell cycle were followed by FACS analysis of DNA content in individual cells. Interestingly, exponentially growing *rad53-ALRR* mutant cells have a higher proportion of cells in the S/G2/M phases than the W303-1a wild-type cells (Fig. 20A). The

doubling time of the *rad53-ALRR* mutant is not longer than that of the WT (data not shown). This result suggests that the *rad53-ALRR* mutant has an accelerated G1 phase relative to the wild type. After G1 synchronization and release, we found that the *rad53-ALRR* mutant recovered and traversed S-phase more rapidly than the W303-1a wild type in 3 of 5 experiments. After G1 synchronization, transient MMS treatment, and release, we found that the *rad53-ALRR* mutant recovered and traversed S-phase more rapidly than the W303-1a wild type in 4 of 5 experiments (Fig. 20B). Overall, these results suggested that the *rad53-ALRR* mutant could re-enter the cell cycle and/or traverse S-phase more rapidly than the W303-1a wild type, but this result was not always reproducible and we have so far been unable to identify the experimental parameter responsible for this variation.

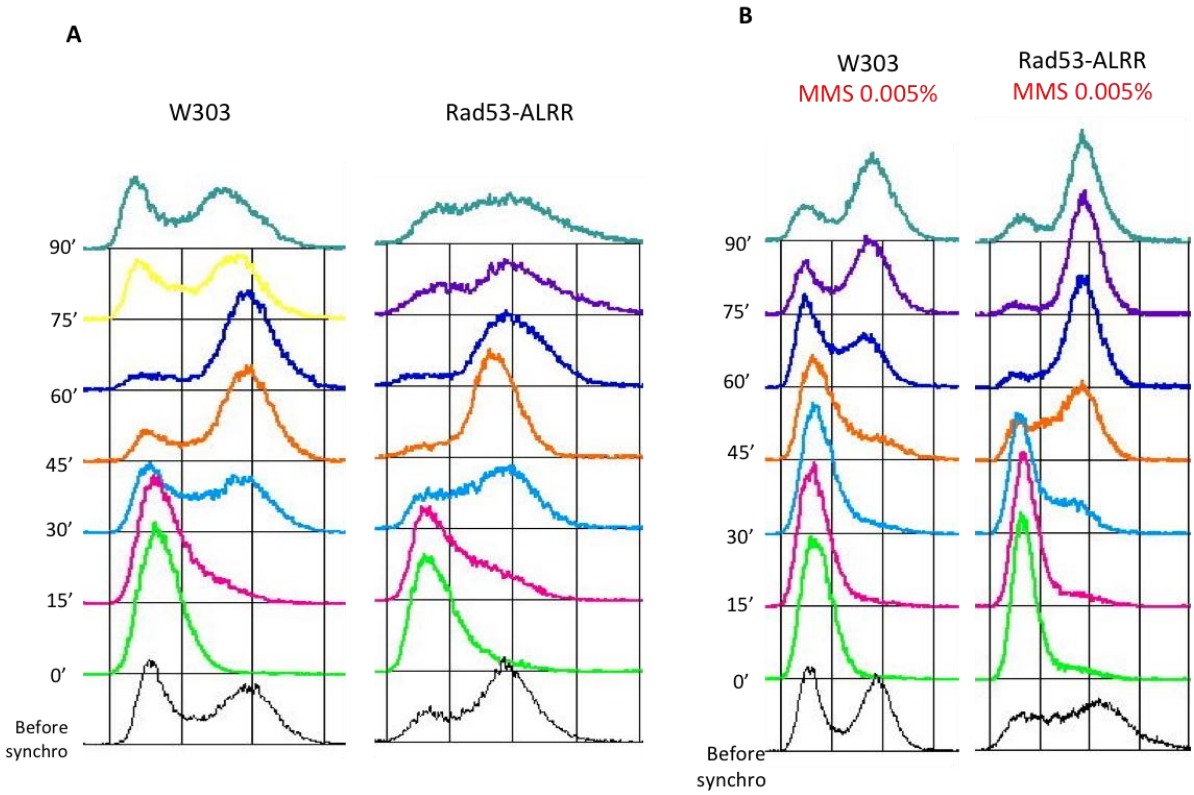

Figure 20. The *rad53-ALRR* mutant re-enters the S-phase more rapidly than W303 in the absence (A), presence (B), of MMS. Shown is the cell cycle distribution of the wild type and the *rad53-ALRR* mutation measured by flow cytometry analysis of DNA content. Cells were synchronized at G1 phase and then released directly into YPD (A) or treated transiently with 0.005% MMS and then released into YPD (B).

3.8 Late origin firing is repressed correctly in the *rad53-ALRR* mutant in the continued presence of HU or MMS

In the presence of genotoxic stress, the activation of Rad53 inhibits late origin firing by phosphorylation of the replisome component Sld3, and by phosphorylation of Dbf4, the regulatory subunit of the Cdc7 kinase (Zegerman et al. 2010; Lopez-Mosqueda et al. 2010). Kinase-dead mutants of Rad53 do not repress late origin firing and thereby complete DNA replication more rapidly than the WT in the continued presence of HU or MMS. We synchronized cells in G1 and then released them into medium containing 200 mM HU or 0.033% MMS to determine whether the *rad53-ALRR* mutant is able to complete S phase more rapidly than the wild type, as would be expected if *rad53-ALRR* could not repress late origin firing. However, the *rad53-ALRR* mutant had only a modest effect on S phase progression in the continued presence of HU or MMS (Fig. 21A). The *rad53-K227A* kinase-defective mutant clearly replicated its DNA more rapidly than the *rad53-ALRR* mutant in the continued presence of MMS (Fig. 21B). This result suggested that the *rad53-ALRR* mutant was competent in blocking late origin firing in response to genotoxic stress.

Further confirmation of this result was obtained through a collaboration with Armelle Lengronne and Philippe Pasero at the Institut de Génétique Humaine de Montpellier. Armelle used quantitative PCR to follow the copy number of an early replicating origin (ARS 305) and three late replicating origins (ARS 809,911, and 1212) in the wild type and *rad53-ALRR* mutant after G1 synchronization and release into 200 mM HU. The *rad53-ALRR* mutant showed significant replication of the early origin, but not the late origins in this assay (Fig. 21C). In contrast, Lengronne and Pasero have previously shown that mutants defective in repressing late origins, such as the *rad53-K227A* mutant, show significant increases in copy number of late origin sequences by this assay (Crabbé et al., 2010). This result confirmed the repression of late origins in the *rad53-ALRR* mutant under conditions of genotoxic stress. It remains possible that *rad53-ALRR* has more subtle effects on S phase progression at the level of replication fork initiation or progression. Armelle Lengronne is examining this possibility by doing pulse labeling with DNA combing and genome-wide analyses of DNA replication in the *rad53-ALRR* mutant.

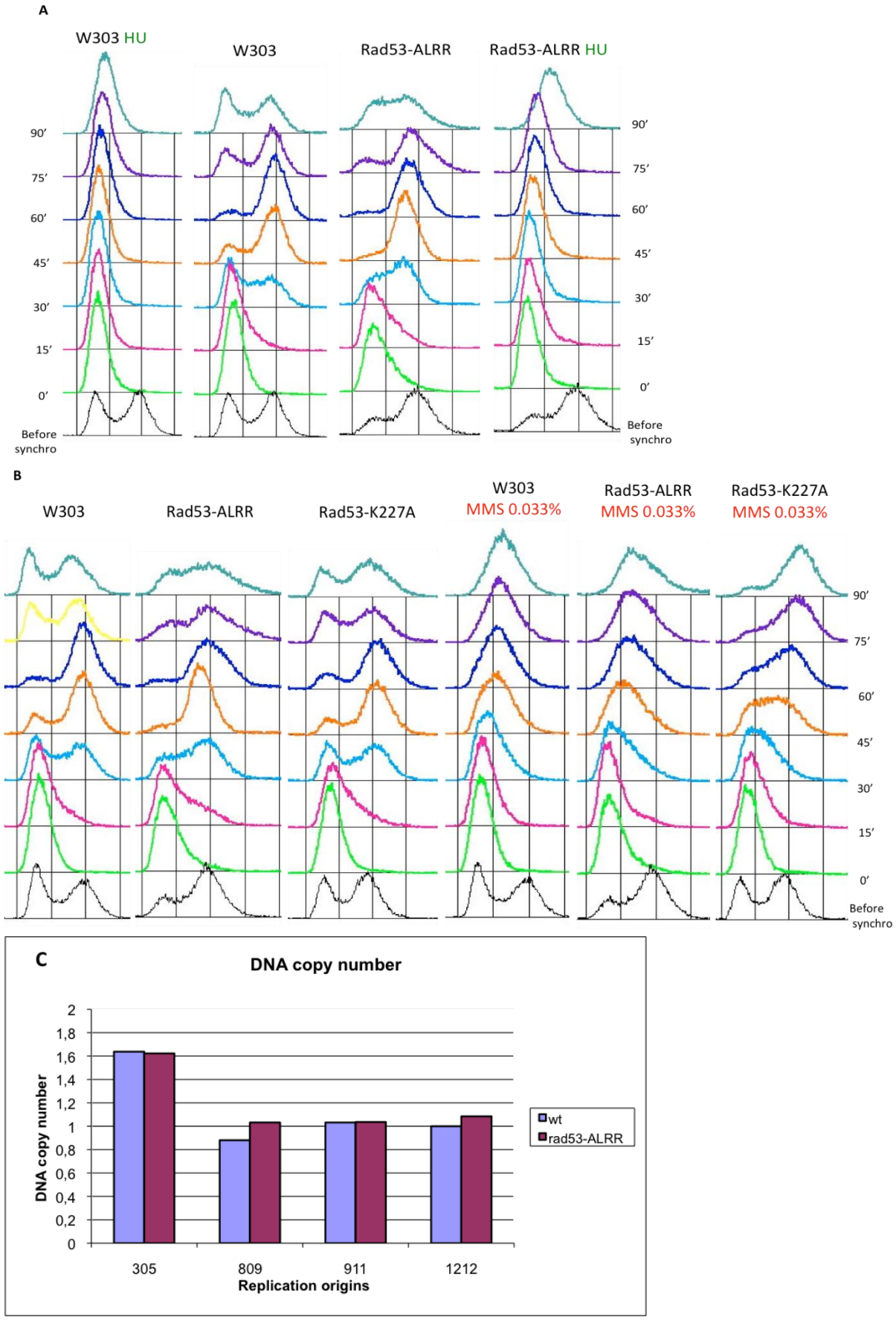
A
W303 HU
W303
Rad53-ALRR
Rad53-ALRR HU
90′
75′
60′
45′
30′
15′
0′
Before synchro
B
W303
Rad53-ALRR
Rad53-K227A
W303 MMS 0.033%
Rad53-ALRR MMS 0.033%
Rad53-K227A MMS 0.033%
C
DNA copy number
DNA copy number
2
1,8
1,6
1,4
1,2
1
0,8
0,6
0,4
0,2
0
305
809
911
1212
Replication origins
wt
rad53-ALRR

Figure 21. The *rad53-ALRR* mutant is competent at repressing late origin firing in the presence of genotoxic stress. (A) the *rad53-ALRR* mutant had only a modest effect on S phase progression in the continued presence of HU or MMS. (B) The *rad53-K227A* kinase-defective mutant that is defective in repressing late origins replicated its DNA more rapidly than the *rad53-ALRR* mutant in the continued presence of MMS. (C) the DNA copy number of early/late origins of the *rad53-ALRR* mutant was examined after G1 synchronization and release into medium containing HU. The significant replication of the early origin (ARS 305), but not the late origins (ARS 809, 911, 1212) was detected.

3.9 Are the effects of *rad53-ALRR* on cell cycle progression due to the disruption of the Asf1-Rad53 interaction?

The *rad53-ALRR* mutation destabilized the Asf1-Rad53 complex (see submitted manuscript Fig. 4B). It is thus possible that the effects of this mutation on cell cycle progression are due to increased levels of free Rad53 and/or Asf1 in the mutant. We sought to further test this possibility by examining the effects of individual over-expression of *RAD53* or *ASF1* in the wild-type strain. We also tested the effect of other mutations that affect the interaction of Asf1 with Rad53, such as the *rad53-TSSDEE*, *rad53-CΔ40NLS* or *rad53CΔ40NLS-asf1T265+270A*.

To determine whether overexpression of Asf1 or Rad53 has an effet on cell cycle progression, we transformed the W303-1a wild-type with 2µ multi-copy plasmids containing the *ASF1* or *RAD53* genes. These plasmids were previously shown to lead to an accumulation of Asf1 and Rad53. After G1 synchronization and release in the absence of MMS treatment, we did not observe an obvious effect of Rad53 or Asf1 overexpression on cell cycle progression (Fig. 22A). In this experiment, we do not observe an effect of the *rad53-ALRR* mutation either. As mentioned above, the accelerated recovery from G1-arrest and S-phase traversal of the *rad53-ALRR* mutant was not always reproducible for unknown reasons. Interestingly however, the *rad53-TSSDEE* and *rad53CΔ40NLS-asf1T265+270A* mutants did show accelerated cell cycle progression in this experiment (Fig. 22A).

We also examined cell cycle progression after G1 arrest, transient treatment with 0.005% MMS for 30 minutes, and then wash and release into normal growth medium. Although Asf1 overexpression did not alter recovery from MMS and subsequent cell cycle progression, Rad53 overexpression did accelerate this process in a manner similar to the *rad53-ALRR* mutation (Fig. 22B). The *rad53-TSSDEE* and *rad53CΔ40NLS-asf1T265+270A* mutants also showed accelerated recovery from MMS and cell cycle progression in this experiment. We also included an *asf1*Δ mutant in this experiment. There is no Asf1 to form a complex with Rad53 in this strain. However, unlike the *rad53-ALRR* mutant, the *asf1*Δ

mutant grows more slowly than the wild type and appears to suffer from endogenous DNA damage that leads to basal activation of Rad53 and accumulation of cells in S/G2/M (Ramey et al., 2004). The *asf1*Δ mutant is also hyper-sensitive to MMS. The FACS analysis indicated that the *asf1*Δ mutant also showed accelerated recovery from MMS and cell cycle progression (Fig. 22B). However, the G1 arrest induced by alpha factor appeared to be less effective, so this experiment should be repeated in optimized synchronization conditions.

Overall, these results suggest that increases in free Rad53 (not complexed with Asf1) in the *rad53-ALRR, rad53-TSSDEE,* and *rad53CΔ40NLS-asf1T265+270A* mutants, or by *RAD53* overexpression in the wild-type strain, can promote more rapid recovery from transient MMS treatment and cell cycle progression. However, it is not clear how these initial effects on recovery from MMS are related to the long-term survival of these strains to MMS. For example, we did not observe obvious differences in the sensitivity of the *rad53-ALRR, rad53-TSSDEE,* and *rad53CΔ40NLS-asf1T265+270A* mutants to MMS relative to the wild type. As shown in our paper, the *rad53-ALRR* mutation does increase the resistance of *rad9* and *rad24* mutants to genotoxic stress, and so we decided to study this phenotype more closely.

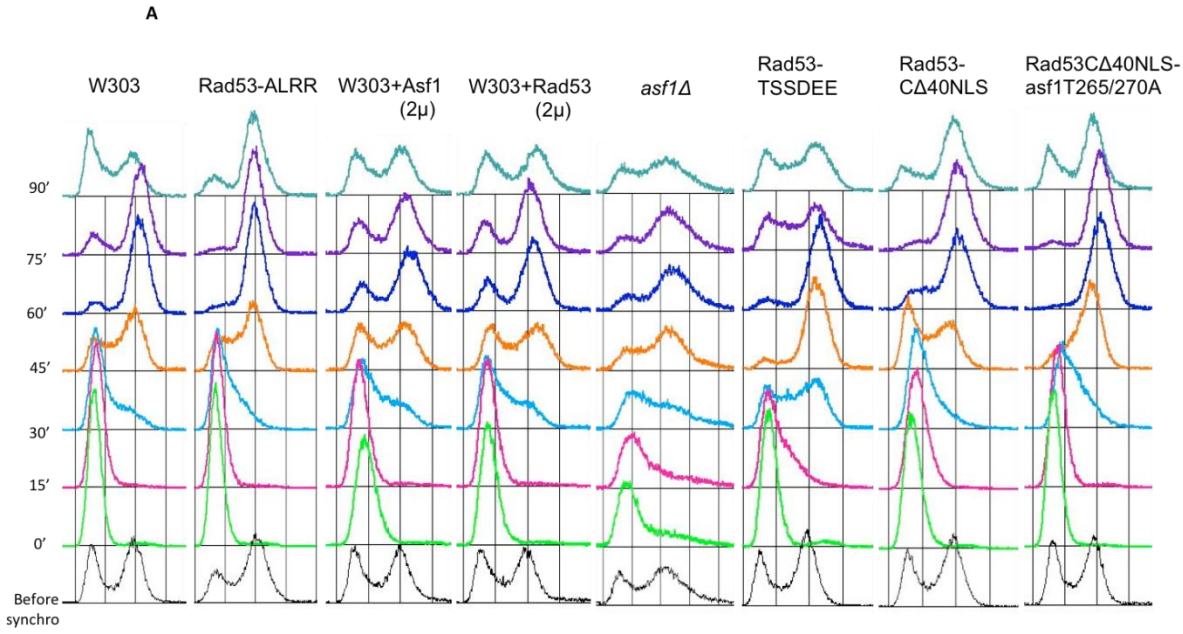

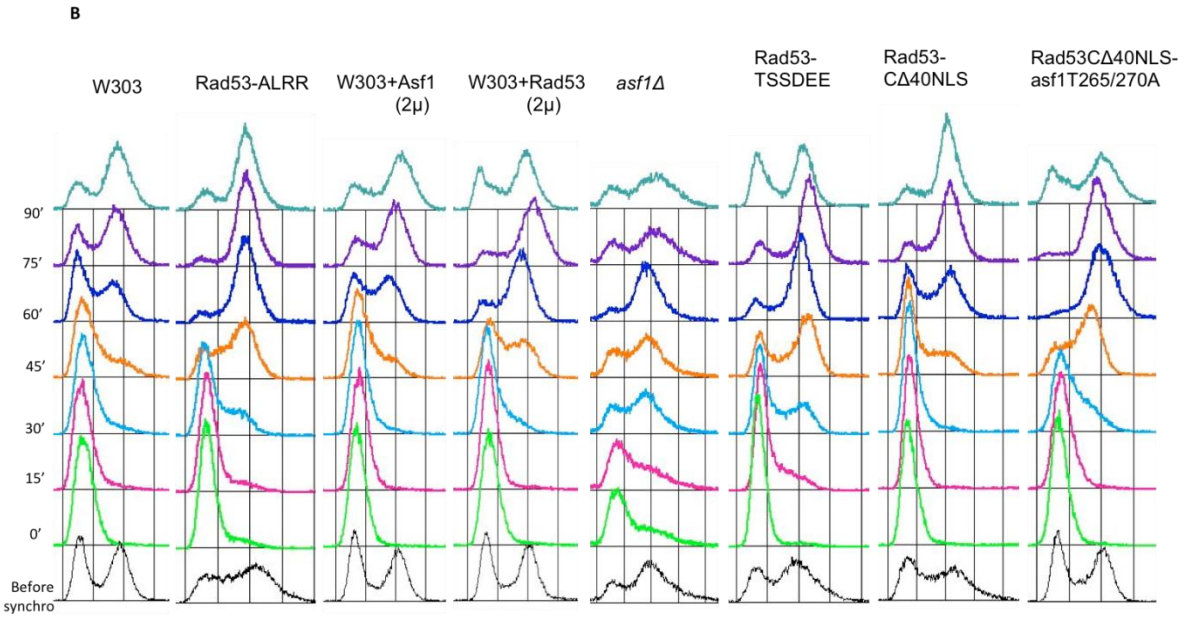

Figure 22. Shown is the cell cycle distribution of different mutations affecting the Asf1-Rad53 interaction mesured by flow cytometry analysis of DNA content. (A) In the absence of MMS, overexpression of Rad53 nor Asf1 has no obvious effect on cell cycle progression, whereas the *rad53-TSSDEE* and *rad53-CΔ40NLS asf1-T265A+270A* mutants accelerated cell cycle progression. (B) In the presence of 0.005% MMS, the ***asf1***Δ, overexpression of Rad53 or *rad53-TSSDEE, rad53CΔ40NLS-asf1T265+270A* mutants accelerated recovery from MMS.

3.10 Recovery of *rad24* versus *rad53-ALRR rad24* mutants to MMS treatment.

We would like to understand how the *rad53-ALRR* mutant increases the resistance of the *rad24* mutant to MMS treatment. We used a microcolony assay to follow the response of individual yeast cells to this treatment. Cells were treated with MMS for 30 minutes, and the cells were then diluted to 10^5-10^6 cells/ml and spread on the surface of the YPD plate. The number of individual cells/micro-colonies was then counted in a microscope after 20 hours of incubation. We classified cells in five different categories: cells that could form a viable microcolony of cells (class MV), cells that formed a microcolony of 16 cells or less indicating that the founding cell had undergone four or fewer divisions, but ultimately all cells were dead (class MM), individual cells that died without a bud (class 0), and individual cells with one, two, or three buds (classes 1, 2 and 3).

After treatment with 0.005% MMS, most WT and *rad53-ALRR* mutant cells formed viable micocolonies, with the remainder mainly in the form of abortive microcolonies of dead cells. In contrast, after treated with 0.05% MMS, most cells formed abortive

microcolonies of dead cells (Fig. 23A, B). As expected, *the rad53-ALRR rad24* mutant was more resistant to MMS compared to the *rad24* single mutant. Interestingly, both strains died mainly in the form of abortive microcolonies, indicating that cells were not permanently blocked in their division cycle after MMS treatment. Instead, cells underwent 3-4 divisions on average before dying with damage incurred by MMS. We were surprised that most cells could undergo several division cycles with ultimately lethal damage. Since Rad24 is implicated in activating one branch of the DNA damage checkpoints, it was possible that these divisions were due to defects in checkpoint activation in the *rad24* mutant. We thus monitored the response of W303-1a wild-type cells, and the *apn1*Δ *apn2*Δ, *rad53-ALRR*, *rad24*, and *rad24 rad53-ALRR* mutant cells to treatment with 0.005% MMS (Fig. 23C). The *apn1*Δ *apn2*Δ mutant is defective for the two APN endonuclease activities in yeast, but has a functional DNA damage checkpoint response. This mutant can excise methylated DNA bases, but is defective in cleaving the DNA strand at the abasic sites and repairing the damage. This repair defect makes the mutant hypersensitive to MMS. Interestingly, the *apn1*Δ *apn2*Δ mutant cells also died almost exclusively in the form of abortive microcolonies. This result contrasts with the response of budding yeast cells to persistent DNA double-strand breaks in which most cells are blocked before nuclear division by the DNA damage checkpoints. We conclude that the lethal damage incurred by yeast cells after MMS treatment is probably not due to DNA double-strand breaks, but rather some other form of damage that is compatible with limited proliferation before cell death. The results suggest that the increased viability after MMS treatment of *rad53-ALRR rad24* compared to the *rad24* may be due to increased repair or tolerance, rather than a difference in recovery from cell cycle arrest.

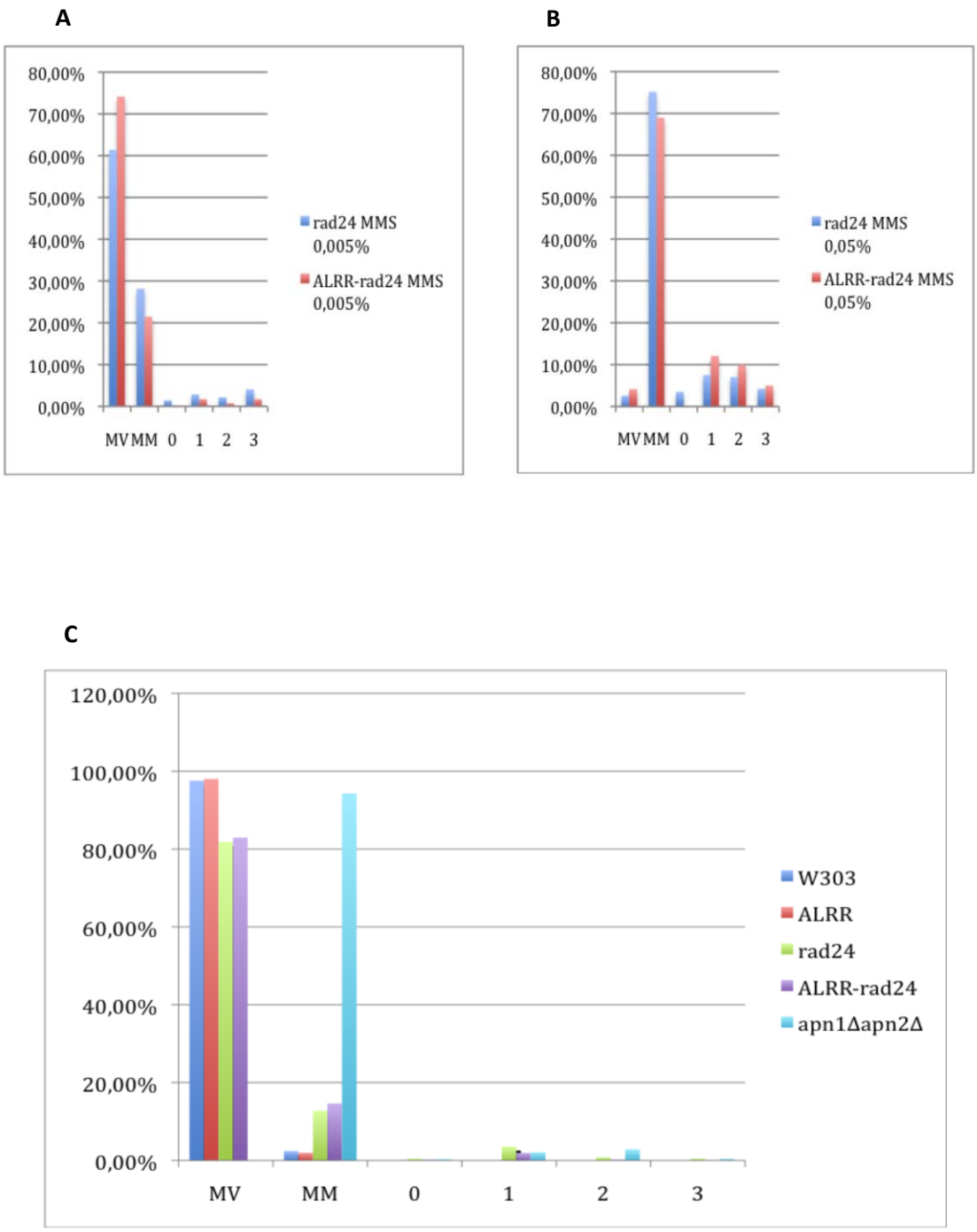

Figure 23. Microcolony viability analysis in *rad24* versus *rad53-ALRR rad24* strains. Cells were treated with 0.005% (A) or 0.05% (B) MMS for 30 minutes, then were released on YPD plates. The number of viable microcolonies (mv), dead microcolonies (mm) or cells with 0,1, 2, 3 buds is expressed as the percentage. (A) most *rad24* and *rad53-ALRR* mutant cells formed viable micocolonies and the remainder mainly formed abortive microcolonies of dead cells after treatment with 0.005% MMS. (B) most cells formed abortive microcolonies of dead cells after treated with 0.05% MMS. (C) most *apn1*Δ *apn2*Δ cells treated with 0.005% MMS also died in the form of abortive microcolonies.

3.11 Adaptation of *rad24* versus *rad53-ALRR rad24* mutants to continuous MMS treatment.

We showed in our submitted m/s that the *rad53-ALRR rad24* mutant grows better in the continued presence of 0.0025% MMS than does the *rad24* single mutant. We used the microcolony assay to examine the behaviour of individual cells in the continued presence of 0.05% MMS to characterize their cell cycle arrest under these conditions. W303, *rad53-ALRR, rad24* and *rad53-ALRR-rad24* cells were synchronized in the G1 phase by alpha factor treatment and cells were spread onto YPD plate containing 0.05% MMS. Individual cells were visualized in a microscope after incubating for 1h30 or 16h (Fig. 24 A,B). We counted the number of buds or individual cell bodies, since cells did not form microcolonies under these conditions of continuous exposure to 0.05% MMS (Fig. 25). The *rad53-ALRR* mutant budded more rapidly than all other strains after 1h30 of incubation in MMS (Fig. 24A), whereas the *rad24* single mutant remained mainly unbudded and the W303-1a wild-type and *rad53-ALRR rad24* double mutant showed intermediate behaviour. After overnight incubation in the presence of MMS, all strains were mainly blocked as single cells with one large bud. There were no major differences in the behaviour of W303-1a wild type, the *rad24* single mutant, and *rad24 rad53-ALRR* double mutant strains. However, the *rad53-ALRR* single mutant did form significantly higher numbers of cells containing three or more cell bodies (Fig. 24B). Altogether, these results suggest that the *rad53-ALRR* mutant shows higher levels of resistance and/or adaptation to the cell cycle arrest provoked by the continuous exposure of cells to 0.05% MMS compared to the wild type. It is possible that this resistance/adaptation contributes to the better growth of *rad53-ALRR rad24* double mutants compared to *rad24* single mutants on plates containing a lower level of MMS (0.0025%).

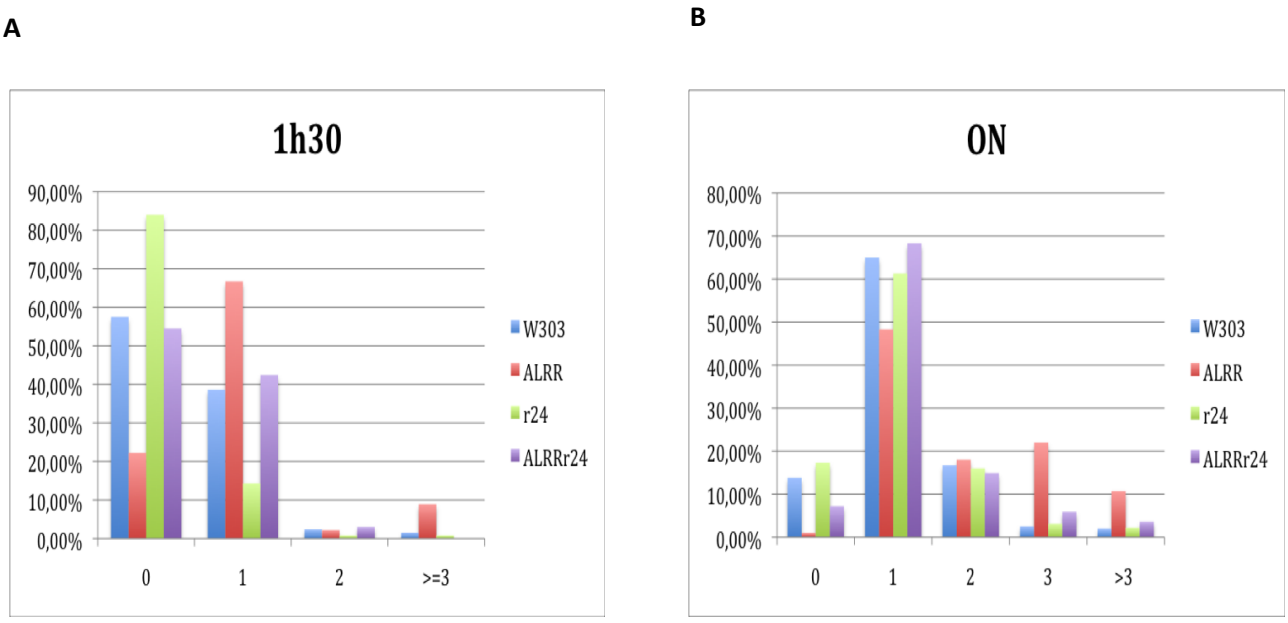

Figure 24. Microcolony analysis of adaptation to MMS-induced cell-cycle arrest in wild type, *rad53-ALRR, rad24* and *rad53-ALRR rad24* strains. Cells were spread on YPD plates containing 0.05% MMS for 1h30 (A) or overnight (ON) (B). The number of cells with 0,1, 2, 3, or more than 3 buds is expressed as the percentage of total cells. The rad53-ALRR mutant showed a better resistance and/or adaptation to the cell cycle arrest.

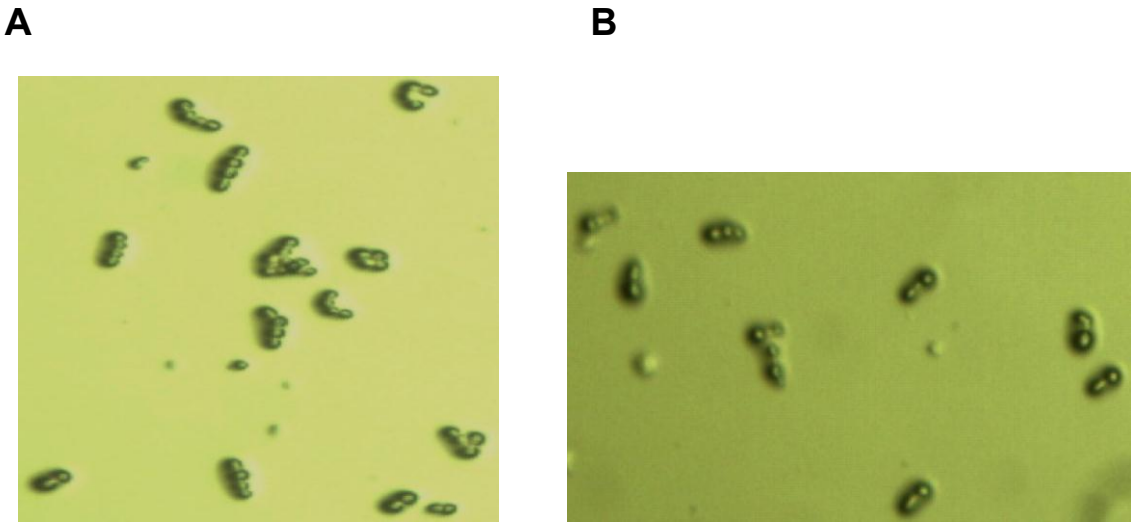

Figure 25. Individual cells were visualized in a microscope after ON treatment with 0.05% MMS. (A) *rad53-ALRR* cells dying with buds. (B) wild-type cells dying with only one or two buds.

3.12 Rad52-YFP foci in *rad53-ALRR* versus the wild type

Rad52 stimulates strand exchange by facilitating a recA-like protein Rad51 binding to single-stranded DNA. It is recruited to resected DNA double-strand breaks where it participates in repair by homologous recombination pathways. The presence of such DSBs in yeast cells can be visualized as intranuclear foci of Rad52-YFP. The quantification of the percentage of yeast cells with Rad52-YFP foci has been used to evaluate the efficiency with which mutant cells can repair DSBs. Wild type and *rad53-ALRR* cells expressing Rad52-YFP were treated with 0.01% MMS for 1h45, washed with PBS, and Rad52-YFP foci were then observed by fluorescence microscopy (Fig. 26). The percentage of wild type cells containing Rad52-YFP foci (26.7%) was similar to that of *rad53-ALRR* cells (23.2%) under these conditions. These observations suggest that there is no obvious difference in the generation or repair of MMS-induced DSBs in the *rad53-ALRR* mutant compared to the wild type.

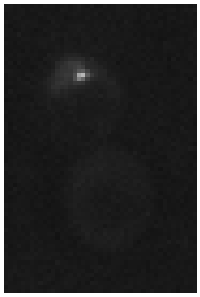

Figure 26. Example of a yeast cell expressing a focus of Rad52-YFP observed by fluorescence microscopy.

Materials and Methods

Co-immunoprecipitation

Cells were harvested at an O.D. 600nm of 0.8 and resuspended in 4 ml extraction buffer (50mM Tris pH 7.5, 100 mM NaCl, 10% glycerol, Roche protease inhibitor cocktail w/o EDTA) and broken in an Eaton press. Extracts were transferred to 50 Ti tubes and centrifuged (40 krpm, 1h, 4°C), and the protein concentration in the supernatant was determined with the Bradford reagent (Bio-Rad). Extracts (5 to 10 mg of protein for anti-myc IP in a final volume of 1 ml) were incubated with anti-myc beads/anti-IgG agarose that had been washed with extraction buffer on a rotating wheel O/N at 4°C. The beads were washed two times with 1 ml extraction buffer + 0.1% Tween-20 and immunoprecipitated proteins were solubilized by heating in the presence of sodium dodecyl sulfate-polyacrylamide gel electrophoresis (SDS-PAGE) sample buffer. Total cell extracts (40 µg) and immunoprecipitated proteins were seperated by SDS-PAGE, transferred to nitrocellulose membranes, incubated with primary antibodies followed by secondary antibodies. Proteins were detected using a Li-Cor Odyssey Imager.

GST-pull down Assay

40 µg purified $(His)_6$-GST-fusion proteins were immobilized on reduced glutathione agarose beads and equilibrated with 20 mM Hepes. 1mg yeast extract containing Asf1-myc was incubated with 50 µl beads for 30 min at 4°C. The beads were collected by centrifugation, washed twice in 20 mM Hepes and two times in 20 mM Hepes, 50 mM NaCl, 0.5% NP40. Bound Asf1 was analyzed by SDS-PAGE and revealed by 9E10 (anti-myc) antibody. (His)6-GST fusion proteins were revealed by anti-GST antibody.

Glycerol gradient centrifugation of yeast cell extracts

10-40% (v/v) glycerol gradients in 20 mM Hepes (pH 7.5) + 100 mM NaCl were poured in SW56 centrifuge tubes. Cells were broken in an Eaton press and 10 mgs of an S100 extract of W303-1a or CMY1562 cells were added to the top of the gradients and the tubes were spun at 45 krpm (200,000 x g) for 18h at 4°C. Proteins in 330 µl fractions were then precipitated by adding TCA to 25% final concentration and incubating on ice for 15 min followed by centrifugation at 22,000 x g for 20 min at 4°C. Pellets were washed with 0.5 ml cold acetone, air dried, and resuspended in SDS-PAGE sample buffer. Glycerol gradients

were calibrated using a mixture of BSA (67 kDa), lactate dehydrogenase (140 kDa), catalase (232 kDa), and ferritin (440 kDa).

Phenotypic analysis

For spotting analyses, cells were resuspended at 10^7/ml, subjected to 10-fold serial dilutions and 3µl of each dilution was spotted on plates of YPD, YPD + 100 mM HU, and YPD + 0.0025% MMS. Growth was assayed at 72h.

Cell synchrony and flow cytometric analysis (FACS)

Yeast cells were arrested with α-factor (30 µM). Cells were then either released into YPD, or treated with 0.005% MMS for 30 min, washed and released into YPD, or treated with 0.033% MMS or 200 mM HU. Cells were harvested every 15 min and fixed in 70% ethanol at 4°C for a minimum of 15 min. Fixed cells were washed in PBS and incubated with 0.25 mg/ml RNase A in PBS for 1h at 50°C. Afterwards, propidium iodide was added to a final concentration of 50 µg/ml and cells were incubated at RT in the dark for 15 min. DNA content was analysed by FACSCalibur (Bekton-Dickinson) and the Cell Quest software (Becton-Dickinson).

Viability test (recovery/adaptation)

Recovery: Cells were synchronized or not in G1 with 30 µM α-factor, then treated with 0.05% MMS or 100 mM HU for 1h30. After washing with YPD, cells were diluted to 10^5-10^6 cells/ml and 5µl of cells were spread on the surface of the a YPD plate. The number of individual cells/micro-colonies was then counted in a microscope after 20h of incubation at 30°C.
Adaptation: Cells were synchronized in G1 with α-factor and washed with YPD, then cells were diluted to 10^5-10^6 cells/ml and 2µl of cells were spread on the surface of the a YPD plate containing 0.05% MMS. The number of individual cells was then counted in a microscope after 1h30 and O/N incubation at 30°C.

Rad52-YPF foci

Cells were treated with 0.01% MMS for 1h45 and washed with PBS. The Rad52-YFP foci were then observed by fluorescent microscopy.

Yeast strains.

All strains were in the W303 background, except for CMY1384, CMY1389 and CMY1520 in the S288C background and CMY1357 and 1360 in the YPH250 background.

W303-1a *MATa ade2-1 his3-11,15 leu2-3, 112 trp1-1 ura3-1*

CMY1139 W303-1a ***rad53::HIS3 sml1-1***

CMY1155 W303-1a ***rad24::URA3***

CMY1156 W303-1a ***rad9::HIS3 rad24::URA3***

CMY1158 W303-1a ***rad9::HIS3***

CMY1227 W303-1a ***rad53::HIS3***/pBAD70 (2µ,*TRP1*)-*RNR1*

CMY1392 W303-1a RAD5+ ***RAD52-YFP*** *bar1::LEU2*

CMY1396 W303-1a ***ASF1-3HA-kanMX6*** *bar1::LEU2 his3-11 leu2-3,112 lys2 trp1-1 ura3-1*

CMY1411 W303-1a ***rad53CΔ40-TAPtag::HIS3MX***

CMY1412 W303-1a ***rad53CΔ63-TAPtag::HIS3MX***

CMY1413 W303-1a ***rad53CΔ91-TAPtag::HIS3MX***

CMY1426 W303-1a ***rad53CΔ21-TAPtag::HIS3MX***

CMY1453 W303-1a ***rad53CΔ40-NLS-TAPtag::HIS3MX***

CMY1501 SEY1127 W303-1a ***mrc1Δ-3::his5+***

CMY1558 W303-1a ***rad53-TSSDEE::URA3::rad53Δ::HIS3***

CMY1561 W303-1a ***rad53-K227A::kanMX***

CMY1562 W303-1a ***rad53-ALRR::URA3::rad53Δ::HIS3***

CMY1563 W303-1a ***RAD53::URA3::rad53Δ::HIS3***

CMY1564 W303-1b ***rad53-ALRR::URA3::rad53Δ::HIS3***

CMY1565 W303-1 ***rad53-ALRR::URA3::rad53Δ::HIS3 mrc1Δ-3::his5+***

CMY1566 W303-1a ***rad53-ALRR::URA3::rad53Δ::HIS3 rad24::kanMX***

CMY1567 W303-1a ***rad53-ALRR::URA3::rad53Δ::HIS3 rad9::LEU2***

CMY1568 W303-1a ***rad53-ALRR::URA3::rad53Δ::HIS3 rad24::kanMX rad9::LEU2***

CMY1569 W303-1a ***rad9::LEU2***

CMY1570 W303-1a ***rad24::kanMX***

CMY1571 W303-1a ***rad24::kanMX rad9::LEU2***

CMY1364 W303-1b ***asf1Δ::kanMX***

CMY1384 EY0986 *MATa his3Δ1 leu2Δ0 met15Δ0 ura3Δ0* ***RAD53-TAP::HIS3MX6*** (Ghaemmaghami et al, 2003)

CMY1389 FY2162 *MATa his3Δ200 leu2Δ1 ura3-52 trp1Δ63 lys2-128∂ Ty912.35-lacZ::his4* ***(hht1-hhf1)Δ::LEU2 (hht2-hhf2)Δ::HIS3***/pDM9=pRS416(CEN URA3)-***HHT1+HHF1***

CMY1520 MATa *his3Δ200 leu2Δ1 ura3-52 trp1Δ63 lys2-128∂ Ty912.35-lacZ::his4* ***(hht1-hhf1)Δ::LEU2 (hht2-hhf2)Δ::HIS3***/ pDM18 (CEN *TRP1*)-***hht2-R129E+HHF2***

CMY1357 YDH6 *ade2–101 his3-200 leu2-1 lys2–801 trp1-1 ura3–52* ***cka1-1::HIS3 cka2-1::TRP1/*** pCEN6-*LEU2*-***CKA2***

CMY1360 YDH13 *ade2–101 his3-200 leu2-1 lys2–801 trp1-1 ura3–52* ***cka1-1::HIS3 cka2-1::TRP1/*** pCEN6-*LEU2*-***cka2-13ts***

Conclusions and perspectives

Our results suggest that the Asf1-Rad53 interaction appears to involve three distinct interaction surfaces. The Rad53-FHA domain binds Asf1 phosphorylated at T270 in its C-terminal acidic tail domain in a casein kinase II-dependant manner. The C-terminal 21 aa of Rad53 binds the same surface of the conserved Asf1 N-terminal domain where the histone co-chaperones HirA/CAF-1 and histone H4. There should be a competition amongst these three proteins to bind the same surface of Asf1. These results explain why they form exclusive complexes with Asf1. The putative third interaction site may involve the histone H3 binding surface of Asf1 with an unknown surface of Rad53 that may reside in its kinase domain. We could further test this third interaction surface by two-hybrid analyses, but structural work will be also required to test this model. We encountered unexpected difficulties in reconstituting a complex of Rad53 and the N-terminal domain of Asf1 from purified recombinant proteins. We suspect the problem to lie in the conformation of the unphosphorylated, inactive Rad53 that seemed incompetent for binding Asf1N in vitro and was readily lost by non-specific sticking to surfaces. We suggest that the proteins must be co-expressed, and/or require specific chaperones, to form a productive complex. We co-expressed the kinase-defective Rad53-K227A (to prevent autophosphorylation) and Asf1N in E. coli, but still failed in obtaining a complex of the two proteins. We should perhaps test co-expression of wild-type Rad53 with Asf1N. Perhaps Asf1N can bind Rad53 and prevent its autophosphorylation in E. coli. However, it is also possible that E. coli does not express appropriate chaperones for this complex. Another possibility would be to test co-expression from baculovirus. The complex can of course be purified from S. cerevisiae, but the yield will not be high unless the complex can be over-expressed. The X-ray structure will no doubt be necessary to give us a complete picture of the unexpected intricacies of this complex.

Rad53 and Asf1 form a complex in yeast cells in the absence of genotoxic stress. We found that the Asf1-Rad53 complex was dissociated when cells were treated with hydroxyurea, a ribonucleotide reductase inhibitor, but not when cells were treated with the methylating agent MMS. The phosphorylation sites of Rad53 are likely to be different in response to HU and MMS. Phosphorylation sites at the putative third interaction surface of the Asf1-Rad53 complex are probably required for dissociation of the complex in presence of HU. Rad53 phosphorylation sites have been mapped after treating cells with MMS, but not HU. Thus, it will be important in the future to search for phosphorylation sites on Rad53 after treating cells with HU. This could be

done by mass spectrometry analyses on TAP-tagged Rad53 purified from HU-treated cells. Identifying phosphorylation sites specific to HU will allow their mutation to test their importance in dissociation of the complex in response to HU and in the general cellular response to HU. They would also pinpoint the surface of Rad53 that is involved in the third interaction surface of the Asf1-Rad53 complex.

From the structure of Asf1N and the Rad53 C-terminal peptide, we were able to identify the residues A806 and L808 of Rad53 as being important for the affinity of the complex. We found that the *rad53-ALRR* mutation destabilized the Asf1-Rad53 complex in yeast cells. Although this mutant did not have an obvious phenotype on its own, we found that it increased the resistance to HU and MMS of *rad9* and *rad24* mutants. Rad9 and Rad24 are implicated in recruitment and activation of Rad53 at DSBs. The *rad53-ALRR* mutation did not significantly modify the profile of Rad53 phosphorylation, so the increased viability of *rad53-ALRR* rad9 rad24 mutants exposed to HU or MMS may not be through effects on Rad53 activity. Though the FACS results of the *rad53-ALRR* mutant were not always reproducible, we observed that the *rad53-ALRR* mutant could re-enter the cell cycle and/or traverse S-phase more rapidly than wild type. The correct repression of late origin firing of this mutant in response to genotoxic stress was confirmed by a collaboration with Armelle Lengronne and Philippe Pasero. They are also examining whether the *rad53-ALRR* mutant has an effect on S phase progression at the level of replication fork initiation or progression by DNA combing and BrdU genome-wide incorporation experiments. Interestingly, Armelle has told us that some *rad53-ALRR* phenotypes resemble those of mutants with increased dNTP pools, such as *sml1*Δ mutants. It will thus be interesting to test dNTP levels in the *rad53-ALRR* mutant. Hopefully, the genome-wide experiments will give us a definitive response of the effect of the mutant on DNA replication and further clues for future experimentation.

The increased viability of *Rad53-ALRR rad24* double mutant compared to *rad24* may due to an increased repair or adaptation. Further work on testing the effect of the mutant on DNA repair after treatment with MMS could potentially be done by pulsed-field gel electrophoresis (PFGE) or by DNA comet analysis. Using G1 synchronized cells for MMS treatment would also allow us to follow Rad53 activity by the Rad9-Rad24 pathway without the contribution of the Mrc1 pathway and may allow us to see effects of the *rad53-ALRR* mutation on adaptation/recovery at the level of the *Rad53-ALRR* mutant kinase.

References

Abraham RT (2001) Cell cycle checkpoint signaling through the ATM and ATR kinases. Genes & Development. pp 2177–2196.

Acilan, C., Potter, D.M., and Saunders, W.S. 2007. DNA repair pathways involved inanaphase bridge formation. *Genes Chromosomes Cancer* **46**(6): 522-531.

Adkins, M. W. & Tyler, J. K. The histone chaperone Asf1p mediates global chromatin disassembly in vivo. *J Biol Chem* **279**, 52069-74 (2004).

Adkins, M. W., Howar, S. R. & Tyler, J. K. Chromatin disassembly mediated by the histone chaperone Asf1 is essential for transcriptional activation of the yeast PHO5 and PHO8 genes. *Mol Cell* **14**, 657-66 (2004).

Adkins (a), M. W., Williams, S. K., Linger, J. & Tyler, J. K. Chromatin disassembly from the PHO5 promoter is essential for the recruitment of the general transcription machinery and coactivators. *Mol Cell Biol* **27**, 6372-82 (2007).

Adkins (b), M. W., Carson, J. J., English, C. M., Ramey, C. J. & Tyler, J. K. The histone chaperone anti-silencing function 1 stimulates the acetylation of newly synthesized histone H3 in S-phase. *J Biol Chem* **282**, 1334-40 (2007).

Agarwal R, Tang Z, Yu H, Cohen-Fix O. 2003. Two distinct pathways for inhibiting pds1 ubiquitination in response to DNA damage. J. Biol. Chem. 278:45027–33

Ahn, J.Y., Schwarz, J.K., Piwnica-Worms, H., and Canman, C.E. (2000). Threonine 68 phosphorylation by ataxia telangiectasia mutated is required for efficient activation of Chk2 in response to ionizing radiation. Cancer Res. 60, 5934–5936.

Ahn, J.Y., Li, X., Davis, H.L., and Canman, C.E. (2002). Phosphorylation of threonine 68 promotes oligomerization and autophosphorylation of the Chk2 protein kinase via the forkhead-associated domain. J. Biol. Chem. 277, 19389–19395.

Ahn, J., Urist, M., and Prives, C. (2004). The Chk2 protein kinase. DNA Repair(Amst.) 3, 1039–1047.

Ahnesorg P, Jackson SP. The non-homologous end-joining protein Nej1p is a target of the DNA damage checkpoint. DNA Repair (Amst) 2007;6:190–201.

Albaugh BN, Kolonko EM, Denu JM. Kinetic mechanism of the Rtt109-Vps75 histone acetyltransferase-chaperone complex. Biochemistry. 2010 Aug 3;49(30):6375-85.

Alcasabas AA, Osborn AJ, Bachant J, Hu F, Werler PJ, Bousset K, Furuya K, Diffley JF, Carr AM, Elledge SJ. Mrc1 transduces signals of DNA replication stress to activate Rad53. Nat Cell Biol. 2001 Nov;3(11):958-65.

Allard S, et al. (1999) NuA4, an essential transcription adaptor/histone H4 acetyltransferase

Allen JB, Zhou Z, Siede W, Friedberg EC, Elledge SJ. The SAD1/RAD53 protein kinase controls multiple checkpoints and DNA damage-induced transcription in yeast. Genes Dev. 1994 Oct 15;8(20):2401-15.

Allis CD, et al. New nomenclature for chromatin-modifying enzymes. Cell 2007;131:633–636.

Andrews, A. J., Downing, G., Brown, K., Park, Y. J. & Luger, K. A thermodynamic model for Nap1-histone interactions. *J Biol Chem* **283**, 32412- 8 (2008).

Aparicio, O. M., Stout, A. M. & Bell, S. P. Differential assembly of Cdc45p and DNA polymerases at early and late origins of DNA replication. *Proc. Natl Acad. Sci. USA* **96**, 9130–9135 (1999).

Arents and Moudrianakis. (1995) The histone fold: a ubiquitous architectural motif utilized in DNA compaction and protein dimerization. *Proc Natl Acad Sci USA*. 92(24):11170-4.

Aylon Y, Kupiec M. The checkpoint protein Rad24 of Saccharomyces cerevisiae is involved in processing double-strand break ends and in recombination partner choice. Mol Cell Biol. 2003 Sep;23(18):6585-96.

Baroni E, Viscardi V, Cartagena-Lirola H, Lucchini G, Longhese MP (2004) The functions of budding yeast Sae2 in the DNA damage response require Mec1- and Tel1-dependent phosphorylation. Mol Cell Biol 24: 4151–4165

Bartek J, Lukas J: Pathways governing G1/S transition and their response to DNA damage. FEBS Lett 2001, 490:117-122.

Bartek, J., C. Lukas, and J. Lukas. 2004. Checking on DNA damage in S phase. Nat. Rev. Mol. Cell Biol. 5:792–804. doi:10.1038/nrm1493

Bartek J, Lukas J. DNA damage checkpoints: from initiation to recovery or adaptation. Curr Opin Cell Biol. 2007

Bartrand, A.J., D. Iyasu, and G.S. Brush. 2004. DNA stimulates Mec1-mediated phosphorylation of replication protein A. *J Biol Chem*. 279:26762-7.

Bashkirov VI, King JS, et al., DNA repair protein Rad55 is a terminal substrate of the DNA damage checkpoints, Mol. Cell. Biol. 20 (2000) 4393–4404.

Bashkirov VI, Bashkirova EV, Haghnazari E, Heyer WD. Direct kinase-to-kinase signaling mediated by the FHA phosphoprotein recognition domain of the Dun1 DNA damage checkpoint kinase. Mol Cell Biol. 2003 Feb;23(4):1441-52

Basrai MA, Velculescu VE, Kinzler KW, Hieter P. NORF5/HUG1 is a component of the MEC1-mediated checkpoint response to DNA damage and replication arrest in Saccharomyces cerevisiae. Mol Cell Biol. 1999 Oct;19(10):7041-9.

Becker PB, Hörz W. ATP-dependent nucleosome remodeling. Annu Rev Biochem. 2002;71:247-73.

Bell SP, Dutta A. DNA replication in eukaryotic cells. Annu Rev Biochem. 2002;71:333-74.

Berndsen CE, et al. (2008) Molecular functions of the histone acetyltransferase chaperone complex Rtt109-Vps75. Nat Struct Mol Biol 15:948–956.

Bird, A. W. *et al.* Acetylation of histone H4 by Esa1 is required for DNA double-strand break repair. *Nature* **419**, 411–415 (2002).

Black BE, Bassett EA. The histone variant CENP-A and centromere specification. Curr Opin Cell Biol. 2008 Feb;20(1):91-100. Epub 2008 Jan 15.

Blow JJ, Dutta A. Preventing re-replication of chromosomal DNA. Nat Rev Mol Cell Biol. 2005 Jun;6(6):476-86.

Bonilla, C. Y., Melo, J. A. & Toczyski, D. P. Colocalization of sensors is sufficient to activate the DNA damage checkpoint in the absence of damage. *Mol. Cell* **30**, 267–276 (2008).

Bortvin, A. & Winston, F. Evidence that Spt6p controls chromatin structure by a direct interaction with histones. *Science* **272**, 1473-6 (1996).

Bosco, E.E., Mayhew, C.N., Hennigan, R.F., Sage, J., Jacks, T., and Knudsen, E.S. 2004. RB signaling prevents replication-dependent DNA double-strand breaks following genotoxic insult. *Nucleic Acids Res* **32**(1): 25-34.

Bousset K, Diffley JF. The Cdc7 protein kinase is required for origin firing during S phase. Genes Dev. 1998 Feb 15;12(4):480-90. Erratum in: Genes Dev 1998 Apr 1;12(7):1072.

Branzei D, Foiani M. The DNA damage response during DNA replication. Curr Opin Cell Biol. 2005 Dec;17(6):568-75.

Branzei D. Foiani M. The Rad53 signal transduction pathway: replication fork stabilization, DNA repair, and adaptation. Exp. Cell Res. 2006;312:2654–2659.

Branzei, D., and M. Foiani. 2008. Regulation of DNA repair throughout the cell cycle. *Nat Rev Mol Cell Biol*. 9:297-308.

Branzei D, Foiani M. The checkpoint response to replication stress. DNA Repair (Amst). 2009 Sep 2;8(9):1038-46.

Brush GS, Morrow DM, Hieter P, Kelly TJ. The ATM homologue MEC1 is required for phosphorylation of replication protein A in yeast. Proc Natl Acad Sci U S A. 1996 Dec 24;93(26):15075-80.

Burgess RJ, Zhang Z. Histones, histone chaperones and nucleosome assembly. Protein Cell. 2010 Jul;1(7):607-12.

Burma S, Chen BP, Murphy M, Kurimasa A, Chen DJ: ATM phosphorylates histone H2AX in response to DNA double-strand breaks. J Biol Chem 2001, 276:42462-42467.

Byeon IJ, Yongkiettrakul S, Tsai MD. Solution structure of the yeast Rad53 FHA2 complexed with a phosphothreonine peptide pTXXL: comparison with the structures of FHA2-pYXL and FHA1-pTXXD complexes. J Mol Biol. 2001 Nov 30;314(3):577-88.

Byeon IJ, Li H, Song H, Gronenborn AM, Tsai MD. Sequential phosphorylation and multisite interactions characterize specific target recognition by the FHA domain of Ki67. Nat Struct Mol Biol. 2005 Nov;12(11):987-93.

Byun TS, Pacek M, Yee MC, Walter JC, Cimprich KA. Functional uncoupling of MCM helicase and DNA polymerase activities activates the ATR- dependent checkpoint. Genes Dev 2005; 19:1040- 52.

Cai Z, Chehab NH, Pavletich NP (2009) Structure and activation mechanism of the CHK2 DNA damage checkpoint kinase. Mol Cell 35: 818–829.

Carrera, P., Moshkin, Y.M., Gronke, S., Sillje, H. H., Nigg, E.A., Jackle, H., and Karch, F. (2003). Tousled-like kinase functions with the chromatin assembly pathway regulating nuclear divisions. Genes Dev. 17: 2578-2590.

Caspari T, Murray JM, Carr AM, Cdc2-cyclin B kinase activity links Crb2 and Rqh1-topoisomerase III, Genes Dev. 16 (2002) 1195–1208.

Celeste A, Fernandez-Capetillo O, Kruhlak MJ, et al. Histone H2AX phosphorylation is dispensable for the initial recognition of DNA breaks. Nat Cell Biol 2003;5:675–679.

Celeste A, Petersen S, Romanienko PJ, et al. Genomic instability in mice lacking histone H2AX. Science 2002;296:922–927.

Celic I, Masumoto H, Griffith WP, Meluh P, Cotter RJ, et al. (2006) The sirtuins hst3 and Hst4p preserve genome integrity by controlling histone h3 lysine 56 deacetylation. Curr Biol 16: 1280–1289.

Chadwick BP, Willard HF. A novel chromatin protein, distantly related to histone H2A, is largely excluded from the inactive X chromosome. J. Cell Biol. 2001;152:375-384.

Chakravarthy S, Luger K: The histone variant macro-H2A preferentially forms ‘hybrid nucleosomes’. J Biol Chem 2006, 281:25522-25531.

Chen SH, Smolka MB, Zhou H. Mechanism of Dun1 activation by Rad53 phosphorylation in Saccharomyces cerevisiae. J Biol Chem. 2007 Jan 12;282(2):986-95.

Chen CC, Carson JJ, Feser J, Tamburini B, Zabaronick S, et al. (2008) Acetylated lysine 56 on histone H3 drives chromatin assembly after repair and signals for the completion of repair. Cell 134: 231–243.

Chen SH, Zhou H. Reconstitution of Rad53 activation by Mec1 through adaptor protein Mrc1. J Biol Chem. 2009 Jul 10;284(28):18593-604.

Cheng L, Hunke L, Hardy CF. 1998. Cell cycle regulation of the Saccharomyces cerevisiae polo-like kinase cdc5p. Mol. Cell Biol. 18:7360–70

Chimura T, Kuzuhara T, Horikoshi M (2002) Identification and characterization of CIA/ASF1 as an interactor of bromodomains associated with TFIID. Proc Natl Acad Sci USA 99:9334–9339.

Chin JK, Bashkirov VI, Heyer WD, Romesberg FE. Esc4/Rtt107 and the control of recombination during replication. DNA Repair (Amst). 2006 May 10;5(5):618-28.

Clerici M, Mantiero D, Lucchini G, Longhese MP (2005) The Saccharomyces cerevisiae Sae2 protein promotes resection and bridging of double-strand break ends. J Biol Chem 280: 38631–38638

Clerici M, Mantiero D, Lucchini G, Longhese MP. 2006. The Saccharomyces cerevisiae Sae2 protein negatively regulates DNA damage checkpoint signaling. EMBO Rep. 7:212– 18

Cobb JA, Bjergbaek L, Shimada K, Frei C, Gasser SM. DNA polymerase stabilization at stalled replication forks requires Mec1 and the RecQ helicase Sgs1. EMBO J. 2003 Aug 15;22(16):4325-36.

Cobb JA, Schleker T, Rojas V, Bjergbaek L, Tercero JA, Gasser SM. Replisome instability, fork collapse, and gross chromosomal rearrangements arise synergistically from Mec1 kinase and RecQ helicase mutations. Genes Dev. 2005 Dec 15;19(24):3055-69.

Cohen-Fix O, KoshCohen-Fix O, Koshland D. 1997. The anaphase inhibitor of Saccharomyces cerevisiae Pds1p is a target of the DNA damage checkpoint pathway. Proc. Natl. Acad. Sci. USA 94:14361–66

Collins SR, Miller KM, Maas NL, Roguev A, Fillingham J, Chu CS, Schuldiner M, Gebbia M, Recht J, Shales M, Ding H, Xu H, Han J, Ingvarsdottir K, Cheng B, Andrews B, Boone C, Berger SL, Hieter P, Zhang Z, Brown GW, Ingles CJ, Emili A, Allis CD, Toczyski DP, Weissman JS, Greenblatt JF, Krogan NJ. Functional dissection of protein complexes involved in yeast chromosome biology using a genetic interaction map. Nature 2007;446:806–810.

Cordón-Preciado V, Ufano S, Bueno A. Limiting amounts of budding yeast Rad53 S-phase checkpoint activity results in increased resistance to DNA alkylation damage. Nucleic Acids Res. 2006;34(20):5852-62.

Cosgrove, M.S., Boeke, J.D., and Wolberger, C. 2004. Regulated nucleosome mobility and the histone code. Nat. Struct. Mol. Biol. **11**: 1037–1043.

Costanzo, V. *et al.* Reconstitution of an ATM-dependent checkpoint that inhibits chromosomal DNA replication following DNA damage. *Mol. Cell* **6**, 649–659 (2000).

Cotta-Ramusino C, Fachinetti D, Lucca C, Doksani Y, Lopes M, Sogo J, Foiani M. Exo1 processes stalled replication forks and counteracts fork reversal in checkpoint-defective cells. Mol Cell. 2005 Jan 7;17(1):153-9.Czornak K, Chughtai S, Chrzanowska KH. Mystery of DNA repair: the role of the MRN complex and ATM kinase in DNA damage repair. J Appl Genet 2008; 49:383-96.

Daganzo SM, Erzberger JP, Lam WM, Skordalakes E, Zhang R, Franco AA, Brill SJ, Adams PD, Berger JM, Kaufman PD. Structure and function of the conserved core of histone deposition protein Asf1. Curr Biol. 2003 Dec 16;13(24):2148-58.

Degrassi, F., Fiore, M., and Palitti, F. 2004. Chromosomal aberrations and genomic instability induced by topoisomerase-targeted antitumour drugs. *Curr Med Chem Anticancer Agents* 4(4): 317-325.

Daley JM, Palmbos PL, Wu D, Wilson TE (2005) Nonhomologous end joining in yeast. Annu Rev Genet 39:431–451.

Das C, Lucia MS, Hansen KC, Tyler JK (2009) CBP/p300-mediated acetylation of histone H3 on lysine 56. Nature 459:113–117.

Davey CA, Sargent DF, Luger K, Maeder AW, Richmond TJ. Solvent mediated interactions in the structure of the nucleosome core particle at 1.9 a resolution. J Mol Biol. 2002 Jun 21;319(5):1097-113.

de Bettignies G, Johnston LH. 2003. The mitotic exit network. Curr. Biol. 13:R301

De Koning L, Corpet A, Haber JE, Almouzni G (2007) Histone chaperones: An escort network regulating histone traffic. Nat Struct Mol Biol 14:997–1007.

Desany BA, Alcasabas AA, Bachant JB, Elledge SJ. Recovery from DNA replicational stress is the essential function of the S-phase checkpoint pathway. Genes Dev. 1998 Sep 15;12(18):2956-70.

Dimitrova, D.S., and D.M. Gilbert. 2000. Temporally coordinated assembly and disassembly of replication factories in the absence of DNA synthesis. Nat. Cell Biol. 2:686–694.

Downs JA, Lowndes NF, Jackson SP: A role for Saccharomyces cerevisiae histone H2A in DNA repair. Nature 2000, 408:1001-1004.

Driscoll R, Hudson A, Jackson SP. Yeast Rtt109 promotes genome stability by acetylating histoneH3 on lysine 56. Science 2007;315:649–652.

Duncker BP, Shimada K, Tsai-Pflugfelder M, Pasero P, Gasser SM. An N-terminal domain of Dbf4p mediates interaction with both origin recognition complex (ORC) and Rad53p and can deregulate late origin firing. Proc Natl Acad Sci U S A. 2002 Dec 10;99(25):16087-92. Epub 2002 Nov 19.

Durocher D, Henckel J, Fersht AR, Jackson SP. The FHA domain is a modular phosphopeptide recognition motif. Mol Cell. 1999 Sep;4(3):387-94.

Durocher D, Taylor IA, Sarbassova D, Haire LF, Westcott SL, Jackson SP, Smerdon SJ, Yaffe MB. The molecular basis of FHA domain:phosphopeptide binding specificity and implications for phospho-dependent signaling mechanisms. Mol Cell. 2000 Nov;6(5):1169-82.

Durocher D, Jackson SP. The FHA domain. FEBS Lett. 2002 Feb 20;513(1):58-66.

Eisen, J. A., K. S. Sweder, and P. C. Hanawalt. 1995. Evolution of theSNF2 family of proteins: subfamilies with distinct sequences andfunctions. Nucleic Acids Res **23:**2715-23.

Eitoku M, Sato L, Senda T, Horikoshi M (2008) Histone chaperones: 30 years from isolation to elucidation of the mechanisms of nucleosome assembly and disassembly. Cell Mol Life Sci 65:414–444.

Elgin, S.C., Grewal, S.I., 2003. Heterochromatin: silence is golden. Curr. Biol. 13, R895–R898.

Elledge, S. J., Zhou, Z. & Allen, J. B. Ribonucleotide reductase: regulation, regulation, regulation. *Trends Biochem Sci* **17**, 119-23 (1992).

Elledge, S. J. (1996). Cell cycle checkpoints: preventing an identity crisis. Science 274(5293): 1664-72.

Emili A. MEC1-dependent phosphorylation of Rad9p in response to DNA damage. Mol Cell. 1998 Aug;2(2):183-9.

Emili A, Schieltz DM, Yates JR, 3rd, Hartwell LH (2001) Dynamic interaction of DNA damage checkpoint protein Rad53 with chromatin assembly factor Asf1. Mol Cell 7:13–20.

English, C. M., Maluf, N. K., Tripet, B., Churchill, M. E. & Tyler, J. K. ASF1 binds to a heterodimer of histones H3 and H4: a two-step mechanism for the assembly of the H3-H4 heterotetramer on DNA. *Biochemistry* 44, 13673-82 (2005).

English, C. M., Adkins, M. W., Carson, J. J., Churchill, M. E. & Tyler, J. K. Structural basis for the histone chaperone activity of Asf1. *Cell* 127, 495-508 (2006).

Faast R, Thonglairoam V, Schulz TC, Beall J, Wells JR, Taylor H, Matthaei K, Rathjen PD, Tremethick DJ, Lyons I. Histone variant H2A.Z is required for early mammalian development. Curr Biol. 2001 Aug 7;11(15):1183-7.

Falbo KB, Shen X. Chromatin remodeling in DNA replication. J Cell Biochem. 2006 Mar 1;97(4):684-9.

Falck J, N. Mailand, R.G. Syljuasen, J. Bartek, J. Lukas, The ATM-Chk2-Cdc25A checkpoint pathway guards against radioresistant DNA synthesis, Nature 410 (2001) 842–847.

Falck J, Coates J, Jackson SP: Conserved modes of recruitment of ATM, ATR and DNA-PKcs to sites of DNA damage. Nature 2005, 434:605-611.

Fan JY, Gordon F, Luger K, Hansen JC, Tremethick DJ: The essential histone variant H2A.Z regulates the equilibrium between different chromatin conformational states. Nat Struct Biol 2002, 19:172-176.

Fiorani S, Mimun G, Caleca L, Piccini D, Pellicioli A. Characterization of the activation domain of the Rad53 checkpoint kinase. Cell Cycle. 2008 Feb 15;7(4):493-9.

Flaus A, Owen-Hughes T. Mechanisms for ATP-dependent chromatin remodelling: farewell to the tuna-can octamer? Curr Opin Genet Dev. 2004 Apr;14(2):165-73.

Flott S, Alabert C, et al., Phosphorylation of Slx4 by Mec1 and Tel1 regulates the single-strand annealing mode of DNA repair in budding yeast, Mol. Cell. Biol. 27 (2007) 6433–6445.

Foiani M, Pellicioli A, Lopes M, Lucca C, Ferrari M, Liberi G, Muzi Falconi M, Plevani P. DNA damage checkpoints and DNA replication controls in Saccharomyces cerevisiae. Mutat Res 2000;451 (1–2):187–96.

Franco, A. A., Lam, W. M., Burgers, P. M. and Kaufman, P. D. (2005). Histone deposition protein Asf1 maintains DNA replisome integrity and interacts with replication factor C. Genes Dev. 19: 1365-1375.

Gambus A, Jones RC, Sanchez-Diaz A, Kanemaki M, van Deursen F, Edmondson RD, Labib K. GINS maintains association of Cdc45 with MCM in replisome progression complexes at eukaryotic DNA replication forks. Nat Cell Biol. 2006 Apr;8(4):358-66.

Garcia BA, et al. Organismal differences in post-translational modifications in histones H3 and H4. J. Biol. Chem 2007;282:7641–7655.

Ge, X. Q., Jackson, D. A. and Blow, J. J. (2007). Dormant origins licensed by excess Mcm2-7 are required for human cells to survive replicative stress. Genes Dev *21*, 3331–41.

Geymonat M, Spanos A, Walker PA, Johnston LH, Sedgwick SG. 2003. In vitro regulation of budding yeast Bfa1/Bub2 GAP activity by Cdc5. J. Biol. Chem. 278:14591–94

Ghaemmaghami S, Huh WK, Bower K, Howson RW, Belle A, Dephoure N, O'Shea EK, Weissman JS. Global analysis of protein expression in yeast. Nature. 2003 Oct 16;425(6959):737-41.

Giannattasio M, Sommariva E, Vercillo R, Lippi-Boncambi F, Liberi G, Foiani M, Plevani P, Muzi-Falconi M. A dominant-negative MEC3 mutant uncovers new functions for the Rad17 complex and Tel1. Proc Natl Acad Sci U S A. 2002 Oct 1;99(20):12997-3002.

Gilbert CS, Green CM, Lowndes NF. Budding yeast Rad9 is an ATP-dependent Rad53 activating machine. Mol Cell. 2001 Jul;8(1):129-36.

Glover JN, Williams SR, Lee MS: Interactions between BRCTrepeats and phosphoproteins: tangled up in two. Trends Biochem Sci 2004, 29:579-585.

Goffeau A, Barrell BG, Bussey H, Davis RW, Dujon B, Feldmann H, Galibert F, Hoheisel JD, Jacq C, Johnston M, Louis EJ, Mewes HW, Murakami Y, Philippsen P, Tettelin H, Oliver SG (Oct 1996). "Life with 6000 genes". *Science* **274** (5287): 546, 563–567.

Goodfellow H, Krejci A, Moshkin Y, Verrijzer CP, Karch F, et al. (2007) Gene- specific targeting of the histone chaperone asf1 to mediate silencing. Dev Cell 13: 593–600.

Green, E. M. et al. Replication-independent histone deposition by the HIR complex and Asf1. *Curr Biol* **15**, 2044-9 (2005).

Grewal S.I. and Elgin, S.C. *2002*. Heterochromatin: New possibilities for the inheritance of structure. Curr. Opin. Genet. Dev. *12*: *178*-187

Grewal SIS & Jia S. 2007. Heterochromatin revisited. *Nature Reviews Genetics* 8 (1): 35-.

Groth, A., Lukas, J., Nigg, E. A., Sillje, H. H., Wernstedt, C., Bartek, J., and Hansen, K. (2003). Human Tousled like kinases are targeted by an ATM- and Chk1-dependent DNA damage checkpoint. EMBO J. 22: 1676-1687.

Groth, A. et al. Human Asf1 regulates the flow of S phase histones during replicational stress. *Mol Cell* 17, 301-11 (2005).

Groth, A., et al. (2007). Regulation of replication fork progression through histone supply and demand. Science 318: 1928-1931.

Gunjan, A. and Verreault, A. (2003). A Rad53 kinase-dependent surveillance mechanism that regulates histone protein levels in S. cerevisiae. Cell *115*, 537–49.

Haber JE: Partners and pathways: repairing a double-strand break. Trends Genet 2000, 16:259-264.

Hammet A, Pike BL, Mitchelhill KI, Teh T, Kobe B, House CM, Kemp BE, Heierhorst J. FHA domain boundaries of the dun1p and rad53p cell cycle checkpoint kinases. FEBS Lett. 2000 Apr 14;471(2-3):141-6.

Han JH (a), Zhou H, Li ZH, Xu RM, Zhang ZG (2007) Acetylation of lysine 56 of histone H3 catalyzed by RTT109 and regulated by ASF1 is required for replisome integrity. J Biol Chem 282:28587–28596.

Han J (b), Zhou H, Li Z, Xu RM, Zhang Z. The Rtt109-Vps75 histone acetyltransferase complex acetylates non-nucleosomal histone H3. J. Biol. Chem 2007;282:14158–14164.

Han J (c), et al. Rtt109 acetylates histone H3 lysine 56 and functions in DNA replication. Science 2007;315:653–655.

Harrison JC, Haber JE (2006) Surviving the breakup: the DNA damage checkpoint. Annu Rev Genet 40: 209–235.41. Kuzminov A (2001) DNA replication meets genetic exchange: chromosomal.

Hartwell, L.H., and THartwell, L.H., and T.A. Weinert. 1989. Checkpoints: controls that ensure the order of cell cycle events. *Science*. 246:629-34.

Hartwell, L., T. Weinert, L. Kadyk and B. Garvik (1994). Cell cycle checkpoints, genomic integrity, and cancer. Cold Spring Harb Symp Quant Biol 59: 259-63.

Heideker J, Lis ET, Romesberg FE: Phosphatases, DNA damage checkpoints and checkpoint deactivation. Cell Cycle 2007, 6:3058-3064.

Henikoff S, Furuyama T, Ahmad K. Histone variants, nucleosome assembly and epigenetic inheritance. Trends Genet. 2004 Jul; 20(7):320-6.

Henikoff S, Ahmad K. Assembly of variant histones into chromatin. Annu Rev Cell Dev Biol. 2005;21:133-53.

Henikoff, S. 2008. Nucleosome destabilization in the epigenetic regulation of gene expression. Nat. Rev. Genet. 9:15–26.

Herzberg K, Bashkirov VI, et al., Phosphorylation of Rad55 on serines 2, 8, and 14 is required for efficient homologous recombination in the recovery of stalled replication forks, Mol. Cell. Biol. 26 (2006) 8396–8409.

Hoch DA, Stratton JJ, Gloss LM: Protein-protein Forster resonance energy transfer analysis of nucleosome core particles containing H2A and H2A.Z. J Mol Biol 2007, 371:971-988.

Hoeijmakers, J.H. (2001). Genome maintenance mechanisms for preventing cancer. Nature *411*, 366-374.

Horn PJ, Peterson CL. Chromatin higher order folding—wrapping up transcription. Science 2002; 297:1824-7.

Hu F, Alcasabas AA, Elledge SJ. Asf1 links Rad53 to control of chromatin assembly. Genes Dev. 2001 May 1;15(9):1061-6.

Hu F, Elledge SJ. 2002. Bub2 is a cell cycle regulated phospho-protein controlled by multiple checkpoints. Cell Cycle 1:351–55

Huang, S. et al. Rtt106p is a histone chaperone involved in heterochromatinmediated silencing. *Proc Natl Acad Sci U S A* 102, 13410-5 (2005).

Huen MS, Grant R, Manke I, et al. RNF8 transduces the DNA-damage signal via histone ubiquitylation and checkpoint protein assembly. Cell 2007;131:901–914.

Huyen, Y. *et al.* Methylated lysine 79 of histone H3 targets 53BP1 to DNA double-strand breaks. *Nature* 432, 406–411 (2004).

Hyland EM, et al. Insights into the role of histone H3 and histone H4 core modifiable residues in Saccharomyces cerevisiae. Mol. Cell. Biol 2005;25:10060–10070.

Ito, T., M. Bulger, M. J. Pazin, R. Kobayashi, and J. T. Kadonaga. 1997. ACF, an ISWI-containing and ATP-utilizing chromatin assembly and remodeling factor. Cell 90:145-55.

Jasencakova Z, Scharf AN, Ask K, Corpet A, Imhof A, Almouzni G, Groth A. Replication stress interferes with histone recycling and predeposition marking of new histones. Mol Cell. 2010 Mar 12;37(5):736-43.

Jazayeri A, Falck J, Lukas C, Bartek J, Smith GC, Lukas J, Jackson SP: ATMandcell cycle-dependent regulation of ATR in response to DNA doublestrandbreaks. Nat Cell Biol 2006, 8(l):37-45.

Jenuwein T., ALLIS C. D. 2001. Translating the histone code. Science 293: 1074.1080.

Johnson, A., and M. O'Donnell. 2005. Cellular DNA replicases: components and dynamics at the replication fork. *Annu Rev Biochem*. 74:283-315.

Kamakaka RT, Biggins S. Histone variants: deviants? Genes Dev. 2005 Feb 1;19(3):295-310.

Kanoh Y, Tamai K, Shirahige K. Different requirements for the association of ATR-ATRIP and 9-1-1 to the stalled replication forks. Gene. 2006 Aug 1;377:88-95.

Karagiannis TC, Harikrishnan KN, El-Osta A. Disparity of histone deacetylase inhibition on repair of radiation-induced DNA damage on euchromatin and constitutive heterochromatin compartments. Oncogene 2007;26:3963–3971.

Kaufman PD, Kobayashi R, Kessler N, Stillman B. The p150 and p60 subunits of chromatin assembly factor I: a molecular link between newly synthesized histones and DNA replication. Cell. 1995 Jun 30;81(7):1105-14.

Kaufman, P. D., Kobayashi, R., and Stillman, B. (1997) Ultraviolet radiation sensitivity and reduction of telomeric silencing in *Saccharomyces cere*V*isiae* cells lacking chromatin assembly factor-I, *Genes De*V*. 11*, 345-357

Keeney S, Kleckner N (1995) Covalent protein–DNA complexes at the 50 strand termini of meiosis-specific double-strand breaks in yeast. Proc Natl Acad Sci USA 92: 11274–11278

Keogh MC, Kim JA, Downey M, Fillingham J, Chowdhury D, Harrison JC, Onishi M, Datta N, Galicia S, Emili A, Lieberman J, Shen X, Buratowski S, Haber JE, Durocher D, Greenblatt JF, Krogan NJ. A phosphatase complex that dephosphorylates gammaH2AX regulates DNA damage checkpoint recovery. Nature. 2006 Jan 26;439(7075):497-501.

Kim UJ, Han M, Kayne P, Grunstein M. Effects of histone H4 depletion on the cell cycle and transcription of Saccharomyces cerevisiae. EMBO J. 1988 Jul; 7(7):2211-9.

Kim ST, Lim DS, Canman CE, Kastan MB. Substrate specificities and identification of putative substrates of ATM kinase family members. J Biol Chem. 1999 Dec 31;274(53):37538-43.

Kim JA, Haber JE (2009) Chromatin assembly factors Asf1 and CAF-1 have overlapping roles in deactivating the DNA damage checkpoint when DNA repair is complete. Proc Natl Acad Sci USA, 106:1151–1156.

Kolas NK, Chapman JR, Nakada S, et al. Orchestration of the DNA-damage response by the RNF8 ubiquitin ligase. Science 2007;318:1637–1640.

Kolodner RD, Putnam CD, Myung K. Maintenance of genome stability in Saccharomyces cerevisiae. *Science.* 2002;297:552–557.

Komata M, Bando M, Araki H, Shirahige K. The direct binding of Mrc1, a checkpoint mediator, to Mcm6, a replication helicase, is essential for the replication checkpoint against methyl methanesulfonate-induced stress. Mol Cell Biol. 2009 Sep;29(18):5008-19.

Kondo T, Higashi H, Nishizawa H, Ishikawa S, Ashizawa S, et al. (2001) Involvement of pRB-related p107 protein in the inhibition of S phase progression in response to genotoxic stress. J Biol Chem 276: 17559–17567.

Kops, G. J., Weaver, B. A. & Cleveland, D. W. On the road to cancer: aneuploidy and the mitotic checkpoint. Nature Rev. Cancer 5, 773–785 (2005).

Korber P, Hörz W (2004) Invitroassembly of the characteristic chromatin organization at the yeast PHO5promoter by a replication-independent extract system. J Biol Chem 279:35113–35120.

Korber, P. et al. The histone chaperone Asf1 increases the rate of histone eviction at the yeast PHO5 and PHO8 promoters. *J Biol Chem* 281, 5539-45 (2006).

Kornberg, R. D., and Y. Lorch. 1999. Twenty-five years of the nucleosome, fundamental particle of the eukaryote chromosome. Cell 98:285-94

Krawitz DC, Kama T, Kaufman PD. Chromatin assembly factor I mutants defective for PCNA binding require Asf1/Hir proteins for silencing. Mol Cell Biol. 2002 Jan;22(2):614-25.

Krejci L, Van Komen S, Li Y, Villemain J, Reddy MS, Klein H, Ellenberger T, Sung P. DNA helicase Srs2 disrupts the Rad51 presynaptic filament. Nature. 2003 May 15;423(6937):305-9.

Lazzaro F, Sapountzi V, et al., Histone methyltransferase Dot1 and Rad9 inhibit single-stranded DNA accumulation at DSBs and uncapped telomeres, EMBO J. 27 (2008) 1502–1512.

Le S, Davis C, Konopka JB, Sternglanz R (1997) Two new S-phase-specific genes from Saccharomyces cerevisiae. Yeast 13:1029–1042.

Lee, M.G., and P. Nurse. 1987. Complementation used to clone a human homologue of the fission yeast cell cycle control gene cdc2. *Nature*. 327:31-5.

Lee SE, Moore JK, Holmes A, Umezu K, Kolodner RD, Haber JE. Saccharomyces Ku70, mre11/rad50 and RPA proteins regulate adaptation to G2/M arrest after DNA damage. Cell. 1998 Aug 7;94(3):399-409.

Lee, C.H., and Chung, J.H. (2001). The hCds1 (Chk2)-FHA domain is essential for a chain of phosphorylation events on hCds1 that is induced by ionizing radiation. J. Biol. Chem. 276, 30537–30541.

Lee (a) SJ, Schwartz MF, Duong JK, Stern DF. Rad53 phosphorylation site clusters are important for Rad53 regulation and signaling. Mol Cell Biol. 2003 Sep;23(17):6300-14.

Lee (b), G. I., Z. Ding, et al. (2003). "NMR structure of the forkhead-associated domain from the Arabidopsis receptor kinase-associated protein phosphatase." Proc Natl Acad Sci U S A 100(20): 11261-6.

Leroy C, Lee SE, Vaze MB, Ochsenbien F, Guerois R, Haber JE, Marsolier-Kergoat MC. PP2C phosphatases Ptc2 and Ptc3 are required for DNA checkpoint inactivation after a double-strand break. Mol Cell. 2003 Mar;11(3):827-35

Li J, Lee GI, Van Doren SR, Walker JC. The FHA domain mediates phosphoprotein interactions. J Cell Sci. 2000 Dec;113 Pt 23:4143-9.

Li, J., Williams, B.L., Haire, L.F., Goldberg, M., Wilker, E., Durocher, D., Yaffe, M.B., Jackson, S.P., and Smerdon, S.J. (2002). Structural and functional versatility of the FHA domain in DNA-damage signaling by the tumor suppressor kinase Chk2. Mol. Cell 9, 1045–1054.

Li, Z., et al. (2008). Acetylation of Histone H3 lysine 56 regulates replication-coupled nucleosome assembly. Cell 134: 244-255.

Liao H, Byeon IJ, Tsai MD. Structure and function of a new phosphopeptide-binding domain containing the FHA2 of Rad53. J Mol Biol. 1999 Dec 10;294(4):1041-9.

Liberi G, Chiolo I, et al., Srs2 DNA helicase is involved in checkpoint response and its regulation requires a functional Mec1-dependent pathway and Cdk1 activity, EMBO J. 19 (2000) 5027–5038.

Limoli, C.L., Giedzinski, E., Bonner, W.M., and Cleaver, J.E. 2002. UV-induced replication arrest in the xeroderma pigmentosum variant leads to DNA doublestrand breaks, gamma -H2AX formation, and Mre11 relocalization. *Proc Natl Acad Sci U S A* 99(1): 233-238.

Linger J, Tyler JK. The yeast histone chaperone chromatin assembly factor 1 protects against double-strand DNA-damaging agents. Genetics. 2005 Dec;171(4):1513-22.

Lisby, M., J.H. Barlow, R.C. Burgess, and R. Rothstein. 2004. Choreography of the DNA damage response: spatiotemporal relationships among checkpoint and repair proteins. *Cell*. 118:699-713.

Liu, P. *et al.* The Chk1-mediated S-phase checkpoint targets initiation factor Cdc45 via a Cdc25A/Cdk2-independent mechanism. *J. Biol. Chem.* 281, 30631–30644 (2006).

Lobachev KS, Gordenin DA, Resnick MA (2002) The Mre11 complex is required for repair of hairpin-capped double-strand breaks and prevention of chromosome rearrangements. Cell 108: 183–193

Longhese MP, Clerici M, Lucchini G. The S-phase checkpoint and its regulation in Saccharomyces cerevisiae. Mutat Res. 2003 Nov 27;532(1-2):41-58.

Longhese MP, Mantiero D, Clerici M (2006) The cellular response to chromosome breakage. Mol Microbiol 60: 1099–1108.

Lopez-Mosqueda J, Maas NL, Jonsson ZO, DefazioEli LG, Wohlschlegel J, Toczyski DP. Damage-induced phosphorylation of Sld3 is important to block late origin firing. Nature 2010; 467:479-83.

Loppin, B., E. Bonnefoy, C. Anselme, A. Laurencon, T. L. Karr, and P. Couble. 2005. The histone H3.3 chaperone HIRA is essential for chromatin assembly in the male pronucleus. Nature 437:1386–1390.

Lou H, Komata M, Katou Y, Guan Z, Reis CC, Budd M, Shirahige K, Campbell JL. Mrc1 and DNA polymerase epsilon function together in linking DNA replication and the S phase checkpoint. Mol Cell. 2008 Oct 10;32(1):106-17.

Loyola A, Almouzni G. Histone chaperones, a supporting role in the limelight. Biochim Biophys Acta. 2004 Mar 15;1677(1-3):3-11.

Loyola A, Bonaldi T, Roche D, Imhof A, Almouzni G. PTMs on H3 variants before chromatin assembly potentiate their final epigenetic state. Mol Cell. 2006 Oct 20;24(2):309-16.

Loyola A, Almouzni G. Marking histone H3 variants: how, when and why? Trends Biochem Sci. 2007 Sep;32(9):425-33. Epub 2007 Aug 30. Review.

Lucca C, Vanoli F, Cotta-Ramusino C, Pellicioli A, Liberi G, Haber J, Foiani M. Checkpoint-mediated control of replisome-fork association and signalling in response to replication pausing. Oncogene. 2004 Feb 12;23(6):1206-13.

Luger, K., Mader, A.W., Richmond, R.K., Sargent, D.F., and Richmond, T.J. (1997). Crystal structure of the nucleosome core particle at 2.8 A° resolution. Nature *389*, 251–260.

Luger K, Richmond TJ. The histone tails of the nucleosome. Curr. Opin. Genet. Dev 1998;8:140–146.

Lydall D, Whitehall S. Chromatin and the DNA damage response. DNA Repair (Amst). 2005 Sep 28;4(10):1195-207.

Maas NL, Miller KM, DeFazio LG, Toczyski DP (2006) Cell cycle and checkpoint regulation of histone H3 K56 acetylation by Hst3 and Hst4. Mol Cell 23: 109–119.

Mahajan A, Yuan C, Pike BL, Heierhorst J, Chang CF, Tsai MD. FHA domain-ligand interactions: importance of integrating chemical and biological approaches. J Am Chem Soc. 2005 Oct 26;127(42):14572-3.

Maier, V. K., M. Chioda and P. B. Becker, 2008 ATP-dependent chromatosome remodeling. Biol. Chem. 389: 345–352.

Mailand N, Bekker-Jensen S, Faustrup H, et al. RNF8 ubiquitylates histones at DNA double-strand breaks and promotes assembly of repair proteins. Cell 2007;131:887–900.

Maison C and Almouzni G, 2004 HP1 and the dynamics of heterochromatin maintenance, Nat. Rev. Mol. Cell Biol. 5, pp. 296–304.

Majka J, Burgers PM. Yeast Rad17/Mec3/Ddc1: a sliding clamp for the DNA damage checkpoint. *Proc Natl Acad Sci U S A.* 2003;100:2249–2254.

Majka J, Binz SK, Wold MS, Burgers PM. Replication protein A directs loading of the DNA damage checkpoint clamp to 5′-DNA junctions. *J Biol Chem.* 2006;281:27855–27861.

Malay, A. D., Umehara, T., Matsubara-Malay, K., Padmanabhan, B. & Yokoyama, S. Crystal structures of fission yeast histone chaperone Asf1 complexed with the Hip1 B-domain or the Cac2 C terminus. *J Biol Chem* 283, 14022-31 (2008).

Malik HS and Henikoff S (2003) Phylogenomics of the nucleosome. Nature Structural Biology 10(11), 882-891.

Marfella, C. G., and A. N. Imbalzano. 2007. The Chd family of chromatin remodelers. Mutat Res 618:30-40.

Mantiero D, Clerici M, Lucchini G, Longhese MP (2007) Dual role for Saccharomyces cerevisiae Tel1 in the checkpoint response to double-strand breaks. EMBO Rep 8: 380–387.

Masumoto H, Sugino A, Araki H: Dpb11 controls the association between DNA polymerases alpha and epsilon and the autonomously replicating sequence region of budding yeast. Mol Cell Biol 2000, 20:2809-2817.

Masumoto H, Hawke D, Kobayashi R, Verreault A. A role for cell-cycle-regulated histone H3 lysine 56 acetylation in the DNA damage response. Nature 2005;436:294–298.

Matsuoka, S., Rotman, G., Ogawa, A., Shiloh, Y., Tamai, K., and Elledge, S.J. (2000). Ataxia telangiectasia-mutated phosphorylates Chk2 in vivo and in vitro. Proc. Natl. Acad. Sci. USA 97, 10389–10394.

Méchali M. Eukaryotic DNA replication origins: many choices for appropriate answers. Nat Rev Mol Cell Biol. 2010 Oct;11(10):728-38.

Melchionna, R., Chen, X.B., Blasina, A., and McGowan, C.H. (2000). Threonine 68 is required for radiation-induced phosphorylation and activation of Cds1. Nat. Cell Biol. 2, 762–765.

Mello JA, Sillje HH, Roche DM, Kirschner DB, Nigg EA, et al. (2002) Human Asf1 and CAF-1 interact and synergize in a repair-coupled nucleosome assembly pathway. EMBO Rep 3: 329–334.

Melo JA, Cohen J, Toczyski DP. Two checkpoint complexes are independently recruited to sites of DNA damage in vivo. *Genes Dev.* 2001;15:2809–2821.

Melo, J. V. & Barnes, D. J. Chronic myeloid leukaemia as a model of disease evolution in human cancer. Nature Rev. Cancer 7, 441–453 (2007).

Meneghini MD, Wu M, Madhani HD. Conserved histone variant H2A.Z protects euchromatin from the ectopic spread of silent heterochromatin. Cell. 2003 Mar 7;112(5):725-36.

Mitelman, F., Johansson, B. & Mertens, F. The impact of translocations and gene fusions on cancer causation. Nature Rev. Cancer 7, 233–245 (2007).

Mito Y, Henikoff JG, Henikoff S. Genome-scale profiling of histone H3.3 replacement patterns. Nat Genet. 2005 Oct; 37(10):1090-7.

Moggs, J. G., Grandi, P., Quivy, J. P., Jonsson, Z. O., Hubscher, U., Becker, P. B., and Almouzni, G. (2000) A CAF-1-PCNAmediated chromatin assembly pathway triggered by sensing DNA damage, *Mol. Cell. Biol*. *20*, 1206-1218.

Mordes DA, Nam EA, Cortez D: Dpb11 activates the Mec1-Ddc2 complex. Proc Natl Acad Sci U S A 2008, 105:18730-18734.

Morrow DM, Tagle DA, Shiloh Y, Collins FS, Hieter P. *TEL1*, an *S. cerevisiae* homolog of the human gene mutated in ataxia telangiectasia, is functionally related to the yeast checkpoint gene *MEC1*. *Cell.* 1995;82:831–840.

Moshkin YM, Armstrong JA, Maeda RK, Tamkun JW, Verrijzer P, et al. (2002) Histone chaperone ASF1 cooperates with the Brahma chromatin-remodelling machinery. Genes Dev 16: 2621–2626.

Mousson F, Lautrette A, Thuret JY, Agez M, Courbeyrette R, Amigues B, Becker E, Neumann JM, Guerois R, Mann C, Ochsenbein F. Structural basis for the interaction of Asf1 with histone H3 and its functional implications. Proc Natl Acad Sci U S A. 2005 Apr 26;102(17):5975-80.

Mousson, F., Ochsenbein, F. and Mann, C. (2007). The histone chaperone Asf1 at the crossroads of chromatin and DNA checkpoint pathways. Chromosoma 116: 79-93.

Munakata T, Adachi N, Yokoyama N, Kuzuhara T, Horikoshi M. A human homologue of yeast anti-silencing factor has histone chaperone activity. Genes Cells. 2000 Mar;5(3):221-33.

Murr R, Loizou JI, Yang YG, Cuenin C, Li H, Wang ZQ, Herceg Z. Histone acetylation by Trrap-Tip60 modulates loading of repair proteins and repair of DNA double-strand breaks. Nat Cell Biol. 2006 Jan;8(1):91-9. Epub 2005 Dec 11.

Murr, R., Vaissiere, T., Sawan, C., Shukla, V. & Herceg, Z. Orchestration of chromatin-based processes: mind the TRRAP. *Oncogene* **26**, 5358–5372 (2007).

Myung, K., A. Datta and R. D. Kolodner, 2001 Suppression of spontaneous chromosomal rearrangements by S phase checkpoint functions in Saccharomyces cerevisiae. Cell 104: 397–408.

Myung K, Kolodner RD. Suppression of genome instability by redundant S-phase checkpoint pathways in Saccharomyces cerevisiae. *Proc Natl Acad Sci U S A.* 2002;99:4500–4507.

Myung, K., Pennaneach, V., Kats, E. S. & Kolodner, R. D. Saccharomy cescerevisiae chromatin-assembly factors that act during DNA replication function in the maintenance of genome stability. *Proc Natl Acad Sci U S A* 100, 6640-5 (2003).

Nabatiyan, A., and T. Krude. 2004. Silencing of chromatin assembly factor 1 in human cells leads to cell death and loss of chromatin assembly during DNA synthesis. Mol. Cell. Biol. 24:2853–2862.

Naiki, T., T. Wakayama, et al. (2004). "Association of Rad9 with double-strand breaks through a Mec1-dependent mechanism." Mol Cell Biol 24(8): 3277-85.

Nakada D, Matsumoto K, Sugimoto K. ATM-related Tel1 associates with double-strand breaks through an Xrs2-dependent mechanism. *Genes Dev.* 2003;17:1957–1962.

Nakamura TM, Du LL, Redon C, Russell P: Histone H2A phosphorylation controls Crb2 recruitment at DNA breaks, maintains checkpoint arrest, and influences DNA repair in fission yeast. Mol Cell Biol 2004, 24:6215-6230

Nakatani Y, Ray-Gallet D, Quivy JP, Tagami H, Almouzni G. Two distinct nucleosome assembly pathways: dependent or independent of DNA synthesis promoted by

histone H3.1 and H3.3 complexes. Cold Spring Harb Symp Quant Biol. 2004;69:273-80.

Nakayama, T., K. Nishioka, Y. X. Dong, T. Shimojima, and S. Hirose. 2007. Drosophila GAGA factor directs histone H3.3 replacement that prevents the heterochromatin spreading. Genes Dev. 21:552–561.

Natsume, R. et al. Structure and function of the histone chaperone CIA/ASF1 complexed with histones H3 and H4. *Nature* 446, 338-41 (2007).

Navadgi-Patil VM, Burgers PM: Yeast DNA replication protein Dpb11 activates the Mec1/ATR checkpoint kinase. J Biol Chem 2008, 283:35853-35859.

Neale MJ, Ramachandran M, Trelles-Sticken E, Scherthan H, Goldman AS (2002) Wild-type levels of Spo11-induced DSBs are required for normal single-strand resection during meiosis. Mol Cell 9: 835–846

Nedelcheva MN, Roguev A, Dolapchiev LB, Shevchenko A, Taskov HB, et al. (2005) Uncoupling of unwinding from DNA synthesis implies regulation of MCM helicase by Tof1/Mrc1/Csm3 checkpoint complex. J Mol Biol 347: 509–521.

Nelson, D. M., X. Ye, C. Hall, H. Santos, T. Ma, G. D. Kao, T. J. Yen, J. W. Harper, and P. D. Adams. 2002. Coupling of DNA synthesis and histone synthesis in S phase independent of cyclin/cdk2 activity. Mol. Cell. Biol. 22:7459–7472.

Neumann, H. et al. A method for genetically installing site-specific acetylation in recombinant histones defines the effects of H3 K56 acetylation. *Mol Cell* 36, 153-63 (2009).

Nourani, A., F. Robert, and F. Winston. 2006. Evidence that Spt2/Sin1, an HMG-like factor, plays roles in transcription elongation, chromatin structure, and genome stability in Saccharomyces cerevisiae. Mol. Cell. Biol. 26: 1496–1509.

Nyberg,K.A., Michelson,R.J., Putnam,C.W. and Weinert,T.A. (2002) Toward maintaining the genome: DNA damage and replication checkpoints. Annu. Rev. Genet., 36, 617–656.

Orphanides, G., Wu, W. H., Lane, W. S., Hampsey, M. & Reinberg, D. The chromatin-specific transcription elongation factor FACT comprises human SPT16 and SSRP1 proteins. *Nature* 400, 284-8 (1999).

Osborn AJ, Elledge SJ. Mrc1 is a replication fork component whose phosphorylation in response to DNA replication stress activates Rad53. Genes Dev. 2003 Jul 15;17(14):1755-67.

Paciotti, V., M. Clerici, G. Lucchini, and M.P. Longhese. 2000. The checkpoint protein Ddc2, functionally related to S. pombe Rad26, interacts with Mec1 and is regulated by Mec1- dependent phosphorylation in budding yeast. *Genes Dev*. 14:2046-59.

Park YJ, Dyer PN, Tremethick DJ, Luger K: A new fluorescence resonance energy transfer approach demonstrates that the histone variant H2AZ stabilizes the histone octamer within the nucleosome. J Biol Chem 2004, 279:24274-24282.

Park YJ, Luger K (2008) Histone chaperones in nucleosome eviction and histone exchange. Curr Opin Struct Biol 18:282–289.

Parthun MR, Widom J, Gottschling DE. The major cytoplasmic histone acetyltransferase in yeast: links to chromatin replication and histone metabolism. Cell. 1996 Oct 4;87(1):85-94.

Paulovich AG, Hartwell LH (1995) A checkpoint regulates the rate of progression through S phase in S. cerevisiae in response to DNA damage. Cell 82: 841–847.

Pellicioli A, Lucca C, Liberi G, Marini F, Lopes M, Plevani P, Romano A, Di Fiore PP, Foiani M. Activation of Rad53 kinase in response to DNA damage and its effect in modulating phosphorylation of the lagging strand DNA polymerase. EMBO J. 1999 Nov 15;18(22):6561-72.

Pellicioli A, Foiani M. Signal transduction: how rad53 kinase is activated. Curr Biol. 2005 Sep 20;15(18):R769-71.

Perego, P., G.S. Jimenez, L. Gatti, S.B. Howell, and F. Zunino. 2000. Yeast mutants as a model system for identification of determinants of chemosensitivity. *Pharmacol Rev*. 52:477-92.

Pike BL, Yongkiettrakul S, Tsai MD, Heierhorst J. Diverse but overlapping functions of the two forkhead-associated (FHA) domains in Rad53 checkpoint kinase activation. J Biol Chem. 2003 Aug 15;278(33):30421-4. Epub 2003 Jun 12.

Pilyugin M, Demmers J, Verrijzer CP, Karch F, Moshkin YM (2009) Phosphorylation-mediated control of histone chaperone ASF1 levels by Tousled-like kinases. PLoS ONE 4: e8328

Pommier Y, Redon C, Rao VA, Seiler JA, Sordet O, Takemura H, Antony S, Meng L, Liao Z, Kohlhagen G, Zhang H, Kohn KW (2003) Repair of and checkpoint response to topoisomerase Imediated DNA damage. Mutat Res 532:173–203

Prado, F., Cortes-Ledesma, F. & Aguilera, A. The absence of the yeast chromatin assembly factor Asf1 increases genomic instability and sister chromatid exchange. *EMBO Rep* **5**, 497-502 (2004).

Prather, D., N. J. Krogan, A. Emili, J. F. Greenblatt, and F. Winston. 2005. Identification and characterization of Elf1, a conserved transcription elongation factor in Saccharomyces cerevisiae. Mol. Cell. Biol. 25:10122–10135.

Qin D, Lee H, Yuan C, Ju Y, Tsai MD. Identification of potential binding sites for the FHA domain of human Chk2 by in vitro binding studies. Biochem Biophys Res Commun. 2003 Nov 28;311(4):803-8.

Raisner RM, Madhani HD. Patterning chromatin: form and function for H2A.Z variant nucleosomes. *Curr Opin Genet Dev.* 2006;16:119–124.

Ramakrishnan, V. 1997. Histone H1 and chromatin higher-order structure.Crit. Rev. Eukaryot. Gene Expr. 7:215–230.

Ramey CJ, et al. (2004) Activation of the DNA damage checkpoint in yeast lacking the

histone chaperone anti-silencing function 1. Mol Cell Biol 24:10313–10327.

Rattray AJ, McGill CB, Shafer BK, Strathern JN (2001) Fidelity of mitotic double-strand-break repair in Saccharomyces cerevisiae: a role for SAE2/COM1. Genetics 158: 109–122

Ray-Gallet, D., J. P. Quivy, C. Scamps, E. M. Martini, M. Lipinski, and G. Almouzni. 2002. HIRA is critical for a nucleosome assembly pathway independent of DNA synthesis. Mol. Cell 9:1091–1100.

Recht, J., Tsubota, T., Tanny, J. C., Diaz, R. L., Berger, J. M., Zhang, X., Garcia, B. A., Shabanowitz, J., Burlingame, A. L., Hunt, D. F., Kaufman, P. D., and Allis, C. D. (2006) *Proc. Natl. Acad. Sci. U. S. A.* 103, 6988–6993

Redon C, Pilch D, Rogakou E, Sedelnikova O, Newrock K and Bonner W (2002). Histone H2A variants H2AX and H2AZ. Curr Opin Genet Dev, 12(2), 162-169.

Redon C, Pilch DR, Rogakou EP, Orr AH, Lowndes NF, Bonner WM: Yeast histone 2A serine 129 is essential for the efficient repair of checkpoint-blind DNA damage. EMBO Rep 2003, 4:678-684.

Roberts TM, Kobor MS, Bastin-Shanower SA, Ii M, Horte SA, Gin JW, Emili A, Rine J, Brill SJ, Brown GW. Slx4 regulates DNA damage checkpoint-dependent phosphorylation of the BRCT domain protein Rtt107/Esc4. Mol Biol Cell 2006;17:539–548.

Rogakou EP, Pilch DR, Orr AH, Ivanova VS, Bonner WM:DNA double-stranded breaks induce histone H2AX phosphorylation on serine 139. J Biol Chem 1998, 273:5858-5868.

Roth SY, Denu JM, Allis CD (2001) Histone acetyltransferases. Annu Rev Biochem 70:81–120.

Rouse J and Jackson SP. Interfaces between the detection, signaling, and repair of D NA damage. Science. 2002; 297: 547- 551.

Rouse J. Esc4p, a new target of Mec1p (ATR), promotes resumption of DNA synthesis after DNA damage. Embo J 2004;23:1188–1197.

Saha A, Wittmeyer J, Cairns BR. Mechanisms for nucleosome movement by ATP-dependent chromatin remodeling complexes. Results Probl Cell Differ. 2006;41:127-48.

Sancar, A., L.A. Lindsey-Boltz, K. Unsal-Kacmaz, and S. Linn. 2004. Molecular mechanisms of mammalian DNA repair and the DNA damage checkpoints. *Annu Rev Biochem*. 73:39-85.

Sanchez Y, Desany BA, Jones WJ, Liu Q, Wang B, Elledge SJ. Regulation of RAD53 by the ATM-like kinases MEC1 and TEL1 in yeast cell cycle checkpoint pathways. *Science.* 1996;271:357–360.

Sanchez Y, Bachant J, Wang H, Hu F, Liu D, et al. 1999. Control of the DNA damage checkpoint by chk1 and rad53 protein kinases through distinct mechanisms. Science 286:1166–71

Sanematsu, F. et al. Asf1 is required for viability and chromatin assembly during DNA replication in vertebrate cells. *J Biol Chem* 281, 13817-27 (2006).

Santisteban MS, Kalashnikova T, Smith MM. Histone H2A.Z regulats transcription and is partially redundant with nucleosome remodeling complexes. Cell. 2000 Oct 27;103(3):411-22.

Santocanale C, Diffley JF (1998) A Mec1- and Rad53-dependent checkpoint controls late-firing origins of DNA replication. Nature 395: 615–618.

Santocanale C, Sharma K, Diffley JF. Activation of dormant origins of DNA replication in budding yeast. Genes Dev. 1999 Sep 15;13(18):2360-4.

Schneider, J., Bajwa, P., Johnson, F. C., Bhaumik, S. R. & Shilatifard, A. Rtt109 is required for proper H3K56 acetylation: a chromatin mark associated with the elongating RNA polymerase II. *J Biol Chem* 281, 37270-4 (2006).

Schwabish MA, Struhl K (2006) Asf1 mediates histone eviction and deposition during elongation by RNA polymerase II. Mol Cell 22:415–422.

Schwartz MF, Duong JK, Sun Z, Morrow JS, Pradhan D, Stern DF. Rad9 phosphorylation sites couple Rad53 to the Saccharomyces cerevisiae DNA damage checkpoint. Mol Cell. 2002 May;9(5):1055-65.

Schwartz MF, Lee SJ, Duong JK, Eminaga S, Stern DF. FHA domain-mediated DNA checkpoint regulation of Rad53. Cell Cycle. 2003 Jul-Aug;2(4):384-96.

Schwartz BE, Ahmad K. Transcriptional activation triggers deposition and removal of the histone variant H3.3. Genes Dev. 2005 Apr 1;19(7):804-14.

Segurado M, Diffley JF: Separate roles for the DNA damage checkpoint protein kinases in stabilizing DNA replication forks. Genes Dev 2008, 22:1816-1827. □

Segurado M, Tercero JA: The S-phase checkpoint: targeting the replication fork. Biol Cell 2009, 101:617-627. Designer deletion strains derived from Saccharomyces cerevisiae S288C:

Selth, L. & Svejstrup, J. Q. Vps75, a new yeast member of the NAP histone chaperone family. *J Biol Chem* 282, 12358-62 (2007).

Selth, L. A. et al. An rtt109-independent role for vps75 in transcription-associated nucleosome dynamics. *Mol Cell Biol* 29, 4220-34 (2009).

Sharp JA, Fouts ET, Krawitz DC, Kaufman PD (2001) Yeast histone deposition protein Asf1p requires Hir proteins and PCNA for heterochromatic silencing. Curr Biol 11:463–473.

Sharp JA, Rizki G, Kaufman PD (2005) Regulation of histone deposition proteins Asf1/Hir1 by multiple DNA damage checkpoint kinases in Saccharomyces cerevisiae. Genetics 171:885– 899.

Shibahara, K., and Stillman, B. (1999) Replication-dependent marking of DNA by PCNA facilitates CAF-1-coupled inheritance of chromatin, *Cell 96*, 575-585.

Shiloh, Y. ATM and related protein kinases: safeguarding genome integrity. Nature Rev. Cancer 3, 155–168 (2003).

Shirahige K, Hori Y, Shiraishi K, Yamashita M, Takahashi K, Obuse C, Tsurimoto T, Yoshikawa H. 1998. Regulation of DNA-replication origins during cell-cycle progression. Nature 395: 618–621.

Shogren-Knaak M, Ishii H, Sun JM, Pazin MJ, Davie JR, Peterson CL. Histone H4-K16 acetylation controls chromatin structure and protein interactions. Science. 2006 Feb 10;311(5762):844-7.

Shroff R, Arbel-Eden A, Pilch D, Ira G, Bonner WM, Petrini JH, Haber JE, Lichten M. Distribution and dynamics of chromatin modification induced by a defined DNA double-strand break. Curr Biol. 2004 Oct 5;14(19):1703-11.

Sidorova JM, Breeden LL. Rad53-dependent phosphorylation of Swi6 and down-regulation of CLN1 and CLN2 transcription occur in response to DNA damage in Saccharomyces cerevisiae. Genes Dev. 1997 Nov 15;11(22):3032-45.

Singh RK, Kabbaj MH, Paik J, Gunjan A. Histone levels are regulated by phosphorylation and ubiquitylation-dependent proteolysis. Nat Cell Biol 2009; 11:925-33.

Sillje HH, Nigg EA (2001) Identification of human Asf1 chromatin assembly factors as substrates of Tousled-like kinases. Curr Biol 11: 1068–1073.

Slater, M. L. Effect of reversible inhibition of deoxyribonucleic acid synthesis on the yeast cell cycle. *J Bacteriol* **113**, 263-70 (1973).

Smerdon MJ. DNA repair and the role of chromatin structure. Curr Opin Cell Biol. 1991 Jun;3(3):422-8.

Smith, S., and Stillman, B. (1989) Purification and characterization of CAF-I, a human cell factor required for chromatin assembly during DNA replication in vitro, *Cell 58*, 15-25.

Smogorzewska A, de Lange T. Regulation of telomerase by telomeric proteins. *Annu Rev Biochem.* 2004;**73**:177–208.

Smolka MB, Albuquerque CP, Chen SH, Schmidt KH, Wei XX, Kolodner RD, Zhou H. Dynamic changes in protein-protein interaction and protein phosphorylation probed with amine-reactive isotope tag. Mol Cell Proteomics. 2005 Sep;4(9):1358-69.

Smolka MB, Chen SH, Maddox PS, Enserink JM, Albuquerque CP, Wei XX, Desai A, Kolodner RD, Zhou H. An FHA domain-mediated protein interaction network of Rad53 reveals its role in polarized cell growth. J Cell Biol. 2006 Dec 4;175(5):743-53.

Sobel, R. E., Cook, R. G., Perry, C. A., Annunziato, A. T., and Allis, C. D. (1995) *Proc. Natl. Acad. Sci. U. S. A.* 92, 1237–1241

Sogo JM, Lopes M, Foiani M (2002) Fork reversal and ssDNA accumulation at stalled replication forks owing to checkpoint defects. Science 297: 599–602.stabilizes the replisome independently of the S phase checkpoint during.

Song JJ, Garlick JD, Kingston RE. Structural basis of histone H4 recognition by p55. Genes Dev. 2008 May 15;22(10):1313-8.

Soulier J, Lowndes NF. The BRCT domain of the S. cerevisiae checkpoint protein Rad9 mediates a Rad9-Rad9 interaction after DNA damage. Curr Biol. 1999 May 20;9(10):551-4.

Stiff T, O'Driscoll M, Rief N, Iwabuchi K, Lobrich M, Jeggo PA: ATM and DNA-PK function redundantly to phosphorylate H2AX after exposure to ionizing radiation. Cancer Res 2004,64:2390-2396.

Strahl BD, Allis CD. The language of covalent histone modifications. Nature. 2000;**403**:41–45.

Su, T.T. 2006. Cellular responses to DNA damage: one signal, multiple choices. *Annu Rev Genet*. 40:187-208.

Sutton, A., Bucaria, J., Osley, M. A., and Sternglanz, R. (2001). Yeast ASF1 protein is required for cell cycle regulation of histone gene transcription. Genetics 158: 587-596.

Sun Z, Fay DS, Marini F, Foiani M, Stern DF. Spk1/Rad53 is regulated by Mec1-dependent protein phosphorylation in DNA replication and damage checkpoint pathways. *Genes Dev.* 1996;10:395–406.

Sun Z, Hsiao J, Fay DS, Stern DF. Rad53 FHA domain associated with phosphorylated Rad9 in the DNA damage checkpoint. Science. 1998 Jul 10;281(5374):272-4.

Sweeney FD, Yang F, Chi A, Shabanowitz J, Hunt DF, Durocher D. Saccharomyces cerevisiae Rad9 acts as a Mec1 adaptor to allow Rad53 activation. Curr Biol. 2005 Aug 9;15(15):1364-75.

Szyjka SJ, Viggiani CJ, Aparicio OM. Mrc1 is required for normal progression of replication forks throughout chromatin in S. cerevisiae. Mol Cell. 2005 Sep 2;19(5):691-7.

Tagami, H., D. Ray-Gallet, G. Almouzni, and Y. Nakatani. 2004. Histone H3.1 and H3.3 complexes mediate nucleosome assembly pathways dependent or independent of DNA synthesis. Cell 116:51–61

Talbert PB and Henikoff S (2010). Histone variants--ancient wrap artists of the epigenome. Nat Rev Mol Cell Biol, 11, 264-275.

Tamburini BA, Carson JJ, Adkins MW, Tyler JK. Functional conservation and specialization among eukaryotic anti-silencing function 1 histone chaperones. Eukaryot Cell. 2005 Sep;4(9):1583-90.

Tan BC, Chien CT, Hirose S, Lee SC. Functional cooperation between FACT and MCM helicase facilitates initiation of chromatin DNA replication. EMBO J. 2006 Sep 6;25(17):3975-85.

Tanaka K, Russell P. Mrc1 channels the DNA replication arrest signal to checkpoint kinase Cds1. Nat Cell Biol. 2001 Nov;3(11):966-72.

Tanaka S, Umemori T, Hirai K, Muramatsu S, Kamimura Y, Araki H: CDK-dependent phosphorylation of Sld2 and Sld3 initiates DNA replication in budding yeast. Nature 2007, 445:328-332.

Tang, Y. et al. (2006) Structure of a human ASF1a-HIRA complex and insights into specificity of histone chaperone complex assembly. Nat. Struct. Mol. Biol. 13, 921–929

Tercero JA, Diffley JF. Regulation of DNA replication fork progression through damaged DNA by the Mec1/Rad53 checkpoint. Nature. 2001 Aug 2;412(6846):553-7.

Tercero JA, Longhese MP, Diffley JF. A central role for DNA replication forks in checkpoint activation and response. Mol Cell 2003; 11:1323-36.

Thaminy S, Newcomb B, Kim J, Gatbonton T, Foss E, et al. (2007) Hst3 is regulated by Mec1-dependent proteolysis and controls the S phase checkpoint and sister chromatid cohesion by deacetylating histone H3 at lysine 56. J Biol Chem 282: 37805–37814.

Thomas JO (1999) Histone H1: location and role. Curr Opin Cell Biol 11: 312Y317.

Tjeertes JV, Miller KM, Jackson SP. Screen for DNA-damage-responsive histone modifications identifies H3K9Ac and H3K56Ac in human cells. EMBO J. 2009 Jul 8;28(13):1878-89.

Toh GW, Lowndes NF. Role of the Saccharomyces cerevisiae Rad9 protein in sensing and responding to DNA damage. Biochem Soc Trans. 2003 Feb;31(Pt 1):242-6.

Traven A, Heierhorst J. SQ/TQ cluster domains: concentrated ATM/ATR kinase phosphorylation site regions in DNA-damage-response proteins. Bioessays. 2005 Apr;27(4):397-407.

Tsukiyama_a, T., C. Daniel, J. Tamkun, and C. Wu. 1995. ISWI, a member of the SWI2/SNF2 ATPase family, encodes the 140 kDa subunit of the nucleosome remodeling factor. Cell 83:1021-6.

Tsukiyama_b, T., and C. Wu. 1995. Purification and properties of an ATPdependentnucleosome remodeling factor. Cell 83:1011-20.

Tsubota, T., et al. (2007). Histone H3K56 acetylation is catalyzed by histone chaperone-dependent complexes. Mol. Cell 25: 703-712.

Turner BM (2000) Histone acetylation and an epigenetic code. BioEssays 22: 836-845

Tyler JK, et al. (1999) The RCAF complex mediates chromatin assembly during DNA replication and repair. Nature 402:555–560.

Tyler, J. K., et al. (2001). Interaction between the Drosophila CAF-1 and ASF1 chromatin assembly factors. Mol. Cell. Bio. 21: 6574-6584.

Tyler JK. Chromatin assembly. Cooperation between histone chaperones and ATP-dependent nucleosome remodeling machines. Eur J Biochem. 2002 May; 269(9): 2268-74.

Umehara, T., Chimura, T., Ichikawa, N. & Horikoshi, M. Polyanionic stretchdeleted histone chaperone cia1/Asf1p is functional both in vivo and in vitro. *Genes Cells* **7**, 59-73 (2002).

van der Heijden, G. W., A. A. Derijck, E. Posfai, M. Giele, P. Pelczar, L. Ramos, D. G. Wansink, J. van der Vlag, A. H. Peters, and P. de Boer. 2007. Chromosome-wide nucleosome replacement and H3.3 incorporation during mammalian meiotic sex chromosome inactivation. Nat. Genet. 39:251–258.

Van Vugt JJ, Ranes M, Campsteijn C, Logie C. The ins and outs of ATP-dependent chromatin remodeling in budding yeast: biophysical and proteomic perspectives. Biochim Biophys Acta. 2007 Mar;1769(3):153-71. Epub 2007 Feb 9.

Varga-Weisz, P. D., M. Wilm, E. Bonte, K. Dumas, M. Mann, and P. B.Becker. 1997. Chromatin-remodelling factor CHRAC contains the ATPases ISWI and topoisomerase II. Nature 388:598-602.

Vaze MB, Pellicioli A, et al., Recovery from checkpoint-mediated arrest after repair of a double-strand break requires Srs2 helicase, Mol. Cell 10 (2002) 373–385.

Verreault, A., Kaufman, P. D., Kobayashi, R. & Stillman, B. Nucleosome assembly by a complex of CAF-1 and acetylated histones H3/H4. *Cell* 87, 95- 104 (1996).

Verreault A. De novo nucleosome assembly: new pieces in an old puzzle. Genes Dev. 2000 Jun 15;14(12):1430-8.

Vidanes, G.M., Bonilla, C.Y., and Toczyski, D.P. (2005). Complicated tails: histone modifications and the DNA damage response. Cell 121, 973–976.

Wang P, Byeon IJ, Liao H, Beebe KD, Yongkiettrakul S, Pei D, Tsai MD. II. Structure and specificity of the interaction between the FHA2 domain of Rad53 and phosphotyrosyl peptides. J Mol Biol. 2000 Sep 29;302(4):927-40.

Wang, G. G., C. D. Allis, and P. Chi. 2007. Chromatin remodeling and cancer, Part II: ATP-dependent chromatin remodeling. Trends Mol Med 13:373-80.

Wang AY, Schulze JM, Skordalakes E, Gin JW, Berger JM, Rine J, Kobor MS. Asf1-like structure of the conserved Yaf9 YEATS domain and role in H2A.Z deposition and acetylation. Proc Natl Acad Sci U S A. 2009 Dec 22;106(51):21573-8.

Ward IM, Chen J: Histone H2AX is phosphorylated in an ATR-dependent manner in response to replicational stress. J Biol Chem 2001, 276:47759-47762.

Watanabe, S. et al. Structural characterization of H3K56Q nucleosomes and nucleosomal arrays. *Biochim Biophys Acta* 1799, 480-6 (2010).

Widom J (1998) Chromatin structure: linking structure to function with histone H1. Curr Biol 8: R788YR791.

Williams SK, Truong D, Tyler JK (2008) Acetylation in the globular core of histone H3 on lysine-56 promotes chromatin disassembly during transcriptional activation. Proc Natl Acad Sci USA 105:9000–9005.

Wirbelauer C, Bell O, Schübeler D. Variant histone H3.3 is deposited at sites of nucleosomal displacement throughout transcribed genes while active histone modifications show a promoter-proximal bias. Genes Dev. 2005 Aug 1;19(15):1761-6.

Woodcock CL. Chromatin architecture. Curr Opin Struct Biol 2006;16:213–220.

Wysocki, R. *et al.* Role of Dot1-dependent histone H3 methylation in G1 and S phase DNA damage checkpoint functions of Rad9. *Mol. Cell. Biol.* 25, 8430–8443 (2005).

Xhemalce B, et al. Regulation of histone H3 lysine 56 acetylation in Schizosaccharomyces pombe. J. Biol. Chem 2007;282:15040–15047.

Xu F, Zhang K, Grunstein M. Acetylation in histone H3 globular domain regulates gene expression in yeast. Cell 2005;121:375–385.

Yamamoto A, Guacci V, Koshland D. 1996. Pds1p, an inhibitor of anaphase in budding yeast, plays a critical role in the APC and checkpoint pathway(s). J. Cell Biol. 133:99–110

Ye, X. et al. Defective S phase chromatin assembly causes DNA damage, activation of the S phase checkpoint, and S phase arrest. *Mol Cell* 11, 341-51 (2003).

Ye, J. et al. Histone H4 lysine 91 acetylation a core domain modification associated with chromatin assembly. *Mol Cell* 18, 123-30 (2005).

You Z, Kong L, Newport J. The role of single-stranded DNA and polymerase alpha in establishing the ATR, Hus1 DNA replication checkpoint. J Biol Chem. 2002 Jul 26;277(30):27088-93.

Zabaronick, S. R. and Tyler, J. K. (2005). The histone chaperone anti-silencing function 1 is a global regulator of transcription independent of passage through S phase. Mol. Cell. Biol. 25: 652-660.

Zachos, G., M.D. Rainey, and D.A. Gillespie. 2003. Chk1-deficient tumour cells are viable but exhibit multiple checkpoint and survival defects. EMBO J. 22:713–723.

Zegerman P, Diffley JF: Phosphorylation of Sld2 and Sld3 by cyclin-dependent kinases promotes DNA replication in budding yeast. Nature 2007, 445:281-285. 34.

Zegerman P, Diffley JF. Checkpoint-dependent inhibition of DNA replication initiation by Sld3 and Dbf4 phosphorylation. Nature 2010; 467:474-8.

Zhang, R., Poustovoitov, M. V., Ye, X., Santos, H. A., Chen, W., Daganzo, S. M., Erzberger, J. P., Serebriiskii, I. G., Canutescu, A. A., Dunbrack, R. L., Pehrson, J. R., Berger, J. M., Kaufman, P. D., and Adams, P. D. (2005) *Dev. Cell* 8, 19–30

Zhang Z, Shibahara K, Stillman B. PCNA connects DNA replication to epigenetic inheritance in yeast. Nature. 2000 Nov 9;408(6809):221-5.

Zhao, X., E.G. Muller, and R. Rothstein. 1998. A suppressor of two essential checkpoint genes identifies a novel protein that negatively affects dNTP pools. *Mol Cell*. 2:329-40.

Zhao, X. and R. Rothstein (2002). "The Dun1 checkpoint kinase phosphorylates and regulates the ribonucleotide reductase inhibitor Sml1." Proc Natl Acad Sci U S A 99(6): 3746-51.

Zhou Z, Elledge SJ. DUN1 encodes a protein kinase that controls the DNA damage response in yeast. Cell. 1993 Dec 17;75(6):1119-27.

Zhou, B.B., and S.J. Elledge. 2000. The DNA damage response: putting checkpoints in perspective. *Nature*. 408:433-9.

Zhou H, Madden BJ, Muddiman DC, Zhang Z. Chromatin assembly factor 1 interacts with histone H3 methylated at lysine 79 in the processes of epigenetic silencing and DNA repair. Biochemistry. 2006 Mar 7;45(9):2852-61.

Zou L, Elledge SJ: Sensing DNA damage through ATRIP recognition of RPA-ssDNA complexes. Science 2003, 300:1542-1548.